
Characterization of Uranium Tailings Cover Materials for Radon Flux Reduction

120555031837 2 ANRU
US NRC
SECY PUBLIC DOCUMENT ROOM
BRANCH CHIEF
HST LOBBY
WASHINGTON DC 20555

Prepared by V. C. Rogers, R. F. Overmyer, K. M. Putzig, C. M. Jensen, K. K. Nielson, B. W. Sermon

Argonne National Laboratory and
Ford, Bacon and Davis Utah, Inc.

Prepared for
U. S. Nuclear Regulatory
Commission

POOR ORIGINAL

8003250 394

FDR

NOTICE

This report was prepared as an account of work sponsored by an agency of the United States Government. Neither the United States Government nor any agency thereof, or any of their employees, makes any warranty, expressed or implied, or assumes any legal liability or responsibility for any third party's use, or the results of such use, of any information, apparatus product or process disclosed in this report, or represents that its use by such third party would not infringe privately owned rights.

POOR ORIGINAL

Available from

GPO Sales Program
Division of Technical Information and Document Control
U.S. Nuclear Regulatory Commission
Washington, D.C. 20555

and

National Technical Information Service
Springfield, Virginia 22161

NUREG/CR-1081
FBDU-218-2
RU

Characterization of Uranium Tailings Cover Materials for Radon Flux Reduction

Manuscript Completed: January 1980
Date Published: March 1980

Prepared by
V. C. Rogers, R. F. Overmyer, K. M. Putzig, C. M. Jensen, K. K. Nielson, B. W. Sermon

Argonne National Laboratory
Argonne, IL 60439

Subcontractor: Ford, Bacon and Davis Utah, Inc.
375 Chipeta Way
Salt Lake City, UT 84108

Prepared for
Division of Safeguards, Fuel Cycle and Environmental Research
Office of Nuclear Regulatory Research
U.S. Nuclear Regulatory Commission
Washington, D.C. 20555
NRC FIN No. A-2046

ABSTRACT

Diffusion coefficients are determined for various soils and tailings. Radon flux and concentration measurements are made at a variety of thicknesses of cover material. The flux and concentration data are applied to a theoretical model based on diffusion theory, and diffusion coefficients are derived. D_e (flux) and D_e (concentration) are found to differ in magnitude, but this difference is within the limits to be expected from determining D_e from the measurement of two different parameters. Values of D_e (flux) vary from 1.8×10^{-3} to 3.2×10^{-2} cm^2/s and D_e (concentration) ranges from 1.4×10^{-3} to 1.3×10^{-2} cm^2/s for the soils considered in this report.

An alternate expression describing an exponential decrease in radon flux with cover thickness is defined. The diffusion coefficient associated with this relationship, D_A , is a function of cover thickness. D_A is found to approach D_e at a cover thickness of about three meters for the materials investigated. A mathematical justification for the use of the alternate expression is presented.

Moisture is found to have a large effect on the diffusion coefficients of both the tailing and the cover material. An empirical relationship between the diffusion coefficient and the moisture content of the soil is given. A change of two orders of magnitude in the value of the diffusion coefficient can be observed as the moisture content changes by 20 percent. Knowledge of the moisture content of the soil is critical for predicting the attenuation effects of cover material.

Vegetation growth in the cover material seems to cause a slight increase in radon exhalation when the roots penetrate to the tailings. Test columns containing tailings covered by soil, and in which plants were growing, exhibited a tendency to have wide variations in flux values from measurement to measurement. This variation appears to be associated with moisture retention and evaporation. Further investigation of this phenomenon is needed.

CONTENTS

<u>Chapter</u>	<u>Title</u>	<u>Page</u>
	Abstract	iii
	List of Figures.	vii
	List of Tables	ix
1	INTRODUCTION	
	1.1 Previous Radon Studies.	1-1
	1.2 Study Tasks	1-2
	Chapter 1 References	1-5
2	EXPERIMENTAL PROCEDURES AND EQUIPMENT	
	2.1 Radon Concentration Determination Using Lucas-Type Cells.	2-1
	2.1.1 Sampling and Counting of Radon Gas.	2-1
	2.1.2 Electronic Counting Equipment.	2-2
	2.1.3 Determination of the Concentration from Alpha Counting.	2-2
	2.1.4 Determination of Radon Surface Fluxes Using Lucas Cells	2-3
	2.1.5 Accuracy of Cell Measurements.	2-4
	2.1.6 Lucas Cell Efficiency.	2-4
	2.2 Radon Flux Measurements Using Activated Charcoal Canisters.	2-5
	2.2.1 Use of Charcoal Canisters for Flux Measurements	2-5
	2.2.2 Determination of the Radon Flux Using the ²¹⁴ Bi 0.609-Mev Gamma Ray.	2-6
	2.2.3 Canister Cross Calibration	2-6
	2.2.4 Precision of Canister Data	2-7
	2.3 Monitoring Moisture with a Resistance- Type Probe.	2-7
	2.3.1 Monitor and Probe Construction	2-7
	2.3.2 Probe Calibration.	2-8
	2.3.3 Use of the Moisture Meter.	2-9
	2.4 Emanating Power Measurements of Uranium Mill Tailings	2-10
	2.5 Collection and Handling of the Selected Cover and Tailings Materials.	2-11
	Chapter 2 References	2-24

CONTENTS (Cont)

<u>Chapter</u>	<u>Title</u>	<u>Page</u>
3	GEOLOGY AND SOIL MECHANICAL PROPERTIES OF THE SELECTED COVER MATERIALS	
	3.1 Powder River Basin - Wyoming	3-1
	3.2 Shirley Basin - Wyoming	3-5
	3.3 Gas Hills - Wyoming	3-7
	3.4 Grants Mineral Belt - New Mexico	3-9
	3.5 General Geology of Other Uranium Mining Regions	3-14
	Chapter 3 References	3-37
4	DIFFUSION THEORY EXPRESSIONS USED TO INTERPRET THE LABORATORY DATA	
	4.1 Radon Soil Gas Concentration Using Finite Sources	4-1
	4.1.1 General Diffusion Equation	4-1
	4.1.2 Boundary Condition	4-2
	4.1.3 Source Modeling	4-5
	4.2 Flux as a Function of Thickness of Bare Tailings	4-5
	4.3 Flux as a Function of Cover Material Thickness	4-6
	4.4 Alternative Expression for the Radon Flux as a Function of Cover Thickness	4-6
	Chapter 4 References	4-12
5	EXPERIMENTAL RESULTS AND DISCUSSION	
	5.1 Radon Source Parameters	5-1
	5.1.1 Radium Content and Emanating Power of the Tailings Source	5-1
	5.1.2 Radium Content and Emanating Power of the Selected Cover Materials	5-3
	5.1.3 Radium Content and Emanating Power of Selected Tailings Samples	5-3
	5.1.4 Soil Mechanical Properties	5-4
	5.2 Determination of the Effective Diffusion Coefficient for the Selected Cover Materials	5-5

CONTENTS (Cont)

<u>Chapter</u>	<u>Title</u>	<u>Page</u>
	5.2.1 Determination of the Effective Diffusion Coefficient Using Radon Flux Profiles	5-6
	5.2.2 Determination of the Effective Diffusion Coefficient Using Radon Concentration Profiles	5-6
	5.3 Variation of the Diffusion Coefficient with Moisture Content	5-7
	5.4 Radon Flux Reduction Due to the Bear Creek Configuration	5-8
	5.5 Surface Radon Flux as a Function of Bare Uranium Tailings Depth.	5-8
	5.6 Radon Flux Alterations Due to Vegetative Root Penetration.	5-9
	Chapter 5 References	5-37
6	CONCLUSIONS	
	6.1 Task 1.	6-1
	6.2 Task 2.	6-1
	6.3 Task 3.	6-2
	6.4 Task 4.	6-2
	6.5 General Conclusions	6-2

APPENDIX

- A SOIL MECHANICAL PROPERTIES OF THE SELECTED COVER AND TAILINGS MATERIALS
- B CHARACTERISTICS OF PLANT SPECIES SELECTED

LIST OF FIGURES

<u>Number</u>	<u>Title</u>	<u>Page</u>
1-1	Radioactive Decay Chain of Uranium-238	1-3
2-1	Lucas Cells and Alpha Particle Counting Electronics.	2-12
2-2	Schematic of Direct Deemanation System	2-13
2-3	M-11 Charcoal Canisters and Block Diagram of Electronic Counting System	2-14
2-4	Charcoal Canister Calibration Data	2-15
2-5	Moisture Monitor and Probe	2-16
2-6	Schematic Diagram, Moisture Meter.	2-17
2-7	Moisture Contact Water Probe	2-18
2-8	Probe Deviation from Unit to Unit.	2-19
2-9	Calibration Data and Comparison of Active Sensing Volumes.	2-20
2-10	Calibration in Powder River and Shirley Basin Clays.	2-21
3-1	Physiographic Division Map of the U.S.	3-20
3-2	Major Uranium Mining Districts of Wyoming.	3-21
3-3	Northwestern Uranium Mining Districts of New Mexico	3-22
3-4	Uranium Mining Districts of Colorado and Utah Showing the Principal Uranium in the Paradox Basin.	3-23
3-5	Major Uranium Mining Districts of Texas.	3-24
3-6	Powder River Basin Uranium Areas	3-25
3-7	Shirley Basin Area, Wyoming.	3-26
4-1	Schematic Representation of Radon Source and Cover Material	4-11
5-1	Correlation of Radium Content of Tailings Samples with Particle Size	5-12

LIST OF FIGURES (Cont)

<u>Number</u>	<u>Title</u>	<u>Page</u>
5-2	Correlation of Percent Emanating Power of Tailings Samples with Particle Size.	5-13
5-3	Unified Soil Classification System	5-14
5-4	Radon Flux Profiles of Shirley Basin Soil No. 2.	5-15
5-5	Radon Flux Profiles of Powder River Soil No. 2.	5-16
5-6	Illustration of the Cover Thickness dependence of D_A	5-17
5-7	Radon Concentration Profile of Shirley Basin Soil No. 2	5-18
5-8	Radon Concentration Profile of Ambrosia Lake Soil No. 1	5-19
5-9	Exponential Moisture Dependence of the Diffusion Coefficient.	5-20
5-10	Flux and Moisture Measurements of the RME Configuration as a Function of Time.	5-21
5-11	Flux as a Function of Bare Tailings Depth for Ambrosia Lake Tailings #1-1.	5-22
5-12	Variation of Radon Flux with Time for a Typical Test Column with Native Grass Growth (Column #4).	5-23
5-13	Effect of Moisture on the Radon Flux and Moisture Probe Voltage as a Function of Time for Bare Cover (Column #5)	5-24
5-14	Effect of Moisture on the Radon Flux and Moisture Probe Voltage as a Function of Time for Native Grass (Column #3)	5-25
5-15	Effect of Moisture on the Radon Flux and Moisture Probe Voltage as a Function of Time for Native Grass (Column #4)	5-26

LIST OF TABLES

<u>Number</u>	<u>Title</u>	<u>Page</u>
1-1	Diffusion Coefficients for Radon in Various Media.	1-4
2-1	Canister Calibration Data.	2-22
3-1	Stratigraphic Section in the Powder River Basin, Wyoming	3-27
3-2	Estimated Properties of Set 2 Soil Samples	3-28
3-3	Stratigraphic Sections in the Shirley Basin Area, Wyoming.	3-29
3-4	Soil/Bedrock Sections in the Shirley Basin, Wyoming.	3-30
3-5	Stratigraphic Units Wind River Basin and Gas Hills Mining District.	3-31
3-6	Soil Characteristics Near the Lucky Mc Mine and Mill Site, Gas Hills, Wyoming.	3-32
3-7	Stratigraphic Section, Southeastern Ambrosia Lake Area, Grants, New Mexico.	3-33
3-8	Geologic Section for the Spanish Valley Area, Paradox Basin, Utah/Colorado	3-34
3-9	Stratigraphic Units and Their Water-Bearing Properties, Karnes County, Texas	3-36
5-1	Radium Concentrations and Diffusion Coefficient for the Sources Used with Each Cover Material.	5-27
5-2	Summary of Radon Source Parameters and Soil Mechanical Properties	5-28
5-3	Typical Void Ratios and Porosities for Cohesionless Soils	5-29
5-4	Measured Radon Flux ($\text{pCi/m}^2\text{-s}$) as a Function of Cover Thickness	5-30
5-5	Effective Diffusion Coefficient (D_e) (cm^2/s) Determined for Each Cover Material at the Specified Depth.	5-31

LIST OF TABLES (Cont)

<u>Number</u>	<u>Title</u>	<u>Page</u>
5-6	Alternate Diffusion Coefficient D_A (cm^2/sec) Determined for Each Cover Material at the Specified Depth.	5-32
5-7	Diffusion Coefficient for Each Cover Material. .	5-33
5-8	Experimental Radon Concentration as a Function of Distance from Tailings-Cover Interface. . . .	5-34
5-9	Effective Diffusion Coefficient D_e (cm^2/sec) Determined Using Radon Concentration Profiles. .	5-35
5-10	Diffusion Coefficient Determined for Various Cover Materials as a Function of Moisture Added.	5-36

CHAPTER 1

INTRODUCTION

Ford, Bacon & Davis Utah Inc. has performed experiments to define the effects on radon gas exhalation of various characteristics of cover materials. These experiments have led to results which are predicted by theoretical models that are described in this report. The studies reported here will be helpful in understanding the phenomena of, and finding solutions to, the disposal of radioactive waste products.

One of the most significant sources of exposure to low level radiation from uranium mill tailings is associated with the ionizing radiation from the chemically inert gas ^{222}Rn , a radioactive decay daughter of ^{238}U , in the $4n+2$ decay series as outlined in Figure 1-1. Due to its relatively long half-life, 3.82 days, ^{222}Rn can be transported large distances and elevated concentrations of radon have been reported at distances greater than 10^3 m from tailings piles. (1,2)

1.1 PREVIOUS RADON STUDIES

Researchers have long been interested in the diffusion and transport of radon in the environment. Early studies of radon in the natural environment (4-12) have been supplemented by research specifically dealing with the diffusion and transport of radon produced in uranium mill tailings. (13-16)

The early works of Tanner, (10) Kraner, (11), and Culot (12) have been especially helpful in determining values of the diffusion coefficient for various soils under various conditions. These values, as presented in Table 1-1, were determined under varying laboratory field conditions where unidentified soil substructure and transport effects might affect the diffusion coefficient.

The first major studies concerned with the diffusion of radon from mill tailings were those performed by Culot, Schiager, et al. (13-15) Their experiments were concerned with diffusion of radon through tailings, soil, and concrete. Their results showed soil and concrete to have diffusion coefficients of approximately 5×10^{-2} cm^2/s and 2×10^{-5} cm^2/s respectively. Diffusion theory was also used to model the radon concentration and flux in the material of interest and proved applicable within the tailing and cover material.

More recently, Macbeth et al. (16) have studied the diffusion of radon through dry bentonitic clay and clean sand as well as the flux reduction capabilities of several foams,

(1) See end of chapter for references.

well as the flux reduction capabilities of several foams, epoxies, asphaltic emulsions, and volumetric stabilizers. Their studies determined soil gas concentrations in the sand and clay and correlated the data with theoretical expressions derived from diffusion theory. The studies yielded the effects of temperature, pressure, moisture in the tailings, and wind speed upon the exhalation rate of radon.

1.2 STUDY TASKS

Clay and soil coverings have been suggested as a method of retarding the exhalation and transport of radon, and allowing greater decay within the confines of the tailings pile.⁽¹⁵⁾ Because mechanical properties of the soils may affect their performance, five tasks were performed to characterize and to quantify the flux-retarding capabilities of different soils and clays, and to correlate the results with the mechanical properties of the respective cover materials.

Task I: Determine the effective radon diffusion coefficient for each of eight different soils and clays which are representative of the Wyoming and New Mexico mining regions; determine for each the radium content and other soil mechanical properties which are necessary to characterize the radon source in the cover material; as part of determining the individual effective diffusion coefficients, determine the radon concentration profile and flux as a function of the cover material thickness; perform measurements on the combination of materials proposed for the Bear Creek project⁽¹⁵⁾ to determine their effectiveness in reducing the radon flux.

Task II: Perform laboratory measurements to determine the effect of moisture upon the the diffusion coefficient of two clays. This was performed by measuring the radon flux and determining the effective radon diffusion coefficient.

Task III: Determine the emanating power of at least ten different uranium mill tailings samples. These were obtained to typify tailings, both sandy and slime, from the major uranium mining region outlined in task I.

Task IV: Investigate the possible effects of plant root penetration upon the radon exhalation from revegetated cover materials which have been placed over uranium mill tailings.

Task V: Propose a field study plan which could be undertaken to verify laboratory measurements on the Bear Creek configuration.

The basic measurement methods used provide accurate information in determining radon flux and concentration profiles.⁽¹⁶⁾ The experimental methods, theoretical models, and results of experiments performed to accomplish the above tasks are reported in this document.

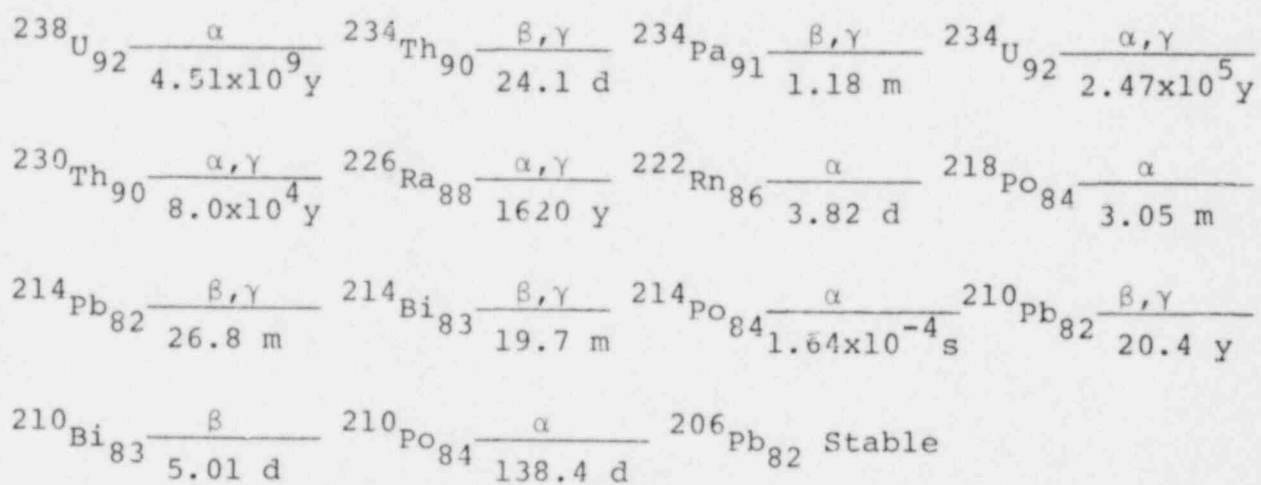


FIGURE 1-1. RADIOACTIVE DECAY CHAIN OF URANIUM-238

TABLE 1.1
DIFFUSION COEFFICIENTS FOR RADON IN VARIOUS MEDIA ⁽¹⁰⁾

Medium	Moisture Content (%)	<u>Effective Diffusion Coefficient</u> Void Fraction D_e/V (cm^2/s)
Air	?	1.0 to 1.2E-1
Water	100	1.13E-5
Sand		
Fine quartz	0	6.8E-2
Building sand (1.40 g/cm ³ , 39% voids)	4	5.4E-2
Fine quartz	8.1	5.0E-2
Fine quartz	15.2	1.0E-2
Fine quartz	17	5.0E-3
Soils		
Granodiorite	?	4.5E-2
Yucca Flats ⁽¹¹⁾ (25% voids)	?	3.6E-2
Metamorphic rock	?	1.8E-2
Granite	?	1.5E-2
Loams	?	8.0E-3
Varved clays	?	7.0E-3
Mud (1.57 g/cm ³)	37.2	5.7E-6
Mud (1.02 g/cm ³)	85.5	2.2E-6
Concrete, 5% voids ⁽¹²⁾		3.4E-4

CHAPTER 1 REFERENCES

1. "Phase II - Title I Engineering Assessment of Inactive Uranium Mill Tailings, Vitro Site, Salt Lake City Utah;" GJT-1; FB&DU; Apr 1976.
2. "Phase II - Title I Engineering Assessment of Inactive Uranium Mill Tailings, Shiprock Site, Shiprock, New Mexico;" GJT-2; FB&DU Mar 1977.
3. G.E. Harrison; "The Thermal Diffusion of Radon Gas Mixtures;" University of Birmingham; 1942.
4. G.E. Harrison; "The Diffusion of Radon Gas Mixtures;" University of Birmingham; 1938.
5. E.M. Kovach; "Meteorological Influences Upon the Radon-Content of Soil-Gas;" Transaction, American Geophysical Union; 26; No. II; 1945.
6. B.J. Giletti and J.L. Kulp; "Radon Leakage from Radioactive Minerals"; Columbia University; 1954.
7. S.L. Jaki and V.F. Hess; "A Study of the Distribution of Radon, Thoron, and Their Decay Products Above and Below the Ground;" Fordham University; 1958.
8. H.B. Evans; "Factors Influencing Permeability and Diffusion of Radon in Synthetic Sandstones;" University of Utah; 1959.
9. H.W. Kraner, G.L. Schroeder, and R.D. Evans; "Measurements of the Effects of Atmospheric Variables on Radon-222 Flux and Soil-Gas Concentrations;" The Natural Radiation Environment; J. A. S. Adams and W. M. Lowder, eds; University of Chicago Press; 1964.
10. Allen B. Tanner; "Radon Migration in the Ground: A Review;" The Natural Radiation Environment; J.A.S. Adams and W.M. Lowder, eds.; University of Chicago Press; 1964.
11. H.W. Kraner, G.L. Schroeder, and R.D. Evans; "Annual Progress Report to AEC;" MIT-952-4; 1967.
12. M.V.J. Culot, H.G. Olson, and K.J. Schiager; "Effective Diffusion Coefficient of Radon In Concrete Theory and Method for Field Measurements;" Health Physics; 30; p. 263; Mar 1976.
13. K.J. Schiager; "Analysis of Radiation Exposures on or Near Uranium Mill Tailings Piles;" Radiation Data and Reports; 15; No. 7; Jul 1974.

14. M.V.J. Culot, H. G. Olson, and K.J. Schiager; "Radon Progeny Control in Buildings;" Colorado State University; Fort Collins, Colorado; May 1973.
15. "Environmental Statement Related to the Operation of the Bear Creek Project;" Rocky Mountain Energy Company; NUREG-0129; Jan 1977.
16. P.J. Macbeth, et al.; "Laboratory Research on Tailings Stabilization Methods and Their Effectiveness in Radiation Containment;" Department of Energy Report GJT-21; Apr 1978.

CHAPTER 2

EXPERIMENTAL PROCEDURES AND EQUIPMENT

Two basic sampling techniques, using Lucas cells and charcoal canisters, were employed in this study to determine radon gas concentrations and radon fluxes. Similar techniques have been used previously and reports of the procedures used are available.⁽¹⁻⁴⁾ Modifications of these techniques were used for the present experimental arrangement, and these modifications are described below.

2.1 RADON CONCENTRATION DETERMINATION USING LUCAS-TYPE CELLS

Early experiments to determine the effects of radiation on man led to the development of the Lucas cell for measuring small amounts of alpha-active radon gas.⁽³⁾ The Lucas cell, a bell-jar-shaped container coated on the interior wall with silver activated zinc sulfide, is filled with air containing radon gas. When alpha particles from radon and radon daughters strike the zinc sulfide it emits photons some of which pass through a clear window in the bottom of the cell and are detected by a photomultiplier (PM) tube. The PM tube produces current pulses that are counted by the appropriate electronics.

Two standard cells of different manufacture were used in this study. The first, a standard commercial Lucas cell, had an effective volume of 100 ml and an average overall counting efficiency of 83%. The second type of cell was made by project personnel by coating the interior walls of a 125 ml Erlenmeyer flask with activated zinc sulfide. Cells constructed in this manner were approximately 40% efficient. With the addition of a reflective aluminized mylar covering as shown in Figure 2-1, the overall efficiency was increased to approximately 81%. All types of cells were fitted with stopcocks through which the cells could be evacuated and the gas samples introduced.

2.1.1 Sampling and Counting of Radon Gas

Sampling of radon gas is accomplished with a Lucas cell that has been evacuated using any typical vacuum pump capable of attaining absolute pressures of approximately 10 to 50 microns. The gas sample is then introduced into the cell through an A/E-type Gelman filter to avoid obtaining extraneous counts from alpha active airborne particulates. The cell is stored after sampling while the radon gas comes to secular equilibrium with its radioactive daughter products through ^{210}Pb , usually for 3 to 4 hr. The gross alpha activity of the cell is then measured with the counting system described in paragraph 2.1.2 and the

(1) See end of chapter for references.

concentration is calculated using the equation given in paragraph 2.1.3. Postcounting evacuation and flushing using aged dry air is performed to reduce the amount of radon daughters which attach to the walls of the cell and increase the background in the cell.

2.1.2 Electronic Counting Equipment

The Lucas cells were counted using a 7.6-cm diameter PM tube connected to a Ludlum 2200 Scaler/Timer. The efficiencies determined for the cells included losses in the PM tube and counting circuitry. Figure 2.1 shows the scaler/timer, 7.6-cm PM tube, a commercial Lucas cell and project-made cells. The scaler/timer is equipped with variable threshold, high voltage and amplifier gain settings. Using a Lucas cell containing radon gas as a source for the PM tube, these settings were varied to obtain an appropriate operating point in the plateau response region where small voltage variations do not alter the counting rate. Consistency of the counting efficiency was checked periodically using a ^{232}Th standard alpha source on a scintillation disk in the PM tube chamber.

2.1.3 Determination of the Concentration from Alpha Counting

After secular equilibrium of the radon daughters has been achieved, the total alpha particles counted in a detector during a time interval t to $t + \Delta t$ is given by

$$C_o = \epsilon A_o \int_t^{t+\Delta t} e^{-\lambda t} dt = \frac{\epsilon A_o}{\lambda} [e^{-\lambda t} - e^{-\lambda(t+\Delta t)}] \quad (1)$$

where

A_o = initial radon activity (pCi)

C_o = counts measured in the counting time Δt (counts)

Δt = counting period (hr)

t = elapsed time since sampling (hr)

λ = radon decay constant (hr^{-1})

ϵ = the detector efficiency

Solving for the initial radon activity gives

$$A_o = \frac{\lambda C_o}{\epsilon [e^{-\lambda t} - e^{-\lambda(t+\Delta t)}]} \quad (2)$$

Dividing by the volume of the sampling cell, the initial radon activity concentration is found to be

$$A = \frac{A_0}{V} = \frac{C_0 \lambda}{\epsilon V [e^{-\lambda t} - e^{-\lambda(t+\Delta t)}]} \quad (3)$$

where

V = the volume of sampling cell (l)

A = initial radon activity concentration (Ci/l)

1.33×10^{14} converts from disintegrations per hour to curies

2.1.4 Determination of Radon Surface Fluxes Using Lucas Cells

Radon surface fluxes over vegetative material were determined by using an accumulator drum sampled with Lucas cells as described by Wilkening.⁽⁴⁾ A relatively large volume container has its open end sealed to the surface across which the flux is to be measured. The initial radon gas concentration in this accumulation drum is the ambient background value. As time passes, the surface flux causes an increase in the radon concentration in the air in the drum. The increase in concentration is linearly proportional to the surface flux until the concentration becomes high enough to inhibit the flux by reduced concentration gradient from the soil gas to the air. Sampling the gas in the drum every 20 min through a sample port allows calculation of the flux using the times involved, the volume of the drum, and the buildup of radon concentration, by the relationship:

$$J = \frac{C V}{A t} \quad (4)$$

where

J = radon surface flux (Ci/m²s)

C = radon gas concentration above background (Ci/l)

V = accumulation drum volume (l)

A = area across which the flux measured (m²)

t = time between sealing the drum to the surface and time the sample is taken (s)

The sampling time must be short compared with the half life of radon and the time it takes for the change in concentration gradient to affect the flux.

2.1.5 Accuracy of Cell Measurements

The accuracy of the Lucas cell measurements is directly related to the counting statistics and the effective volume sampled. Inaccuracies in the volume sampled can also come from incomplete evacuation of the cell before sampling or from termination of the sampling procedure before the gas pressure has come to equilibrium. Careful sampling techniques can reduce inaccuracies to counting statistics only.

The lower limit of detection of the Lucas cell measurements has been reported as approximately 1 pCi/l with long counting times and low backgrounds.⁽⁶⁾ The accuracy and precision of the method are reflected in several repeated determinations of cell efficiencies reported by Percival⁽⁷⁾ where the standard deviation of the efficiency was determined to be +1.2% for many cells and +6% for determinations on individual cells using standard radium solutions for calibration. Repeated efficiency measurements on this project indicate a precision of about +10% for the cells produced by FB&DU.

2.1.6 Lucas Cell Efficiency

Lucas cell efficiencies for cells used in this study were determined using the deemanation method described by Percival.⁽⁷⁾ Figure 2-2 shows the experimental arrangement. A radon bubbler is filled with a standard solution of radium in HCl acid with an activity of 9.77×10^{-7} mCi radium. The evacuated cell is attached to the system, and stopcock 1 is opened. Stopcock 2 is slowly opened and the solution allowed to froth slowly until the system comes to equilibrium. The starting time of deemanation is recorded. Stopcock 3 is opened slightly until the level of the bubbling liquid is approximately 2 in. above the natural level of the liquid. As the pressure equalizes, the frothing decreases, and stopcock 3 may be opened slowly until it is open completely to atmospheric pressure. Deemanation is allowed to continue until only a few small columns of bubbles are rising through the solution. All stopcocks are then closed and the time is recorded. The cell is then allowed to achieve radioactive equilibrium before counting, approximately 3 to 4 hr; it is then counted for 1 hr.

The Lucas cell efficiency is then calculated as follows:

$$\epsilon = \frac{1.004 C}{4.0 \times 10^{14} (1 - e^{-\lambda t_1}) (e^{-\lambda t_2}) 0.99 Ra (V)} \quad (5)$$

where

1.004 = factor to correct for decay of ^{222}Rn during a 1-hr count

C = net cph of sample minus net cph of blank corrected to same time as sample count

4.00×10^{14} = alpha dph/Ci of ^{222}Rn and its daughters

Ra = activity of the standard solution (Ci/ml)

λ = disintegration constant for ^{222}Rn (hr^{-1})

t_1 = time between deemanations allowing for ingrowth of ^{222}Rn in the radium solution (hr)

t_2 = time between completion of deemanation and start of 1-hr count (hr)

0.99 = radium yield

V = volume of the standard solution (ml)

Once several cell efficiencies have been determined in this manner, the efficiencies of other cells can be determined by cross-comparison; sampling a large volume of known concentration with a few cells and comparing the results. The cells' efficiency, as determined by the above methods, for this study were found to be $81\% \pm 6\%$.

2.2 RADON FLUX MEASUREMENTS USING ACTIVATED CHARCOAL CANISTERS

The following paragraphs concerning determination of the precision and accuracy of charcoal canisters were performed as part of an earlier Department of Energy study, GJT-21, (4) and they are given here for completeness. Activated charcoal has been recognized and used as an effective means of trapping radon gas. (1,2) Activated charcoal canisters of the U.S. Military M-11 and M-3 types have been used for radon flux measurements in this study. These canisters are displayed with the counting system in Figure 2-3. The canister on the left had part of the metal housing removed to increase the area for flux measurements. This type of canister has been used by the Health and Safety Laboratory (HASL) (1) and works satisfactorily.

2.2.1 Use of Charcoal Canisters for Flux Measurements

Basically, the activated charcoal in the canister absorbs the radon gas that emanates from the surface over which the canister is placed. The radon is held by the charcoal and subsequently decays. After exposure to the radon-emitting surface, the canister is stored for a minimum of 3 hr for equilibrium to be established between radon and its short-lived daughters. Then gamma-rays from the canister are counted using a well-shielded NaI detector and a pulse height analyzer (PHA) system to determine the integrated peak area for a specific

gamma-ray energy. The flux is then calculated as described in Section 2.2.2.

The precision of the method of determining the radon flux across the surface, by using activated charcoal canisters to accumulate radon gas, has been investigated and is discussed in paragraph 2.2.4. This method gives reliable flux measurements with a precision of approximately 15%. Accuracy is also on the order of 15%.

2.2.2 Determination of the Radon Flux Using the ^{214}Bi 0.609-MeV Gamma Ray

After equilibrium has been achieved, the activity of each radon daughter in the canister is equal to the radon activity; hence, the activity of the ^{214}Bi 0.609-MeV gamma ray is proportional to the radon activity. The 0.609-MeV gamma ray is relatively free of interfering radiation, providing easy determination of the peak area. The 0.609-MeV gamma radiation was detected using a 12.7- x 12.7-cm NaI detector and the Tracor Northern PHA system. The PHA system has the capability of determining net peak areas.

The flux is calculated from:

$$J(\text{Ci}/\text{m}^2\text{s}) = \frac{C \lambda^2}{\epsilon A (1 - e^{-\lambda t_2}) [e^{-\lambda(t_3 - t_2)} - e^{-\lambda(t_4 - t_2)}]} 3.7 \times 10^{10} \quad (6)$$

where

C = net observed counts

λ = radon decay constant (sec)

t_2 = time since start of exposure to radon flux (sec)

t_3 = time since start of exposure to start of count (sec)

t_4 = time since start of exposure to radon flux to end of counting interval (s)

A = area of canister exposed to radon flux (m^2)

ϵ = efficiency (counts/disintegration)

3.7×10^{10} converts disintegrations per second to curies

2.2.3 Canister Cross Calibration

To determine the detection efficiency of the counting system used for the project, several canisters were exposed to uranium mill tailings in test chambers for varying lengths of

time and for different activity levels. The canisters were counted on the 12.7 x 12.7 cm NaI detector at least once before being shipped to the HASL for counting on their previously calibrated system. The canisters were then returned to Utah and counted several times subsequently.

The counting data are shown in Figure 2-4. An apparent radon half-life of 80 hr (instead of the expected 92 hr) is observed. This variation is probably due to radon redistribution within the charcoal in the canister and to leakage from the canister.

Based on the flux determinations provided by HASL, the detection efficiency for the 0.609 MeV gamma peak from ^{214}Bi was determined for each canister and is shown in Table 2-1. Efficiencies were determined using both the actual and the observed apparent half-life of radon in the canister. The 80-hr value narrowed the spread in observed efficiency. The efficiencies obtained from the first counts taken after exposure of the canisters (3 hr after exposure) minimize the differences. These values were averaged for use in the remaining measurements since most counting does take place shortly after exposure. Table 2-1 summarizes the pertinent data, including the HASL flux measurements.

2.2.4 Precision of Canister Data

Measurements have also been performed to check the precision of the canister measurements. Seventeen canisters were placed on a large area source within a 2-ft diameter. The canisters were exposed for 2 hr and counted after 3 hr to allow equilibrium to be established. The measurements yielded a flux of 16.5 pCi/m²s with a standard deviation of 1.9 pCi/m²s. This deviation corresponds to 12% fluctuation in the flux values, assuming that the flux was actually constant over the large source. Allowing for other variations in counting and canister uptake yields a precision of about +15% for all measurements.

2.3 MONITORING MOISTURE WITH A RESISTANCE-TYPE PROBE

An alternating current probe was developed to monitor moisture in tailings and cover material. The caustic nature of the tailings and some cover materials precluded the use of a direct current resistance type probe because of the enhanced corrosion and plating effects which alter the probe geometry and resistance characteristics. To overcome these effects, a probe with a 50% duty cycle at 60 Hz was developed.

2.3.1 Monitor and Probe Construction

In order to carefully measure the water content of the soils used for tailings cover materials, it was necessary to design a specific piece of equipment to provide conductivity

measurements within the range of interest. The conductivity measurement equipment consists of a probe unit, AC resistance measuring unit and AC digital voltmeter as outlined in Figure 2-5. The AC digital voltmeter unit used is a Fluke Model 8020A, which operates from batteries to provide portability. This battery operated unit was also designed to work from the output of the AC resistance measuring box which consists of a 120 Hz pulse generator driving a CMOS flip-flop to provide a 50% duty cycle square wave output at exactly 60 Hz. The power supply voltage for the CMOS flip-flop was derived from a center-tapped 11.2-V mercury battery to provide good voltage regulation. The output of the flip-flop was fed through a 22.5K 1% accurate resistor to the probe unit as outlined in Figure 2-6. The voltage generated across the resistor was measured by the DVM. The bipolar nature of the output signal provides freedom from DC polarization of the electrodes, while the 60-Hz output signal allows simple bench reproduction of these measurements from an AC power source.

The moisture probe was designed using a probe and ring construction to allow easy penetration when forced into soil without opening voids in the soil. Materials used are No. 304 stainless steel and acrylic plastic for the probe insulator. The dimensions of the various parts are detailed in Figure 2-7. The probe head built as outlined was attached to a length of butyrate plastic tubing which acts as a handle. The combination of the stainless steel construction and alternating current applied to the probe provides a very corrosion resistant device with stable electrical characteristics.

2.3.2 Probe Calibration

A series of tests were run to determine the repeatability of measurements among the 24 probes which were constructed. Each unit was placed in an identical location in a gallon of test solution of fixed salinity, using common sodium chloride as the salt. Conductivity measurements using salt concentrations from zero (distilled water) to high concentrations were made of all 24 probes, and the results summarized in Figure 2-8. As can be seen from the figure, the characteristics of the probes are nearly identical.

A concern was felt as to the effect of the volume of material surrounding the probe, and its effect on the absolute accuracy of the measurements. A test was therefore run to determine the moisture content versus resistance for two different volumes of material contained in a spherical glass container and containing various amounts of water as a percentage by weight of the surrounding material. These results are presented in Figure 2-9 for representative materials.

For moisture contents less than 5% and greater than 20% the effect of volume is negligible, while in the range of 10% to 20% moisture, the measure and voltage can be in error as much as

40%. In explanation, it is assumed for small moisture contents (less than 5%) the detector is less sensitive and for moisture contents greater than 20% the electrical path is essentially becoming a short circuit and the sampling volume is very small. In the midrange, the moisture may not make as good a contact with the probe and the measured voltage would become very path dependent.

To overcome this problem during the experiments, care was taken to ensure the use of finer particle sized material around the probe and with complete compaction to ensure good contact with the probe.

Calibration of the probe in the specific materials to be used in the moisture experiments was performed and is given in Figure 2-10.

A calibration was performed for both the Powder River Basin clay and the Shirley Basin clays used with both showing essentially exponential behavior between 5% and 30% moisture. The exceptional point at 25% moisture for the Shirley Basin clay was probably due to non-uniform compaction around the probe and the data point was ignored when calculating moisture content of the clay. In each case an exponential was fit to the data and the equation used to calculate moisture content from the experimental voltage readings. The fit obtained for the Powder River clay gave

$$\% \text{ Moisture} = \frac{1}{0.148} \ln \frac{10.755}{V}$$

where V = the moisture meter voltage in volts. The corresponding equation for the Shirley Basin clay was

$$\% \text{ Moisture} = \frac{1}{0.139} \ln \frac{11.201}{V}$$

The r^2 (i.e. correlation coefficient squared) was 0.985 and 0.992 for the Powder River and Shirley Basin clay respectively. The two equations are in good agreement but do indicate other properties of the soil besides the moisture affect the probe.

2.3.3 Use of the Moisture Meter

Before each measurement of soil conductivity, the open circuit and short circuit voltage output of the AC resistance box was measured, to ensure proper battery voltage. The probe to be measured was then connected to the input of the AC resistance box. The measurement was made, and referred to the calibration chart for determination of moisture content. Using No. 20 wire, probe-to-measurement equipment distances of 100 ft are permissible for deep soil measurements.

2.4 EMANATING POWER MEASUREMENTS OF URANIUM MILL TAILINGS

Emanating power is defined as that fraction of radon produced in some mineral matrix which escapes the matrix and is free to diffuse in the pore spaces. This parameter is used in models to predict radon exhalation from tailings and cover material. Values of the emanating power of uranium ores range from 1% to 91%. The emanating power is dependent on many parameters such as porosity, particle size, mineral species, radium mineralogy, etc.⁽⁸⁾ Emanating powers of approximately 20% have been used to model radon sources from western sites.⁽⁹⁾

The principal method used to determine the emanating power is described by Scott et al.⁽¹⁰⁾ Dry uranium mill tailings were deemanated by evacuating in a bell jar to free the radon gas. This produced no size separations and samples were otherwise untreated in any respect. The tailings were then sealed in a can to trap all radon that emanates from the material. After allowing equilibrium of the radon daughters to be established, the can of tailings was analyzed to determine the initial activity, A_0 , using a NaI detector and a pulse height analyzer, as described in paragraph 2.3. Waiting 30 days allows the radon to grow back into complete equilibrium with its radium progenitor. The additional amount of radon, A_1 , is equal to the amount that had been removed previously from the tailings by deemanation. The percent emanating power of the uranium tailings is then given by:

$$\% \text{ Emanation} = 100 \times \left(1 - \frac{A_0}{A_\infty}\right) \quad (20)$$

where

A_0 = initial activity

A_1 = radon activity deemanated

A_∞ = $A_1 + A_0$ the activity after 30 days

A modification of this procedure was used. The activity was determined at several times after deemanation and the resulting data were fit by the method of least squares to the equation:

$$\text{Activity} = A_0 + A_1(1 - e^{-\lambda t}) \quad (21)$$

to determine the parameters A_0 and A_1 . Using these best fit parameters gives:

$$A_\infty = A_0 + A_1 \quad (22)$$

and the emanating powers can be determined.

To determine the emanating power, several specimens of each sample were made and the emanating power determined.

2.5 COLLECTION AND HANDLING OF THE SELECTED COVER AND TAILING MATERIALS

The cover and tailings materials were both collected during the early winter after a moderate snow storm. The ground was exposed and some increase in moisture content of the clay was probable. In each case, personnel from the operating mills suggested the cover material to be taken, indicating that it was their choice for use in stabilizing the tailings.

At each location three 55-gal containers were obtained of each cover material. The containers were then sealed and maintained in a sealed condition until experimental personnel were ready for their use. No other treatment or handling of the cover material was performed. Compaction of the material for the experiments was performed by loading 10 to 15 cm of soil and then tamping the soil in place. Because of physical restrictions in the laboratory, heavy and cumbersome machinery for compaction could not be used.

The tailings samples were obtained in 5-gallon buckets and also sealed until needed. Samples of each tailings material were taken for sieve analysis, radium content, and emanating power measurements.

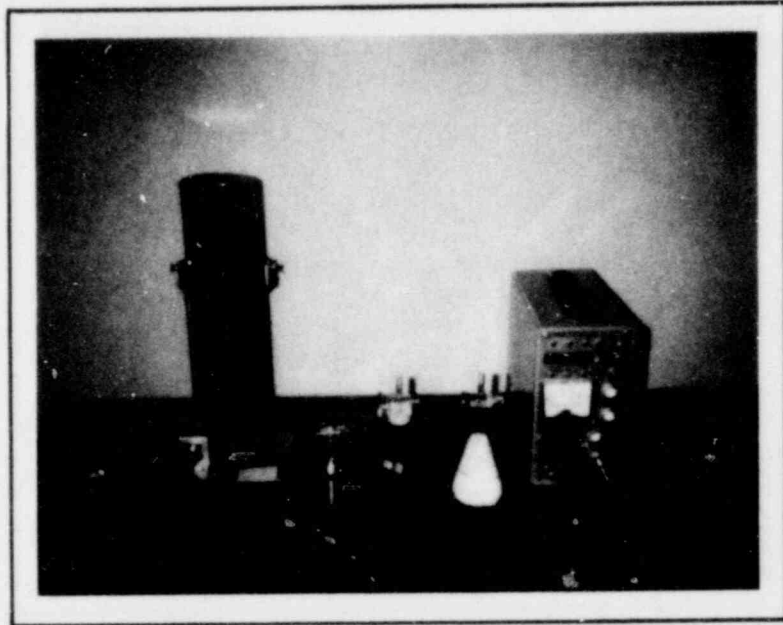


FIGURE 2-1. LUCAS CELLS AND ALPHA PARTICLE COUNTING ELECTRONICS

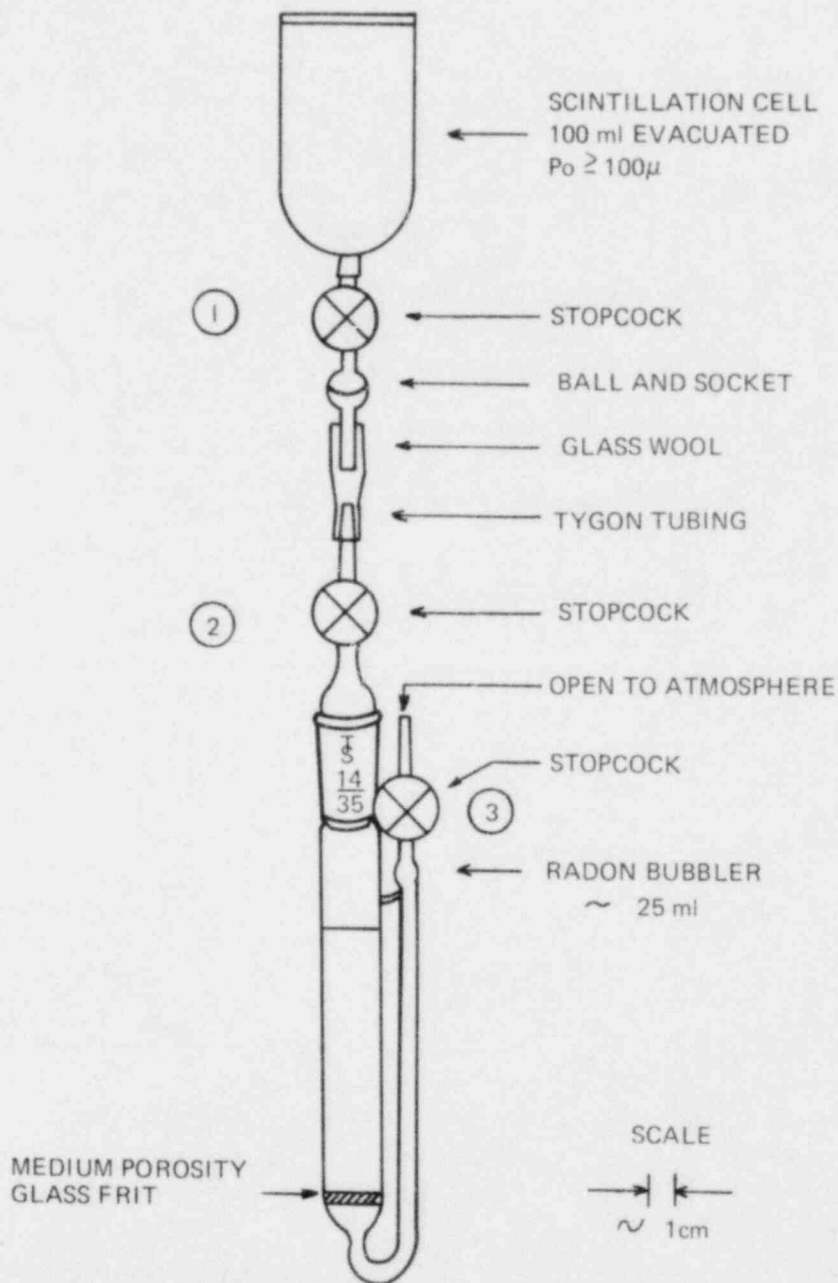


FIGURE 2-2. SCHEMATIC OF DIRECT DEEMANATION SYSTEM

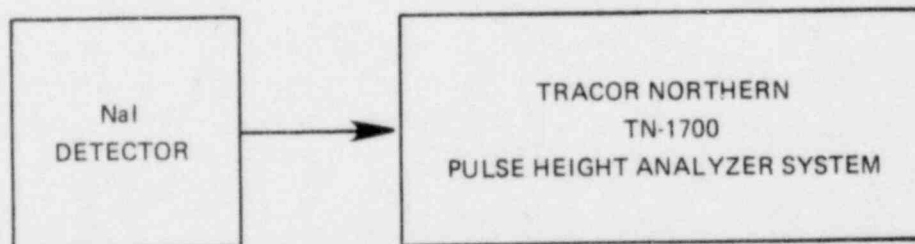


FIGURE 2-3. M-11 CHARCOAL CANISTERS AND BLOCK DIAGRAM OF ELECTRONIC COUNTING SYSTEM

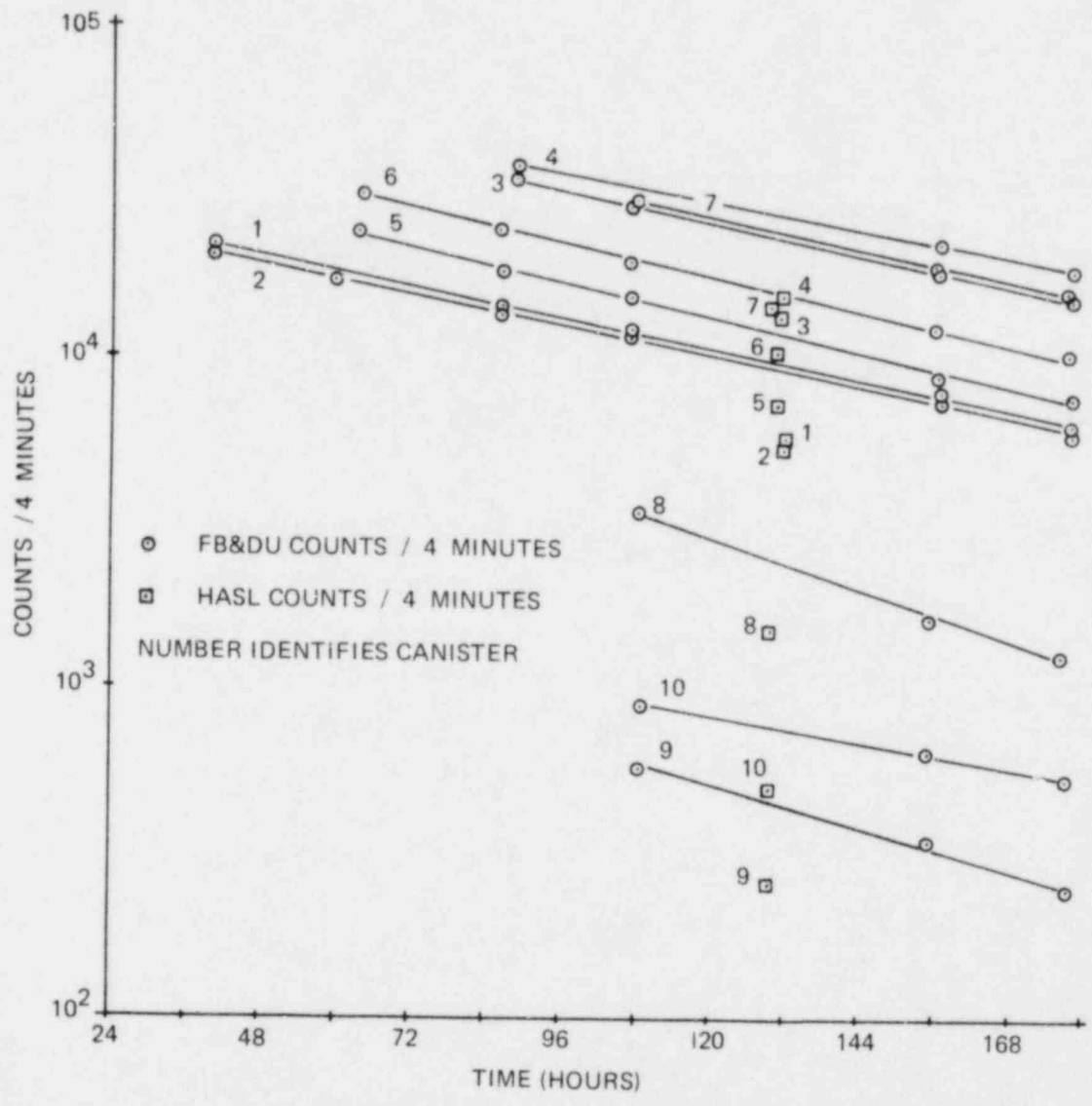


FIGURE 2-4. CHARCOAL CANISTER CALIBRATION DATA

POOR ORIGINAL

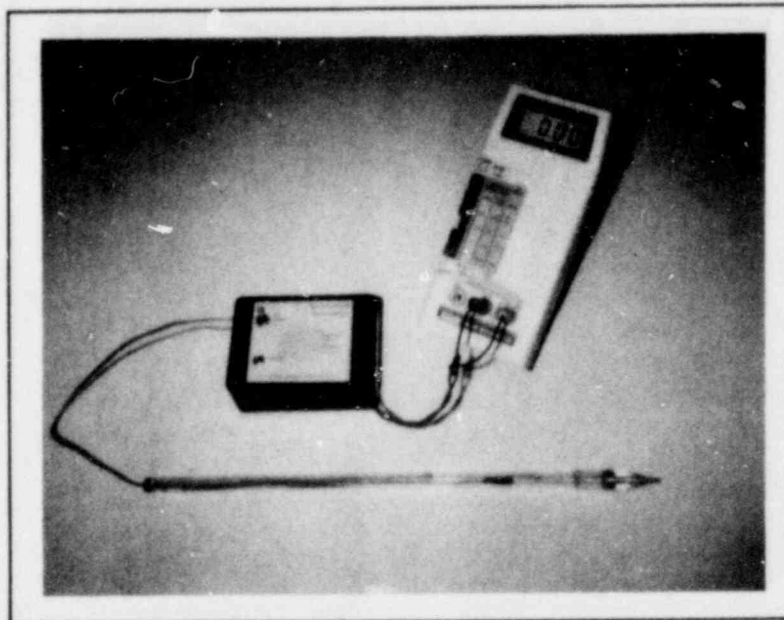


FIGURE 2-5. MOISTURE MONITOR AND PROBE

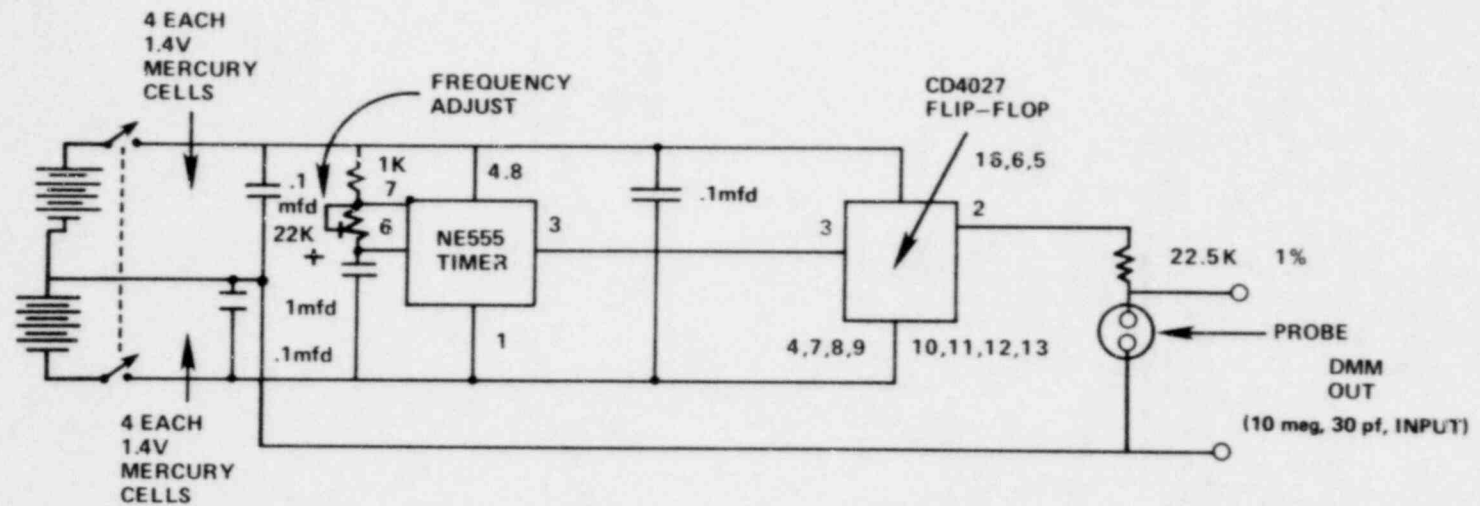
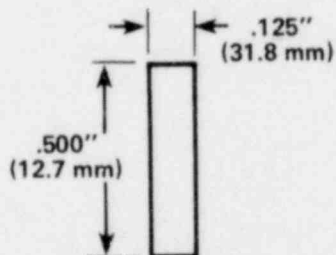
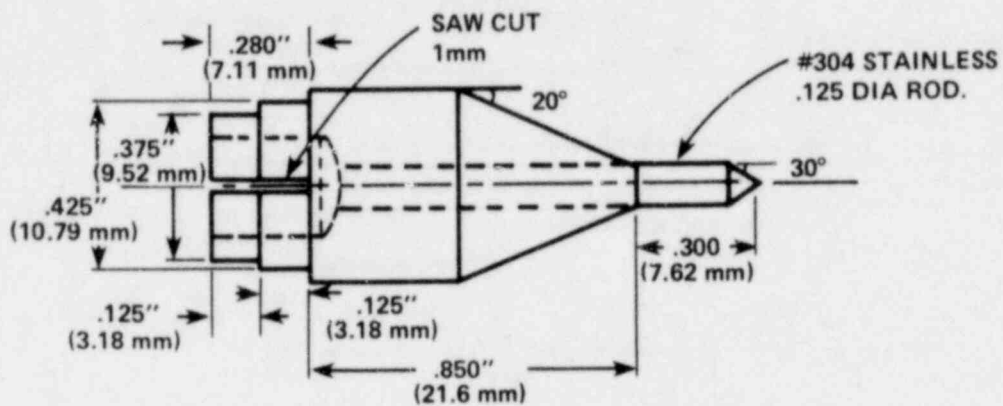
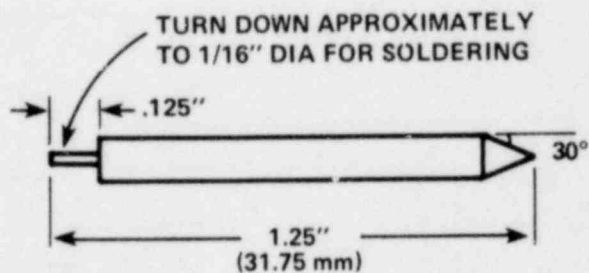


FIGURE 2-6. SCHEMATIC DIAGRAM, MOISTURE METER



RING CONTACT
 .035" WALL
 .500 O.D.
 #304 STAINLESS
 TUBING



PROBE CONTACT
 .125 DIA
 #304 STAINLESS ROD.

FIGURE 2-7. MOISTURE CONTACT WATER PROBE

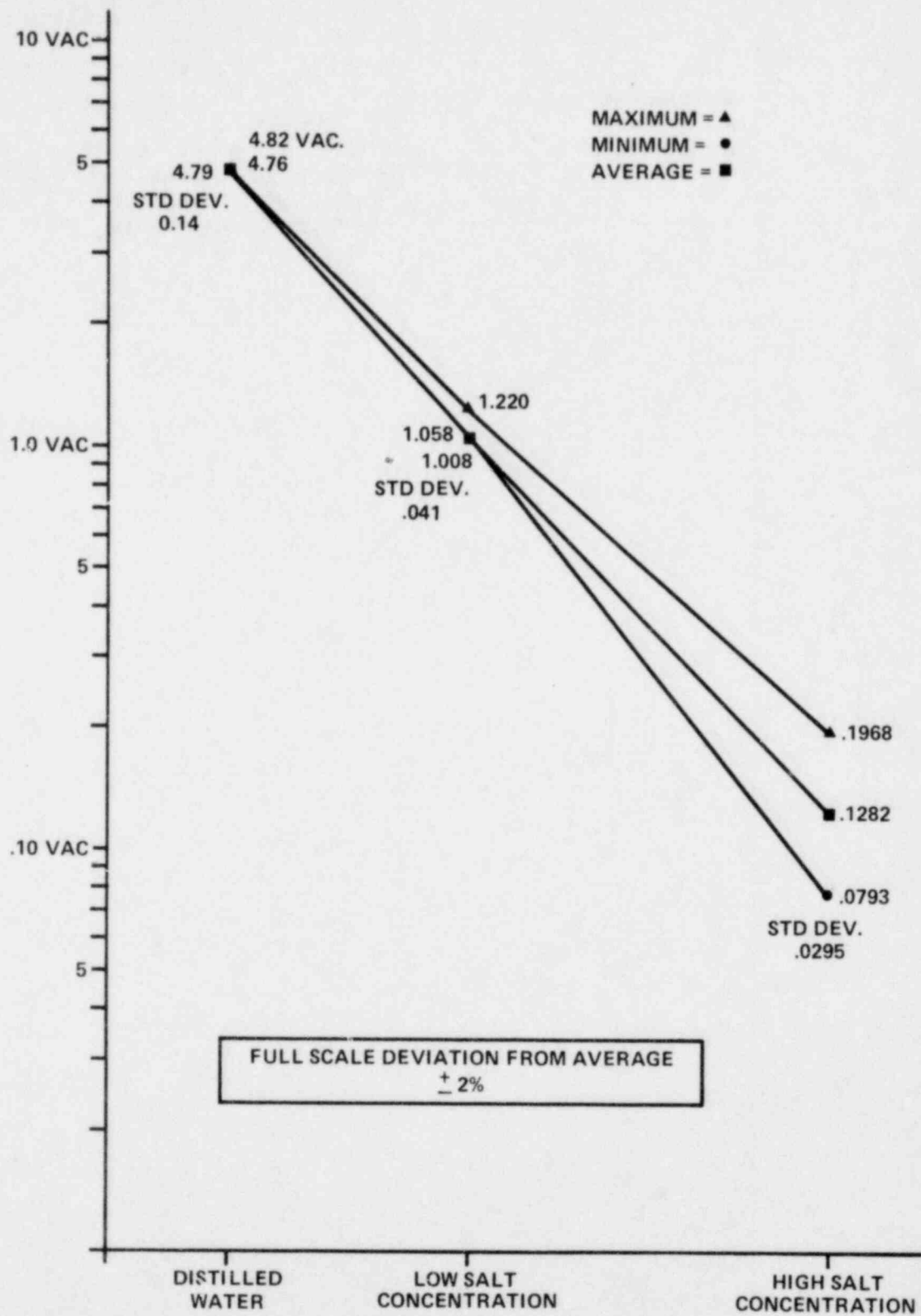


FIGURE 2-8. PROBE DEVIATION FROM UNIT TO UNIT

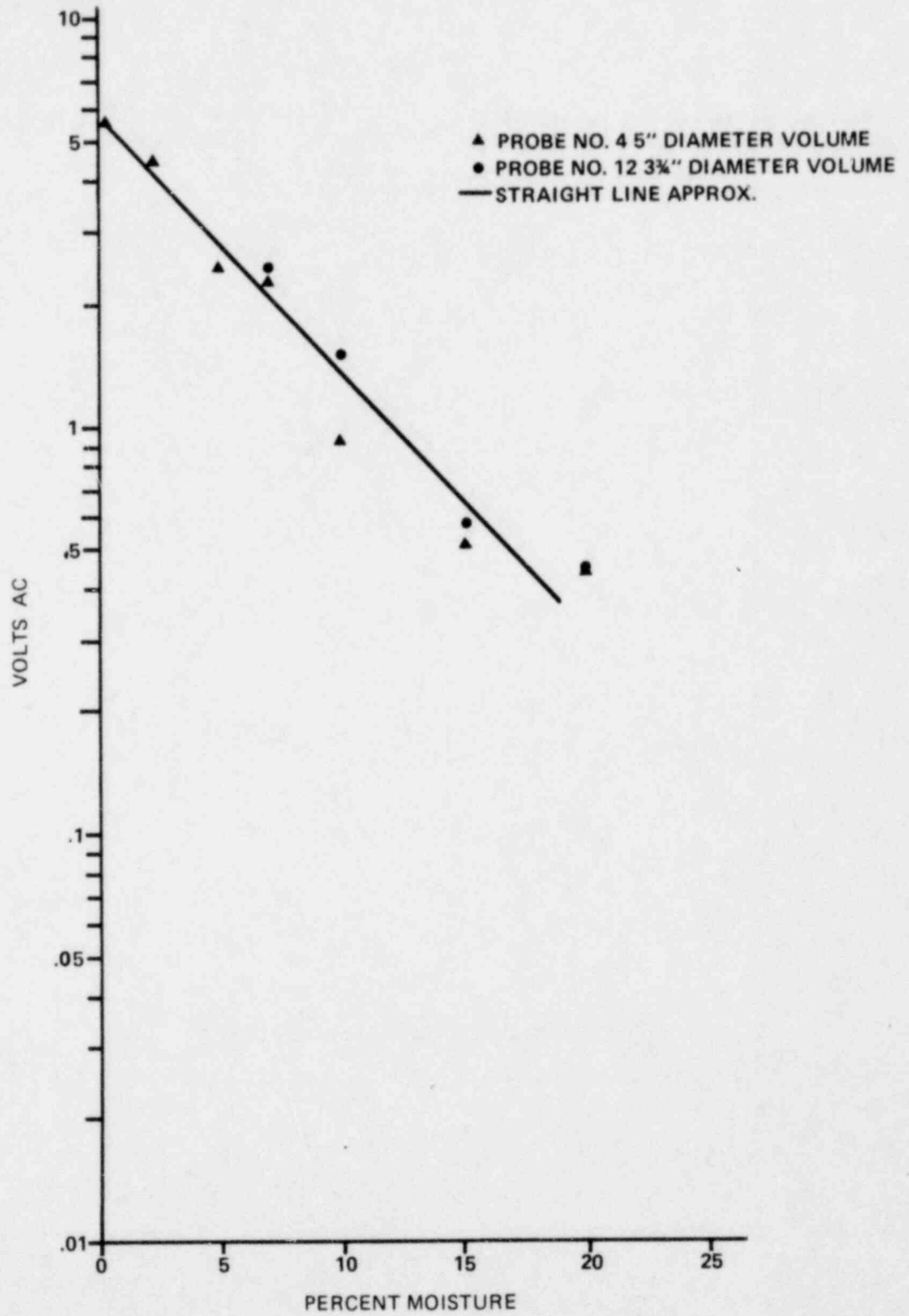


FIGURE 2-9. CALIBRATION DATA AND COMPARISON OF ACTIVE SENSING VOLUMES

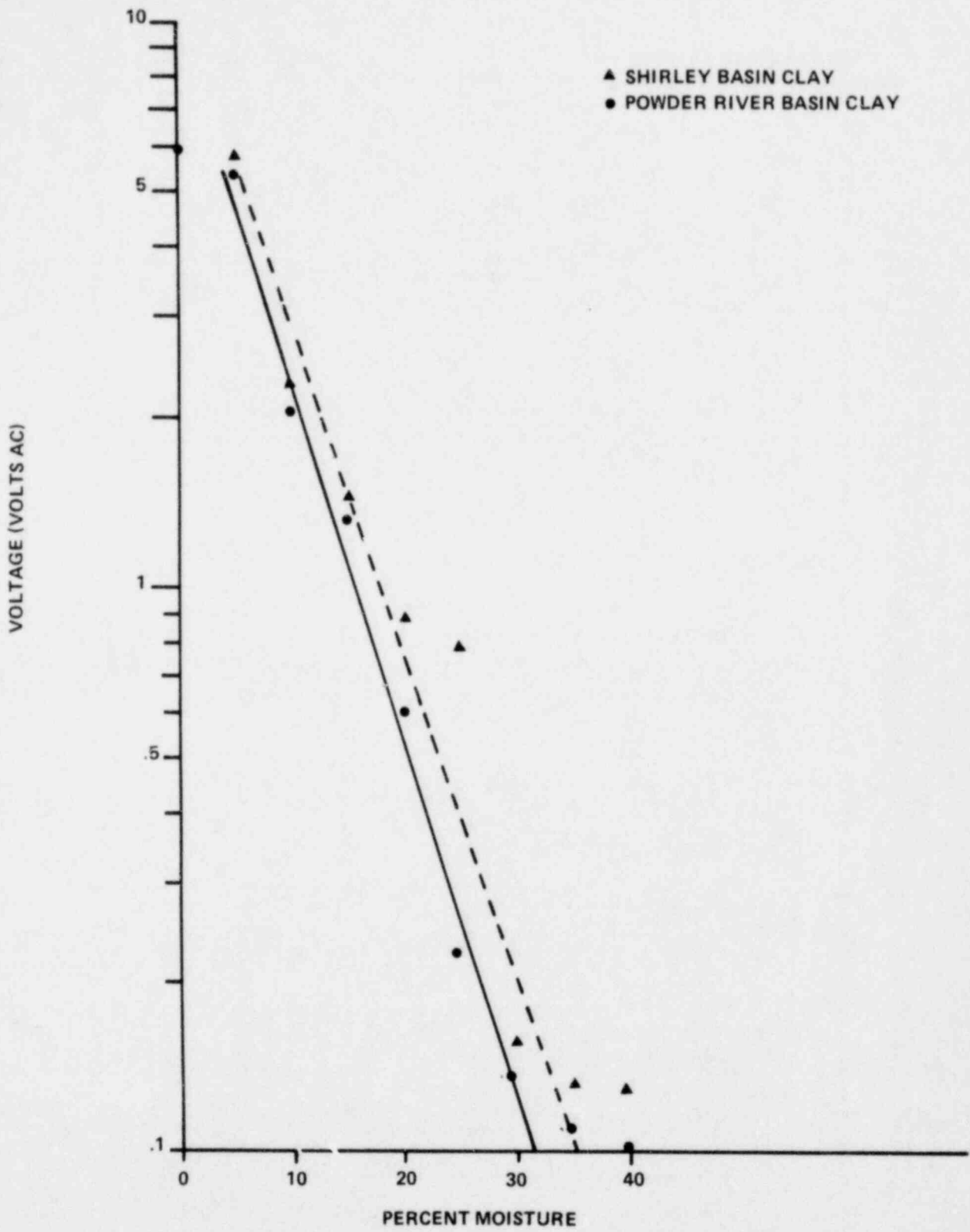


FIGURE 2-10. CALIBRATION IN POWDER RIVER AND SHIRLEY BASIN CLAYS

TABLE 2-1

CANISTER CALIBRATION DATA

Canister and Count	Exposure Times		Count Times		Net Counts in 609KeV Peak	Apparent Efficiency(%)		HASL Flux (fCi/cm ² ·s)
	Start	Stop	Start	Stop		92 hr Tl/2	80 hr Tl/2	
1-1	15:40	36:10	41:04	41:08	21624	3.25	2.88	12.9
1-2	15:40	36:10	60:07	60:11	17678	3.06	2.77	12.9
1-3	15:40	36:10	86:19	86:23	14553	3.08	2.87	12.9
1-4	15:40	36:10	107:35	107:39	12027	3.08	2.85	12.9
1-5*	15:40	36:10	132:15	132:25	14146	--	--	12.9
1-6	15:40	36:10	157:25	157:29	7828	2.83	2.85	12.9
1-7	15:40	36:10	178:37	178:41	5991	2.54	2.62	12.9
2-1	15:40	36:10	40:57	41:01	21527	3.41	3.02	12.2
2-2	15:40	36:10	60:14	60:18	17331	3.18	2.88	12.2
2-3	15:40	36:10	86:30	86:34	13426	3.00	2.80	12.2
2-4	15:40	36:10	107:17	107:21	11397	2.98	2.84	12.2
2-5*	15:40	36:10	132:00	132:10	13484	--	--	12.2
2-6	15:40	36:10	157:19	157:23	7718	2.94	2.75	12.2
2-7	15:40	36:10	178:31	178:35	6340	2.84	2.93	12.2
3-1	15:40	85:41	88:56	89:00	34466	3.01	2.73	7.64
3-2	15:40	85:41	107:11	107:15	28683	2.88	2.66	7.64
3-3*	15:40	85:41	131:40	107:50	33317	--	--	7.64
3-4	15:40	85:41	157:13	157:17	18548	2.71	2.66	7.64
3-5	15:40	85:41	178:24	178:28	15241	2.62	2.62	7.64
4-1	15:40	85:41	89:02	89:06	38639	2.79	2.53	9.25
4-2	15:40	85:41	107:29	107:33	33276	2.77	2.56	9.25
4-3*	15:40	85:41	131:20	131:30	39581	--	--	9.25
4-4	15:40	85:41	157:06	157:10	22358	2.70	2.64	9.25
4-5	15:40	85:41	178:18	178:22	18789	2.66	2.67	9.25
5-1	15:40	60:00	63:31	63:35	23983	3.29	2.94	7.05
5-2	15:40	60:00	86:44	86:48	18521	3.02	2.78	7.05
5-3	15:40	60:00	107:23	107:27	15323	2.92	2.75	7.05
5-4*	15:40	60:00	131:05	131:15	18136	--	--	7.05
5-5	15:40	60:00	156:43	156:47	8886	2.45	2.45	7.05
5-6	15:40	60:00	178:12	178:16	7656	2.50	2.54	7.05

TABLE 2-1 (Cont)

CANISTER CALIBRATION DATA

Canister and Count	Exposure Times		Count Times		Net Counts in 609KeV Peak	Apparent Efficiency(%)		HASL Flux (fCi/cm ² ·s)
	Start	Stop	Start	Stop		92 hr Tl/2	80 hr Tl/2	
6-1	15:40	60:00	64:01	64:05	31163	3.02	2.71	9.99
6-2	15:40	60:00	86:38	86:42	24388	2.80	2.58	9.99
6-3	15:40	60:00	107:41	107:45	19795	2.67	2.51	9.99
6-4*	15:40	60:00	130:45	130:55	25426	--	--	9.99
6-5	15:40	60:00	156:11	156:14	12569	2.44	2.43	9.99
6-6	15:40	60:00	178:06	178:10	10437	2.39	2.44	9.99
7-1	15:40	105:35	108:35	108:39	29820	2169	2.46	6.16
7-2*	15:40	105:35	130:30	130:40	37126	--	--	6.16
7-3	15:40	15:35	156:22	156:26	18756	2.42	2.34	6.16
7-4	15:40	105:35	177:44	177:54	39034	2.37	2.34	6.16
8-1	86:10	105:27	108:43	108:47	3406	3.27	2.89	2.11
8-2*	86:10	105:27	130:15	130:25	3722	--	--	2.11
8-3	86:10	105:27	155:21	155:31	4179	2.28	2.12	2.11
8-4	86:10	105:27	176:53	177:03	3243	2.08	1.99	2.11
9-1	86:14	105:24	108:49	108:53	578	2.95	2.60	0.40
9-2*	86:14	105:24	129:40	129:50	629	--	--	0.40
9-3	86:14	105:24	155:09	155:19	872	2.53	2.35	0.40
9-4	86:14	105:24	177:10	177:20	593	2.03	1.93	0.40
10-1	86:14	105:24	108:55	108:59	899	2.86	2.53	0.64
10-2*	86:14	105:24	130:00	130:10	1236	--	--	0.64
10-3	86:14	105:24	154:56	155:06	1553	2.80	2.61	0.64
10-4	86:14	105:24	177:26	177:36	1345	2.88	2.75	0.64

Average Efficiencies

Average of All Measurements

2.79_±0.32 2.62_±0.24

Average of 1st Count for Each Canister

3.05_±0.24 2.73_±0.20

* HASL Counts

CHAPTER 2 REFERENCES

1. R.J. Countless; " ^{222}Rn Flux Measurement with a Charcoal Canister;" *Health Physics*; Vol 31; p. 455; 1976.
2. K. Megumi and T. Mamura; "A Method for Measuring Radon and Thoron Exhalation from the Ground;" *Journal of Geophysical Research*; Vol 77; p. 3052; 1972.
3. H.F. Lucas; "A Fast and Accurate Survey Technique for Both Radon-222 and Radium-226;" The Natural Radiation Environment; J.A.S. Adams and W.M. Lowder, eds; University of Chicago Press; 1964.
4. P.J. Macbeth, et al.; "Laboratory Research on Tailings Stabilization Methods and Their Effectiveness in Radiation Containment;" U.S. Department of Energy Report GJT-21; Apr 1978.
5. Wilkening and Hand; "Radon at the Earth-Air Interface;" *Journal of Geophysical Research*; Vol 65; No. 10; Oct 1960.
6. A.J. Breslin; "Monitoring Instrumentation in the Uranium Mining Industry;" unpublished report; AEC; HASL; 1972.
7. D.R. Percival; ERDA Health Services Laboratory, Idaho Operations Office; private communication; 1976.
8. S.R. Austin; "A Laboratory Study of Radon Emanation from Domestic Uranium Ores;" *Radon in Uranium Mining*; IAEA-PL-565/8; 1975.
9. K.J. Schiager; "Analysis of Radiation Exposures on or Near Uranium Mill Tailings Piles;" *Radiation Data and Reports*; EPA; Vol 15, No. 7; July 1974.
10. J.H. Scott and P.H. Dodd; "Gamma-Only Assaying for Disequilibrium Corrections;" RME-135; *Geology and Mineralogy*; Apr 1960.

CHAPTER 3

GEOLOGY AND SOIL MECHANICAL PROPERTIES OF THE SELECTED COVER MATERIALS

Geologically, the major uranium deposit areas in the United States are located in the Colorado Plateau of the western U.S. between the Southern Rocky Mountains and the Great Basin and Range Province.⁽¹⁾ These major deposits exist in the States of Wyoming, Utah, New Mexico and Colorado. Major known deposits and mining operations also exist in South Texas in the Gulf Coast Area of the Coastal Plain Province. Figure 3-1 shows the major areas in relation to the general physiography of the U.S. More specifically, divided into regions by state, the uranium deposit areas of Wyoming exist in the northern portion of the Colorado Plateau (Wyoming Basin) between the Southern Rocky Mountains on the east and the Big Horn Range of the Northern Rocky Mountains to the west. The known major uranium deposits are located in the Powder River Basin, Shirley Basin, Gas Hills, and the Red Desert Region, north, south, west and southwest of Casper, Wyoming, respectively. The locations of the basins deposits are shown in Figure 3-2.

The uranium deposits of New Mexico are located primarily in the Southern Colorado Plateau: in northwestern New Mexico in an area known as the Grants Mineral Belt as shown in Figure 3-3.

In Colorado and Utah, the major uranium deposits are contained primarily in the Paradox Basin area of the Central Colorado Plateau Region as shown in Figure 3-4.

Figure 3-5 illustrates the locations of the major uranium districts of Texas which are situated in the southern portion of the state primarily in the west Gulf Coastal Plain region.

The major uranium deposit areas of the western United States are described in more detail as to geologic occurrence, bedrock classification, major structural features, general ore deposits, hydrologic conditions, soil overburden characteristics and the soil sampling/testing program in the following sections. (As part of the project study, overburden soil samples were taken for laboratory analysis in the Powder River and Shirley Basins and in the Gas Hills Region of Wyoming, and from the Grants Mineral Belt of New Mexico.)

3.1 POWDER RIVER BASIN - WYOMING⁽²⁾

The Powder River Basin is a structural basin open to the north; and bounded on the south by the Laramie Range and the

(1) See end of chapter for references.

Hartville Uplift; on the east by the Black Hills, and on the west by the Big Horn Mountains and the Casper Arch. The Basin comprises an area of nearly 12,000 mi². All the major uranium deposits are found in the Tertiary rock formations. Most of the important uranium deposits are in the Wasatch and Fort Union Formations. (See Table 3-1 and Figure 3-6.)

The basin began taking shape in the late Cretaceous time owing to several uplifts and widespread deposition into the Paleocene. The Fort Union Formation (early Paleocene) consists of soft shales and sandstones (mainly fine-grained clastics). Interbedded wedges of coarse-to-fine sand (ancient alluvial fans) are characteristic of the Fort Union Formation. Dark gray carbonaceous shales exist between these arkosic sand units within the finer grained Fort Union Formation. The carbonaceous shales correlate with several coal beds in the northern portion of the basin. Heavy mineralization is found in the coarse facie units located between the Fort Union and the unconformably overlying Wasatch Formation. Also, the Fort Union coarse sands may be the source of uranium mineralization in other parts of the Basin. These sediments are found at dips of near 6 degrees.

Additional structural deformation and uplift of major mountain blocks seen today occurred during the close of Paleocene time. Large amounts of coarse clastics, forming large fans and braided stream deposits, were formed during the Eocene. Also, several coal beds were formed indicating inactive swamps and low cycles of sediment deposition. Major contributing streams from the southern Laramie Mountains and Hartville Uplift caused erosion left deposits of continuous sediment which formed the passageways and allowed deposition of the mineralized uranium solutions being mined today.

The mineralized sandstone units range from 10 to over 200 ft in thickness, from 1 to 30 mi in length, and from a few hundred feet to a few miles wide. Smaller sand units exist as isolated lenses or pods and in roll-front type deposits.⁽³⁾ It is common for the main sandstone units to be separated by 100-200 ft of silts and claystones. Degradation of the area continued throughout the Eocene. During the Oligocene, Miocene and Pliocene vast thicknesses of sandstone and tuffaceous (weathered and fine-grained volcanics) sediments accumulated. After considerable volcanic activity, uplift and moderate to severe erosion by stream action, the area has been reduced to the low relief and highly eroded surface topography of today.

Specifically, uranium deposits are found throughout the Powder River Basin contained in the coarse-grained fluvial arkosic sandstone units. The deposits represent several stratigraphically separate units usually existing in a widespread vertical zone from 1,200 to 1,400 ft thick, especially in the Wasatch Formation. The sandstones are locally separated by gray-to-black carbonaceous shales, siltstones and claystones. It is these fine-grained sediments that are being removed and

discarded as mining overburden/waste which has the potential use as a tailings cover material.

Some of the mining also occurs in the shallow near surface formations of the upper Fort Union and Box Creek Formations where similar coarse sand and fine shale sediments exist, only with generally thinner bedding and more interbedding relationships.⁽⁴⁾ This makes selection of uniform tailings cover materials difficult. However, most areas in the Basin are believed to contain adequate amounts of suitable tailings cover materials. But specific areas will differ as to type, quantity, thickness and stratigraphic position within the deposit.

The sandstone units containing the mineralization usually exhibit high permeability and transmissivity values. Corresponding values for the interbedded and/or overlying shales are generally low.

Generally, groundwater conditions in the basin are controlled by a regional asymmetrical syncline which causes the general flow gradient to trend north-northwest. Locally, shallow aquifer flow is controlled by discharge and recharge within and along the drainages into the alluvial deposits. Recharge is through precipitation, springs and wells. Discharge would be from evaporation, transpiration and well pumpage. Water levels in the alluvium is shallow ranging between 5 and about 25 ft, and is usually concordant to stream channel flow. The Wasatch Formation, which underlies most of the basin, comprises the upper bedrock aquifer and includes both confined (artesian) and unconfined flow/storage conditions depending upon location and depth. Water quality is in the calcium sulfate class with TDS ranging from less than 200 to more than 8,000 mg/l.

Considerable alteration has occurred in the deposits and many zones of variable mineral concentration exist. The mineral deposition and subsequent alteration has resulted primarily in the high occurrence of sulfates, even though relatively high amounts of chromium, selenium, manganese, pyrite, and hematite are present. Primary uranium ores identified are uraninite and vanadium with a host of associated oxide minerals.

Soils in the basin range between weathered and altered shale, sandstone, siltstone and claystone bedrock to fine-to-coarse alluvial sands, silts, and clays. Gravels are not common but do exist locally where harder rock materials occur. As many as 43 different soil types have been identified in the Basin by the U.S. Soil Conservation Service.⁽⁵⁾

Complete classification of these soils and information as to gradation, density, permeability, thickness, origin and erosion/runoff potential is available in varying forms of completeness. Generally, surface soils are thin (1-3 ft) except in drainages where some thicker (5-20 ft) accumulations occur;

they are sandy loam with moderate to low permeability; they have medium density (less than 100 lb/ft³); and they have originated from weathering/alteration of nearby up gradient surface bedrock formations. The soils are usually easily strippable and contain vegetation (sage brush, low grasses, etc.) with root systems extending from 0.5 to 1.5 ft. Most of the soils support rangeland and wildlife habitat at a 2.5 acre per animal ratio.⁽⁵⁾ Surface runoff is moderate as is the erosion rate, except in major drainages where dry-wash conditions usually exist as an intermittent or ephemeral streams but change to brief, swift flowing streams during periods of rainfall and snow melt runoff. Considerable scour and cutting can and usually does result during these periods of accelerated erosion. Again, it must be noted that soil conditions change locally and characteristics will differ from the typical examples discussed here. Overall, the natural soils and residual (weathered bedrock) soils found in the basin seem to have suitable characteristics to be used as tailings cover material. As mentioned, however, due to the variability, site-specific studies would have to be made to determine suitability of existing soils.

Selected clay and sandy soils were sampled by FB&DU and analyzed by an independent soils laboratory. Results of the tests are included in the Appendix A. Tests performed included sieve analysis, liquid limits, maximum density, recompacted density and permeability.

Test results of March 6, 1978 (Appendix A) showed the soils (S-2) to be a silty fine to medium sand (SM) having an optimum moisture content of 15.0% and a maximum dry density of 112.0 lb/ft³. Liquid/plastic limit tests showed the soil to be nonplastic. Significantly, permeability tests indicated a value range as follows:

<u>% Compaction</u>	<u>% Collapse</u>	<u>10⁻⁶ cm/s</u>
75.1	13.5	358
84.8	8.5	90.1
90.0	2.0	31.5

As can be noted, the permeability rate and percent collapse are almost directly proportional to the percent compaction (maximum density). The tests were performed at a constant surcharge loading of 500 lb/ft². Obviously, compaction of the soil cover materials would result in a thinner layer of cover material dependent upon the degree of compaction.

Test results of March 6, 1978 also showed the clay soils (C-2) to be a silty clay with some fine sand (CL). Maximum density of the clay was reported as 107 lb/ft³ with an 18% optimum moisture content. The clay was found to have a liquid limit of 33.8 with a plasticity index of 14.6. Permeabilities/collapse were again proportional to the percent compaction and

ranged between 23 and 83×10^{-6} cm/s permeability. Surchage loading was increased to 1,000 lb/ft² to compensate for higher head pressures and percent compaction of fine-grained embankment soils. It should be noted that even though the clay soils have lower permeability rates, they are also more susceptible to shrinkage and cracking when allowed to dry, thus allowing percolation of surface runoff waters. The properties of the Powder River Soils used for the set 2 radon experiments are summarized in Table 3-2.

In conclusion, the Basin typically can be expected to contain: from 0-30 ft of alluvial soils in major drainages; from 0-5 ft of residual surface soils; moderate to low permeability and low potentiometric gradient due to overall fine grained sediments; slow movement of groundwater and moderate surface runoff; uranium deposits contained in the Wasatch and Fort Union Tertiary sandstone formations with depths ranging between 0-30 ft (Wasatch) and 30-400 ft (Fort Union); groundwater existing as confined (artesian) and unconfined at depths between about 25 and 1,000 ft; TDS range from 500-1,000 mg/l and associated concentrations of heavy metals (selenium, iron, chromium, and manganese).⁽⁶⁾ Overall quantity and quality of soil overburden as potential tailings cover is good at specific locations but would have to be transported at others. Overburden is available as mine waste or can be stripped with adequate provisions for reclamation. Soils range in the clayey loam to sandy shale classification and exhibit suitable characteristics for placement and compaction as cover materials under controlled engineering specifications.

3.2 SHIRLEY BASIN - WYOMING

The Shirley Basin⁽⁷⁾ of Wyoming is located south of Casper, covers four counties and comprises four geographic units: the Shirley Basin, Bates Hole, Bates Creek drainage, and the Laramie Mountains (see Figure 3-7). The Basin is structural/stratigraphic controlled containing rocks in age from Precambrian to Quaternary. It is an area of low to moderate relief with perennial streams draining all four subareas. The Precambrian rocks are found in the Laramie Mountains and exist as metasediments and intrusive granitic batholiths and mafic dikes. Current exposure is in the core of the mountains. Paleozoic sediments are fully represented in the Basin and consist of a thick series of marine, littoral and continental sediments comprising limestones, sandstones, shales, mud, silt, and claystones.

Coarse clastic deposits originating from the higher elevations were deposited in the Basin during late Cretaceous times. Some folding and faulting of these sediments have occurred, and a syncline trends southeastward through the western part of the area. The sediments dip from 2-12 degrees southwest on the eastern limb of the syncline with flatter dips on the western limb. Doming that occurred in later Tertiary

time accounts for the current approximate 1 degree dip of exposed sediments. The few localized displacements are due to associated faulting.

The uranium deposits of the Basin are of major significance and at one time constituted about 1/6 of the nation's supply. The deposits are found in the Wind River Formation of early Eocene age. They consist of two thick sandstone intervals separated by silt and claystone beds. (See Table 3-3.) The deposits are classified as roll-front (large tongues of altered sandstone) and exist at the Basin margins with more tabular layers at the top and bottom zones. As in the Powder River Basin, the uranium deposits exist in coarse arkosic sandstones separated by softer shales which, as waste, could be utilized as a source of tailings cover material. Uraninite is the only identified ore mineral but accessory minerals such as pyrite, marcasite, calcite, hematite, selenium, beryllium, and vanadium also exist.

Ground water conditions in the Basin indicate that the watertable lies from less than 20 ft to 100 ft or more below the surface. The hydraulic gradient is to the south at about 10-30 ft/mile. Information from dewatering efforts by mining operations indicate that the water is contained in the ore bearing sandstones. Ground water flow is also reported in overlying aquifer beds and as perched zones. Moderate to high permeabilities and transmissivities are reported indicating good interconnection within and between sandstone aquifers. Ground water quality studies⁽⁷⁾ show that the principal anions are sulfate and bicarbonate; radioelements include uranium, radium and radon. The average pH is approximately 7.7.

Soils in the Basin consist primarily of clay and sandy loams. Some 8-10 major classifications have been identified which range in thickness from 0-60 in. The soils are found as thin layers on ridge and low relief erosional surfaces and as thicker sections in the major depressions and drainages. Most of the natural soils have originated from sedimentary bedrock deposits. Residual soils (weathered bedrock) exist where surface outcrops occur in loosely consolidated shales and fine grained, poorly cemented sandstones. Surface erosion and runoff are moderate to severe depending upon topographic relief. Ephemeral and intermittent drainages experience brief, but high volume flow during periods of rainfall and snow melt runoff. Permeability of these soils is generally low, owing to their fine-grained nature.

Interbedded shales above and within the mineralized zone possess soil-like characteristics due to their low level of lithification. These sediments constitute overburden waste material during mining operations and should be considered as having the highest potential for use as tailings cover material. The sediments are mostly fine-grained clay and siltstones that could be easily stripped and would be suitable

borrow material for placement and compaction. Currently these sediments are stockpiled as waste deposits near the mining operations. Table 3-4 shows the relative thicknesses, depths and lithologic description of the bedrock materials of the Wind River Formation found in the Shirley Basin.

Alluvial soils also exist throughout the basin. Older alluvium, as much as 30 ft in thickness, exists in parts of the basin as fine-grained eroded-stream dissected deposits. Younger alluvium is now being deposited by streams as flood-plain deposits and channel fill. Most of the deposits are fine-grained material derived from the soft Tertiary rocks in the upper drainage basins. Some highly cemented coarser grained soil sediments exist as topographically high areas due to their high silica matrix and resistance to weathering. Origin of these deposits is from pre-Tertiary siliceous sediments. These sediments would not make suitable cover material due to their more permeable nature, higher resistance to stripping, lesser quantity and more sporadic and nonuniform occurrences.

Similar laboratory test analyses were conducted on the Shirley Basin soils as were conducted on those from the Powder River Basin. Detailed results of the tests are contained in the Appendix A. In general, the test results (March 6, 1978) showed that the soils (S-1) are classified as silty clays with trace fine-to-coarse sand. An optimum moisture content of 26% and a maximum density of 94 lb/ft³ were reported. The liquid limit was found to be 64.2, and a plasticity index of 36.7 was determined. Permeability ranged between 0.13 and 635 x 10⁻⁶ cm/s at a uniform surcharge loading of 500 lb/ft². It should be noted that the percent fines (less than 200 sieve-silt/clay fraction) strongly affects the permeability level--the higher the fines content, the lower the permeability. Therefore, to select suitable cover materials, site-specific studies should be conducted using select soils to evaluate important parameters such as permeability, density and compactive feasibility. Properties of the Shirley Basin soils used for the set 2 radon experiments are summarized in Table 3-2.

3.3 GAS HILLS - WYOMING(8)

The Gas Hills area is located west of Casper as shown in Figure 3-2. The area is within the southeastern portion of the Wind River Basin along the western flank of the Dutton Basin Anticline, which plunges northwest exposing rocks of Precambrian through Tertiary Ages. The uranium deposits are generally found in the Eocene Wind River Formation, a two-member unit containing fine-grained siltstones and mudstones in the lower member, and coarse-grained poorly sorted arkosic sandstones and pebble conglomerates in the upper member. Total thickness of the formation is near 750 ft. The Wind River formation lies unconformably over the steeply dipping Cretaceous and Jurassic sediments which outcrop to the west and east of the basin

forming the Gas Hills. Table 3-5 illustrates the stratigraphic relationship in the area.

The Cody Shale (Cretaceous) exists at the surface in some areas of the basin and acts as a retention unit where tailings pond systems are located.⁽⁹⁾ The shale is very fine grained, consisting of mostly thin inter-bedded sandstones, siltstone and grey to black shales. However, these sediments do not occur in the thicknesses or easily strippable positions as do the somewhat comparable sediments in the Powder River Basin or Shirley Basin which can be used as tailings cover material. At most areas in the basin the Cody is found at depths well below the surface.

The present surface drainage pattern is locally variable but generally follows the northwestern trend of the Dutton anticline.⁽⁸⁾ There are no perennial streams or lakes in the area except for those caused by tailings discharge streams and ponds. Most streams are intermittent, flowing only in response to spring runoff and rainfall.

Ground water conditions in the basin also vary locally but again are generally controlled by the anticlinal feature. Area gradient is reported to be northwesterly with local variances common in relation to drainage pattern characteristics. Recharge is mainly from precipitation along the eastern flank of the basin and from the eroded portions of the water-bearing strata of the anticlinal structures. Ground water occurs primarily under unconfined water table conditions but occurrence of artesian (confined) flow in the Wind River formation has been noted. Depth to water ranges between 30 and 200 ft with an average gradient of 90 ft/mi.⁽⁸⁾ Shallower occurrences of ground water could be expected in alluvial sediments within drainage basins and valleys. Four bedrock formations have been identified as containing water-bearing aquifers: the Wind River (Tertiary, Eocene), Cloverly-Morrison (Cretaceous), Phosphoria (Permian) and the Tensleep Sandstone (Pennsylvanian).

Water quality is generally in the calcium sulfate range and usually very hard. High amounts of radioactivity are reported in uraniferous-bearing formations and in the Cloverly Formation. High amounts of sulfate and fluoride were reported in the Tensleep Formation.⁽⁸⁾

Soil conditions at the site vary locally with 10 different series identified. Table 3-6 illustrates the characteristics of the soils found near the center of the basin at the Lucky Mc mining operation. Twenty-six soils are strongly calcareous and are classified as clay loam, fine sandy loam and silty clay loam. Surface-occurring siltstones, sandstones and claystones have soil-like characteristics where residual weathering has occurred.

As part of the field sampling program, soil samples were

taken in the Gas Hills for comparison with soils in other mining districts of Wyoming. The samples were tested by an independent laboratory and results are included in Appendix A. Test results for the report dated February 6, 1978 indicated that the soil (S-3) was in the SC/CL (sandy, fine-to-medium clay) classification range and had a liquid limit of 39.2, a plastic limit of 19.1, and a plasticity index of 20.1. Samples tested for permeability varied between 4.70×10^{-6} and 75.7×10^{-6} cm/s at 89.4 and 74.4% compaction, respectively. Soil (S-4), being much coarser and nonplastic, exhibited much higher values of permeability (2.190×10^{-6} - 6.640×10^{-6} cm/s) at a similar surcharge load pressure of 500 lb/ft². The S-4 soil was classified as a fine-to-medium sand with some silt (SP/SM).

Of the clay samples tested, sample C-3 had a liquid limit of 37.2, a plastic limit of 20.3, and a plasticity index of 16.9. The soil was classified as a sandy fine-to-medium clay (CL/SC). Permeabilities were found to range between 2.4×10^{-6} to 21.9×10^{-6} cm/s at 90.0 and 74.9% compaction, respectively. Surcharge loading was set at 1,000 lb/ft². Clay sample (C-4) was classified as a silty clay with some fine-to-coarse sand and further classified as a highly weathered residual shale. A liquid limit of 28.7, a plastic limit of 15.2, and a plasticity index of 13.5 were also reported. Permeabilities of 0.128×10^{-6} to 0.240×10^{-6} cm/s were reported at a percent compaction of 90.0 and 75.3, respectively. Surcharge loading was similar to C-3 at 1,000 lb/ft².

In summary, it can be said that the existing soils/weathered shale readily available in the Gas Hills area are not as extensive, accessible or characteristically suitable as soils in the Powder River and Shirley Basins. Considerable more expense and effort would have to be expended in the Gas Hills to obtain cover materials as suitable as those found in the other basins. Also, it should be noted that the Powder River Basin soils are not as available or suitable as those found in the Shirley Basin.

3.4 GRANTS MINERAL BELT - NEW MEXICO

Several samples were collected in McKinley County in northwestern New Mexico in the southwestern corner of the Colorado Plateau. The sites are found on the Chaco Slope where the beds dip 2 to 5 degrees to the northeast towards the San Juan Basin. The Chaco Slope is characterized by a series of elongated valleys separated by ridges or cuestas formed by the differential erosion of the slightly tilted sedimentary rocks. Shales generally underlie the valleys and the ridges are formed from the more resistant sandstone and limestone rocks. These beds comprise a broad homocline locally modified by tertiary folds and faults. The area is characterized by associated intrusive and extrusive rocks of the Mount Taylor and Zuni volcanic fields of both Tertiary and Quarternary Ages. The beds of the Chaco Slope dip away from the Zuni Uplift

to the south. Pre-Cambrian rocks comprise the core of the Zuni Uplift, and the sedimentary beds which slope away from the core are Pennsylvanian and progressively younger. A columnar section of the exposed bedrock is shown in Table 3-7.

This area of the Colorado Plateau is in the Grants Uranium Belt Region,⁽¹⁰⁾ as seen in Figure 3-3. The belt is from 15 to 20 mi wide and extends from Gallup and the Gallup Sag in the west to the western edge of the Rio Grande Trough on the east. There are three main uranium producing areas in the belt: the Gallup, Grants and Laguna mining districts.

A sample of highly decomposed shale bedrock was obtained in the Ambrosia Lake area north of Grants. The sample was taken from a knoll just east of Phillips United Nuclear Mill in Section 28, Township 4 North, Range 9 West, New Mexico Principal Meridian at 55 deg 24 min 30 sec north latitude and 107 deg 47 min 55 sec west longitude.⁽¹¹⁾ The sample was taken in one of the northwest-southeast trending valleys. This valley is cut into the shales of the Mancos Formation of Cretaceous age.⁽¹²⁾ The older Dakota Sandstone bounds the valley to the southwest and the younger Crevasse Canyon Formation outcrops to the northeast.

The Mancos Formation consists largely of a dark gray friable silty shale with minor amounts of light brown sandstone and gray fissil shale. There are three significant sandstone layers in the lower Mancos called the Tres Hermanos. These sandstones are shaly, yellowish brown to pale yellowish gray, fine- and medium-grained sandstones. Several hundred feet of this Mancos shale bedrock prevents downward and upward migration of ground waters. Since almost 75% of the formations underlying the area are impermeable shales, most recharge to the interbedded aquifers is through outcrops. The most significant aquifer in this area is found in the underlying Westwater Canyon Member of the Morrison Formation.⁽¹³⁾ Lesser amounts of ground water occur in the Dakota Formation, Gloreata Sandstone, San Andres Limestone, Bluff Sandstone and in the sandstone layers of the Mancos Shale. All of the confined ground water moves downdip in a northeasterly direction, opposite the direction of surface drainage.

The sample site lies on a pediment that slopes southwestward from the base of San Mateo Mesa. There are several intermittent drainages from the Mesa which empty into the southeastern-trending Arroyo del Puerto, a tributary to San Mateo Creek.⁽¹⁴⁾ There is an irregular cover of Quaternary alluvium and saprolite (weathered bedrock) overlying the bedrock in this area.

In general, the alluvium is derived from the weathered Mancos Formation and consists largely of clay and silt with some clean sand and pebbles. There are isolated stringers and lenses of fine-grained, clean to silty eolian sand interbedded with

thinner coarse-grained alluvial sand, gravel and clay beds. Since the climate in this area is semiarid, this alluvium is generally dry except where recharged by mill or ion-exchange process waters. Any groundwaters that are present move to the southwest towards Arroyo Del Puerto.

Soils in this area have been classified⁽¹⁵⁾ as a Las-Lucas-Little, Persayo Association by the New Mexico Soil Conservation Service and New Mexico State University. This association occurs dominantly on gentle to strongly sloping and rolling uplands. While slopes are generally less than 10%, some of the Persayo soils have slopes up to 25%. Steep to very steep escarpments and break areas included in this association consist of shale and sandstone.

The soils are generally formed in materials weathered from gray or olive shales. They tend to be light to moderately light, calcareous and highly erodible.

A description of the soil characteristics as per Maker et al., 1974, is as follows:

"Las Lucas soils occur on gently sloping and undulating alluvial fan and valley side slopes. They typically have a surface layer of pale brown calcareous loam or light clay loam. Their subsoil consists of a yellowish-brown to brown strongly calcareous silty clay loam with a few threads and small soft masses of lime. This grades through a light yellowish-brown clay loam or light silty clay loam to the underlying shale, which commonly occurs at depths between 40 and 60 inches.

Little soils, which are also extensive in this association, occur on gently sloping and undulating uplands. They are forming in fine-textured material weathered residually from the underlying shale. The depth to shale varies from 20 to 40 inches. These soils usually have a thin surface layer of light olive-brown calcareous silty clay loam and a subsoil of light yellowish-brown clay or silty clay. Thin threads of lime and gypsum crystals are common in the subsoil immediately above the underlying shale.

Persayo soils, which are light colored and shallow, are forming on gently to strongly sloping and rolling shale ridges and knolls. They have a thin surface layer of light yellowish-brown calcareous silt loam or silty clay loam. This grades through a light yellowish-brown silty clay loam that usually contains some partly weathered shale fragments, to the underlying shale which occurs at a depth of less than 20 inches. Gypsum crystals and threads and small soft masses of lime are common in the subsurface layers."

Most of these soils are clays and silty clay loams which

are classified as CL soils under the Unified Soil Classification System, except for the top 5 in. or so of the Las Lucas soils which tend to be coarser grained and classified as ML soils. The weathered shale sample that was taken probably includes some of the above soils as well as the weathered shale. This sample was crushed for gradation analysis and was classified as a CH soil or an inorganic clay of high plasticity. Therefore, crushed samples of weathered shales from this area will yield a finer grained sample than will the associated soils which contain more of the sands derived from the sandstones present in the area.

The sample had an optimum moisture content of 28.5% and a dry density of 1.5 g/cm³. Liquid/plastic limit tests showed the soil to have a liquid limit of 70.5, a plastic limit of 29.5, and a plasticity index of 41. Permeability ranged between 0.217 and 0.320 x 10⁻⁶ cm/s at a uniform surcharge loading of 1,000 lb/ft². Properties of the Ambrosia Lake soils used for the set 2 radon experiments are summarized in Table 3-2.

Once again site-specific studies should be carried out when selecting suitable cover material, because the soils vary throughout the area. In this area weathered shale at the surface might serve as well as, or better than, the soils found here.

A soil sample was obtained for analysis from the Church Rock area, northeast of Gallup. The sample was taken from the slopes just east of the United Nuclear Corporation's Church Rocks tailings, which are in Section 2, Township 16 N, Range 16 W. The sample was taken in Pipeline Valley, a northeast-southwest trending valley system which transects the outcrops of the Chaco Slope. The sample was taken in an area of the valley which is cut into the Crevasse Canyon Formation of Cretaceous Age.⁽¹⁶⁾ This formation and the Gallup Formation are both stratigraphically above the Mancos Formation, from which the shale sample was obtained. However, these younger formations are intertongued with the Mancos Shale in this area.

The sample was taken in an area where the Dalton Member of the Crevasse Canyon Formation forms the prominent cliffs framing the Valley; the Dilco Coal Member of the formation is the immediately underlying bedrock. There are several sandstone layers in the upper part of the Dilco which may serve as minor aquifers in this area. Generally speaking, yields from the Dilco would be small and of poor quality because of the close association with coal and carbonaceous shale. Below these sandy layers approximately 110 ft of sandy and carbonaceous shales, thin lenticular sandstones and coal, also of the Dilco, separate the "Dilco Sands" from the "Gallup Aquifer." It is unlikely that there is any recharge of the Gallup in this area because of this thick sequence of impermeable beds. This aquifer is probably recharged largely farther to the south in areas where it outcrops. Groundwater also occurs in the deeper Dakota

Sandstone, Westwater Canyon Member of the Morrison Formation, San Andres Limestone and the Glorieta Sandstone. These aquifers are even further separated from overlying aquifers by interbedded impermeable formations. Recharge to all of these aquifers is largely through distant outcrops. The confined groundwater in these formations moves downdip in a north-northeasterly direction--opposite the direction of surface drainage in this vicinity. There may be some unconfined groundwater in the alluvium of the valley which would move in the direction of surface flow, to the southwest.

Surface drainage is generally from the northeast to the southwest down Pipeline Valley, a tributary drainage to the Rio Puerco River. A relatively broad floodplain is bordered by steep-sided slopes extending upwards to both the northwest and the southeast. The sample was obtained on the southeast side of the valley.

There is an irregular cover of Quaternary alluvium and saprolite overlying the bedrock in this area. In general, the alluvium is derived largely from the weathered shales and sandstones of the Crevasse Canyon and younger formations. It ranges from a few feet to over a hundred feet in depth. The soils are generally sandy and silty clays of medium plasticity with some sandy silts and silty sands.

Soils in this area have been classified as either Rockland-Travesilla associations or Lohmiller-San Mateo associations by the New Mexico Soil Conservation Service and New Mexico State University. The Rockland-Travesilla association occurs largely in areas with rough broken topography. Steep canyon walls, narrow valleys, gently sloping to rolling mesa tops and upland areas, and gently to strongly sloping alluvial fans and valley floors are all represented. A description of the two major soil types in this association is given by Maker et al., 1974, as follows:

"Rockland, which is dominant in this association, consists of a complex of shallow soils and outcrops of sandstone and other types of sedimentary rocks. It characteristically occupies the steep and very steep mesa side slope escarpments, and breaks in which ledges and stair step topography are common. The outcrops of bedrock commonly occur as vertical or nearly vertical exposures or ledges. A thin mantle of stony soil generally occurs between the ledges or outcrops of bedrock. Although shallow soils and rock outcrops are dominant, small isolated pockets of moderately deep to deep soils occur on the escarpments where benches or areas with a lesser slope gradient have formed.

Travesilla soils, which are underlain by sandstone at shallow depths, occur on gently sloping moderately steep and rolling upland areas and mesa tops. They have a thin

surface layer of light brownish-gray or light brown, slightly calcareous fine sandy loam or stony fine sandy loam. This grades through soil of similar color and texture to the underlying sandstone bedrock at depths which typically range from 8 to 12 inches, but may be as little as 4 inches or as much as 20 inches. A few small angular fragments of sandstone are common at the surface and typically become more numerous with depth."

The Rockland soils were most predominant in the area where the sample was taken. These soils are classified as SM or silty sands under the Unified Soil Classification System. It is probable that the soil we collected was a Rockland soil, which is supported by the SM classification arrived at using a gradation analysis. The soil had an optimum moisture content of 12% and a maximum dry density of 1.81 g/cm³. Liquid/plastic limit tests showed the soil to be nonplastic. Permeability ranged between 225 and 1,910 x 10⁻⁶ cm/s at a uniform surcharge loading of 500 lb/ft².

The Lohmiller-San Mateo soils are found in the valley bottoms and on flood plains and terraces adjacent to intermittent drainages. Slopes are generally less than 5%. The soils are derived largely from sandstone and shale formations. Gully erosion often occurs in the valley bottoms filled with this soil. The Lohmiller-San Mateo soils are deep, fine textured soils occurring on the nearly level to gently sloping flood plains and shales. This association is characterized by a surface calcareous loam or clay loam underlain by stratified loams, fine sandy loams, silty clay loams, clay loams and clays. These soils are classified as CL-clays of high plasticity. These soils are found at slightly lower elevations than that where the soil sample was collected. If finer material is found to be a more effective cover, it might possibly be obtained at the lower elevations.

3.5 GENERAL GEOLOGY OF OTHER URANIUM MINING REGIONS

COLORADO - UTAH

There is a concentration of uranium deposits in the Paradox Basin and the surrounding area which is found on the eastern central part of the Colorado plateau. This cratonic basin is formed by rocks of Permian-Pennsylvanian Ages. During this time the basin was bounded to the east and northeast by the Uncompahgre and San Luis uplifts, to the northwest and west by the Emery uplift, to the southwest by the Kaibab-Supai shelf, and the south by the Defiance uplift. After the Laramide Deformation the area took on its present shape (see Figure 3-4) and the San Rafael and the Circle Cliffs uplifts are on the west of the basin. The Tyende Saddle separates the Black Mesa Basin from the Paradox Basin in the southwest. The San Juan Dome or Mountains are found to the east. (17)

The Paradox Basin occupies much of southeastern Utah, southwestern Colorado, and a small part of northeastern Arizona and comprises an area of nearly 19,000 mi². It is a strongly asymmetrical basin having its thickest deposits on its northeast flank. In general the sedimentary rocks are flat to gently dipping. Steeply dipping beds are associated with the anticlines, broad monoclines and domes. The basin is characterized by nearly flat or gently sloping mesas dissected by steep canyons. There are many northwest-southeast trending faults and valleys in this basin. Surface outcrops are generally of Mesozoic Age except along the associated salt anticlines and along Monument upwarp where the Permian and Pennsylvanian rocks are exposed. The sedimentary rocks in this area include such unusual types of material as extremely thick beds of salt and gypsum, red beds of great variety, thick eolian sandstones, arkosic formations and wide-spread river accumulations. These beds reflect continental conditions and peculiar marine environments. Apparently this area has been dominated by arid and semiarid climates for long periods. Even when the sea invaded the area a powerful evaporation effect produced the extensive salt and gypsum beds.

The uranium-bearing minerals have been found in almost every rock type in the area including limestone and coal.⁽¹⁸⁾ While the deposits have been found in numerous formations, the majority of the commercial deposits are found in the sandstone beds of the Morrison Formation, of late Jurassic Age. The ores are concentrated in the Salt Wash Member of the Morrison Formation, as seen in Table 3-8.⁽¹⁹⁾

The ore seems to be contained largely in sandstone which occurs as composite lenses or channels surrounded by shale or mudstone. The proportions of sandstone and mudstone appear to be about equal in the Salt Wash Sandstone member of the Morrison. In the overlying Brushy Basin Shale the finer clastics predominate.⁽²⁰⁾ The sandstone beds of the Morrison containing the carnotite deposits are lenticular and are in places 50 ft or more thick. A minimum thickness of 40 ft of sandstone is indicated for locating favorable deposits. The presence of abundant carbonaceous material also appears to be indicative of ore-bearing sandstone. The ores generally occur in a pale to light-yellow-brown sandstone speckled with limonite stains. Also, although normally red, mudstones near ore deposits are altered to gray. The most valuable deposits have been found in the Uravan mineral belt. This belt produced over 78% of the yield from southwestern Colorado and southeastern Utah during the 1936-43 period.⁽²¹⁾ Almost all the mines producing more than 10,000 tons of ore during this time were in the Uravan mineral belt.

Most ore deposits occur in tabular deposits which parallel the bedding. Below the oxidized zones common uranium minerals are uranite or pitchblend and coffinite. These unoxidized deposits are generally associated with vanadium minerals

including montroseite and several micaceous silicates. Copper sulfides are also closely associated with the deposits. The oxidized zones contain many secondary minerals of uranium, vanadium and copper. Carnotite and tyuyamunite are the most common ore mineral where both uranium and vanadium are present. (22)

Ground water in this area is highly controlled by the various structural features in the Paradox Basin. In general however, the recharge is from the west flank of the San Juan mountains and along the west side of the Uncompahgre Uplift. The general direction of ground water is towards the southwest and the topographic lows along the Colorado River.

Water above the Pennsylvanian contains fresh to moderately saline water with relatively few cases of true brines occurring. Below the Permian, however, due to the underlying salt formation most water samples are brines of the sodium chloride type. (23) Ground water is contained under both unconfined and confined conditions in the sandstones in the basin. The principal water bearing formations are the Permian Cutler Formation, the Triassic Wingate sandstone, the Jurassic Navajo sandstone, the Cretaceous Dakota sands and Burro Canyon formations and the Quaternary unconsolidated deposits. In general, the ore beds of the Morrison do not yield water to wells. Unconfined reservoirs in the Quaternary valley deposits are important sources for water yield to wells in this area. (23) Depth to the water table is highly variable but is generally quite low due to the arid nature of the area. It is from several hundred to more than 1,000 ft below the surface in much of the region. However, in alluvium the water is often less than 50 ft from the surface. (24)

Due to the great range of relief in the Paradox Basin soil types vary greatly as do soil depths. Deposits are generally thinner on the ridges and thicker in the depressions and drainages. Colluvial and alluvial deposits get as much as 360 ft deep in some valleys where very thin residual mantles are often all that is present on the adjacent plateaus. Most of the soils of the Paradox Basin are probably soils of the great groups Torriorthents, having little or no development of pedogenic horizons. (25) Most of these valley soils are derived from the sandstone substrata in the area and could probably not be used as suitable cover material. However, residual mantle deposits on shales and siltstones are fairly deep and include high percentages of clay-size particles. These residual soils, where present, could serve as cover material. It is also possible that the shale which is interbedded in the vicinity of the ore deposits could be crushed and used as cover material. The Morrison Formation itself is predominantly made up of shales which do not generally contain very high-grade ore and are now probably disposed of as waste material during mining operations. It may be possible to use this waste material as cover material.

TEXAS

Most of the uranium deposits in Texas are found on the West Gulf Coastal Plain.⁽²⁶⁾ (See Figure 3-5.) In this area, sedimentary beds of Cretaceous and younger ages dip towards the Gulf of Mexico at rates ranging from 20 to more than 200 ft/mi. The dip of the older beds is generally slightly more than that of the younger beds. The beds run parallel to the coast and thin landward. Ridges are formed by the resistant formations and the less resistant form the valleys.

The sediments of the Gulf Coastal Plain are more folded and faulted than those of the Atlantic Plain. The domes and basins are usually accompanied by faulting which parallels the strike of the formations. In some areas the faulting, although present, is not associated with folding. Generally the block towards the coast is the downthrown block. Often these features are associated with salt plugs. However, most of the salt plugs are farther east than the areas associated with uranium deposits.

The geologic formations of the Gulf Coast are sedimentary deposits representing on-shore, near-shore and off-shore environments. The Plain was submerged during much of Cenozoic time. During the Paleocene the sea advanced and the Midway deposits were laid down. Following Midway time, deposits were laid down in lagoons and embayments, along the shore and in the sea at or near the oscillating shoreline. The sea withdrew from the area in the later part of the Tertiary and has been above sea level since then. Beds of volcanic ash and tuff were deposited at times throughout the Tertiary. Faulting and uplift of the area occurred in Pliocene time, followed by deposition of much gravel and silt. Erosion has lowered the plain to the present altitude.

The uranium is usually associated with tuffaceous sand and conglomerate, but has also been found in the silts and bentonitic clays in the area.⁽²⁷⁾ When found in the clay, the ore occurs as coatings and fillings along joint and bedding planes in the clay immediately underlying the sands. The uranium is generally associated with the upper Jackson sediments of late Eocene time; however, uranium minerals have been found in at least seven other stratigraphic positions, ranging from the late Eocene Jackson sediments to Pliocene Goliad sands.

The upper Jackson Group consists largely of tuffaceous sand interbedded with bentonitic clay. The middle and lower sections are largely clay with some interbedded sands. The largest deposits of ore are in the lower sands of the Stones Switch Member of the Whitsitt Formation (the upper part of the Jackson group). The Stones Switch Member consists of two sandstone layers separated by clay and carbonaceous siltstone. The Stones Switch Member is approximately 50 ft thick.

Ore deposits are generally from 20 to 40 ft deep. However, some zones of mineralization have been found downdip from the surface deposits at depths of 100 ft and more. The mineralization occurs largely as several varieties of yellow to greenish-yellow, oxidized uranium minerals including uranyl phosphates, arseno-phosphates, silicates, phospho-silicates, molybdates and vanadates. Some uraninite ore has been found in silty clays underlying the thickest and richest deposits. The uranyl phosphate minerals, autunite and meta-autunite are the most abundant. The mineralogy is more typical of the Wyoming oxidized near-surface deposits of Tertiary Age than of the Colorado Plateau deposits, which are high in vanadium and contain carnotite as the dominant mineral.

In Table 3-9 it can be seen that clays are present throughout the stratigraphic units in this area. In mining areas, the intervening layers of waste or the overburden might often be silts, silt clays, clays and tuffaceous and bentonitic clays which could be suitable as tailings cover material. In areas where in-situ mining is being done, the cover material could most likely be obtained from local surficial outcrops of clays or from soils derived largely from these clays.

Ground water is at or near the surface in the valleys and as much as 100 ft below the surface along the interstream divides. (28) The hydraulic gradient is to the southeast from 50-200 ft/mi. Although all the beds underlying the area are saturated, only the sandy beds yield water freely to wells. Water occurs in the ore-bearing beds of the Jackson Group as well as in the underlying and overlying beds. Water table conditions are reported in outcrop areas but artesian conditions develop further downdip where the aquifers are confined by less permeable beds. Although ground water studies show highly variable quality, water in this area is often at least slightly saline since most deposits have contained salty water because they were deposited in the sea or in brackish areas near the sea, or because the sea flooded the area shortly after deposition. Fresh water is found in outcrop areas where fresh water has had a chance to flush the salty water out. Due to the low permeability of the rocks, ground water has become alkaline and highly mineralized with sodium, calcium, silica, potassium and other soluble constituents released from the alteration of the prevalent volcanics. These conditions set up the conditions for the concentration of the uranium and associated phosphorous, arsenic, molybdenum and vanadium. Arid conditions in the late Tertiary to middle Pleistocene caused extensive caliche development and silica induration in this area often associated with other mineralization. (29)

Soils in this area are generally quite deep. Many soil types would be present in different areas dependent on the formations from which they were derived. Deposits are thinner on the ridges and rolling hills and deeper in the depressions and drainages. Almost all of the soils are derived from the

local sedimentary bedrock. Residual soils exist in most areas, especially near outcrops. Soil textures indicate that recharge to the ground water reservoir from infiltration of surface water is small.

The interbedded clays in this area will have high potential for use as tailings cover material due to their low level of lithification. Where fine-grained clays and siltstones were predominant in the soils they easily could be stripped and used as material for placement and compaction. The higher part of the area often will be covered with sand and gravel, remnants of the Uvalde gravel, so lower areas would be better areas to obtain stripable materials.

Alluvial soils also exist throughout the area. Alluvial terraces are found in areas from 20 to 50 ft above the streams. These deposits consist largely of fine sand, silt, clay and some gravel and range in thickness from 0 to 30 ft. Alluvium is presently being deposited along flood plains and in stream channels. Due to the discontinuous nature of these deposits they would not be as reliable as sources of cover material.

POOR ORIGINAL

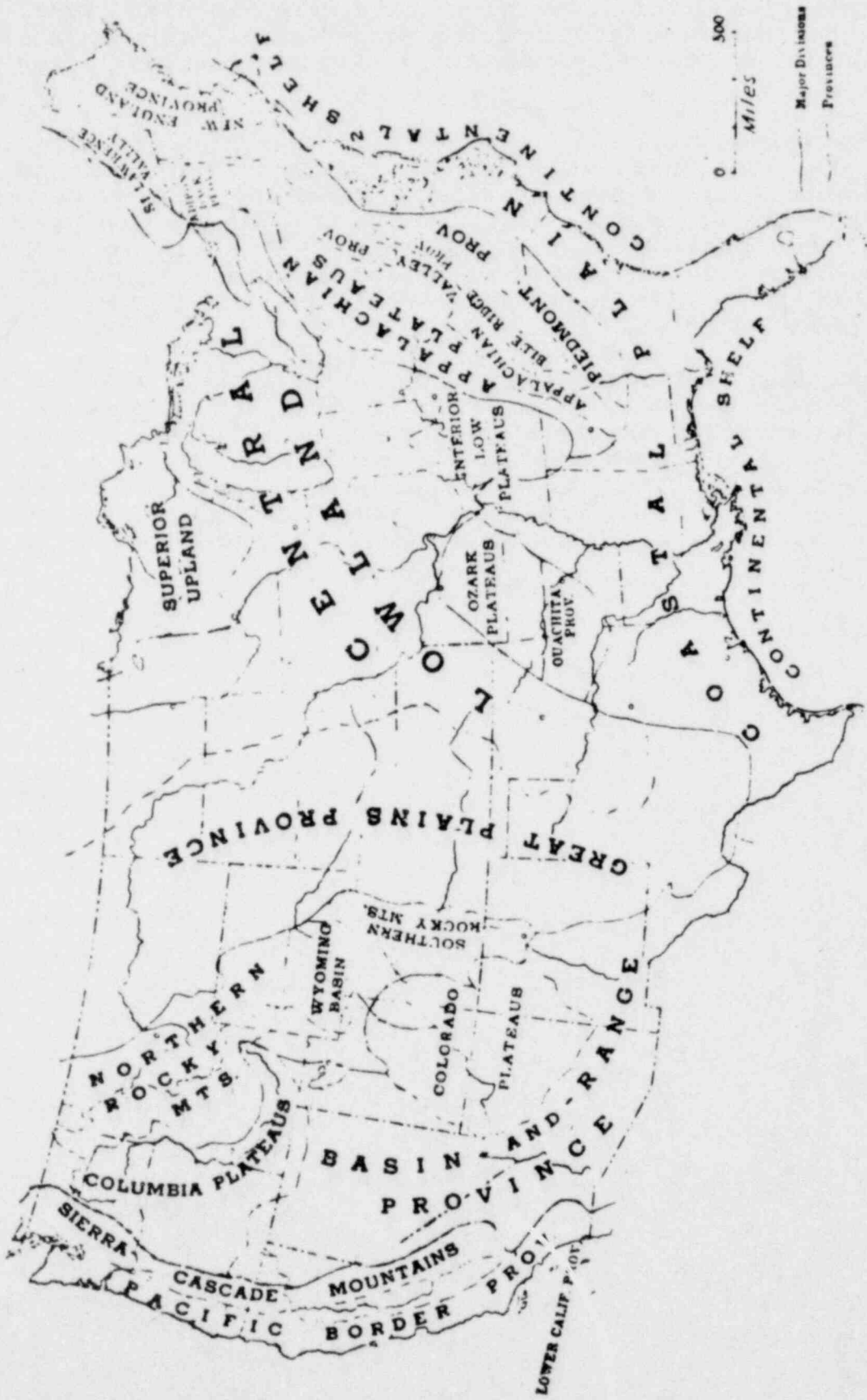


FIGURE 3-1. PHYSIOGRAPHIC DIVISION MAP OF THE U.S. ³⁰

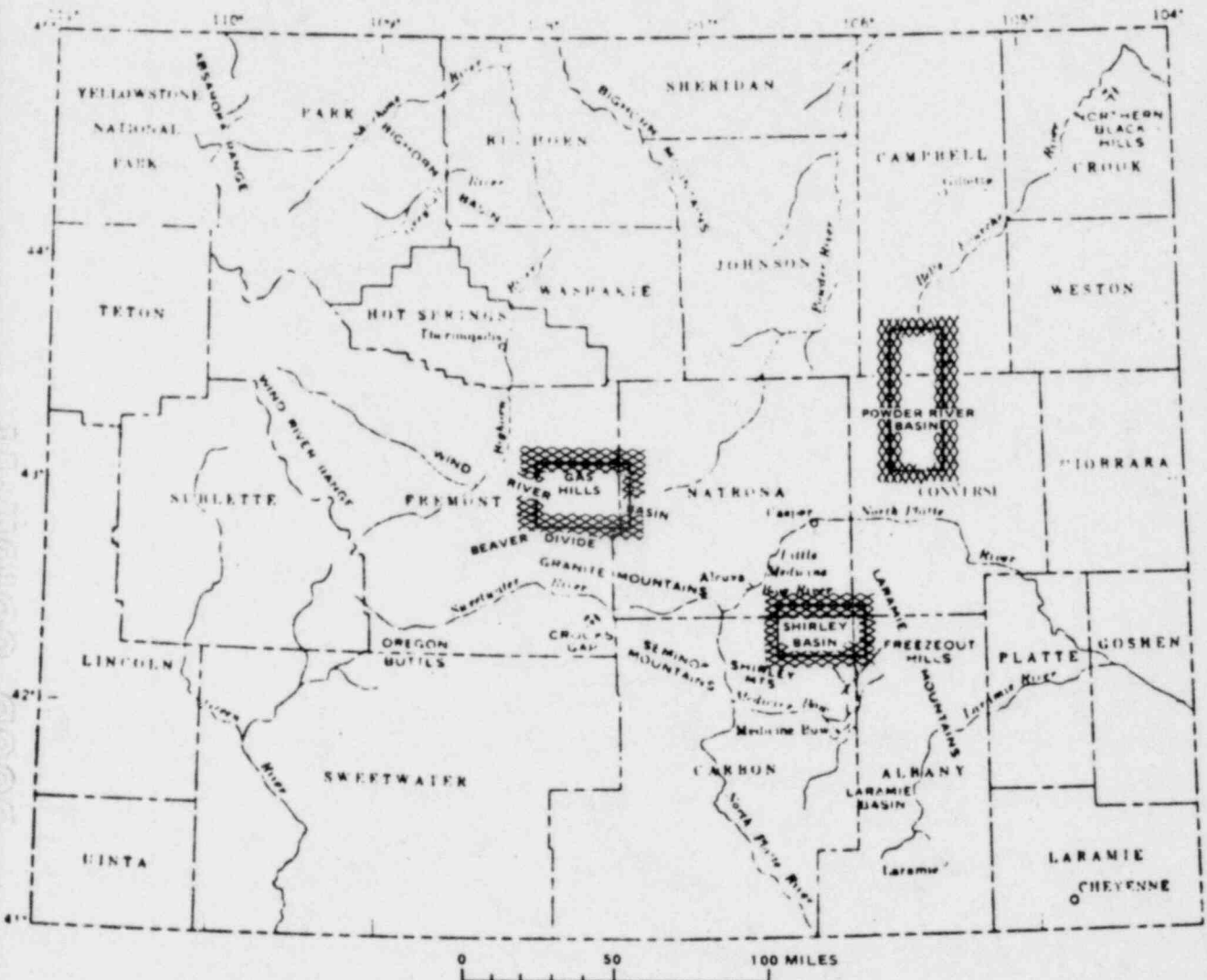


FIGURE 3-2. MAJOR URANIUM MINING DISTRICTS OF WYOMING^⑦

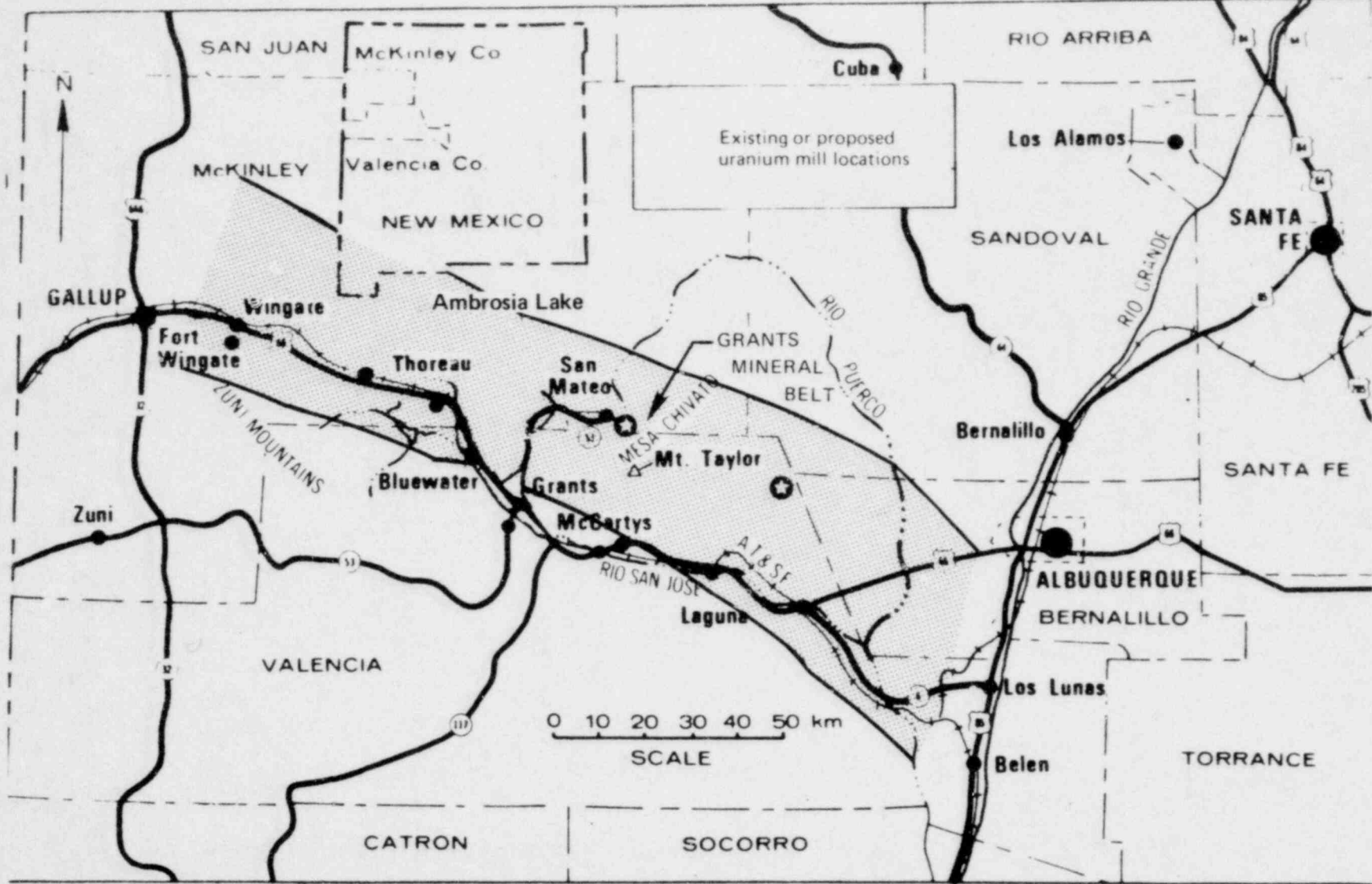


FIGURE 3-3. NORTHWESTERN URANIUM MINING DISTRICTS OF NEW MEXICO ¹⁰

POOR ORIGINAL

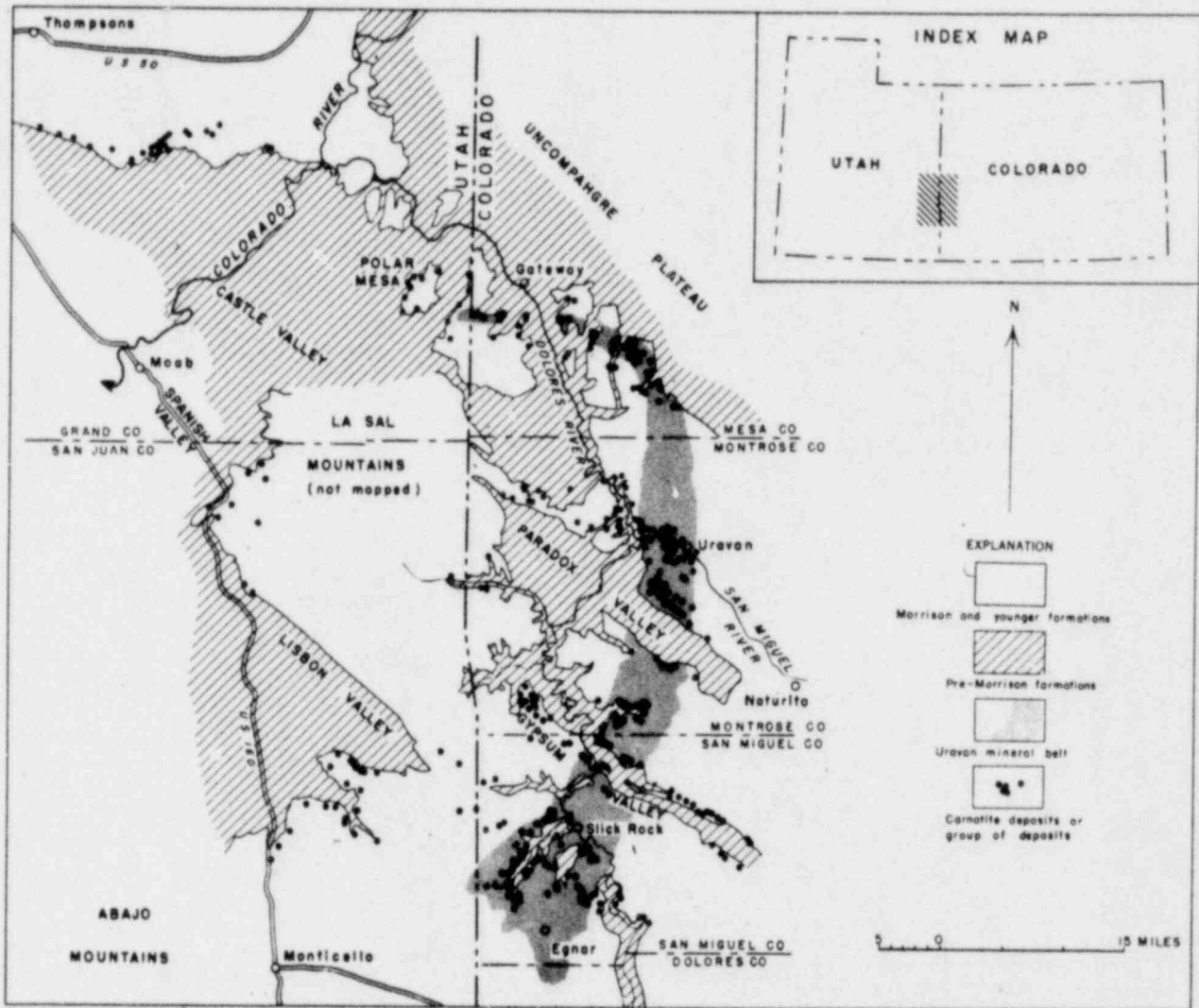


FIGURE 3-4. URANIUM MINING DISTRICTS OF COLORADO AND UTAH SHOWING THE PRINCIPAL URANIUM IN THE PARADOX BASIN. (21)

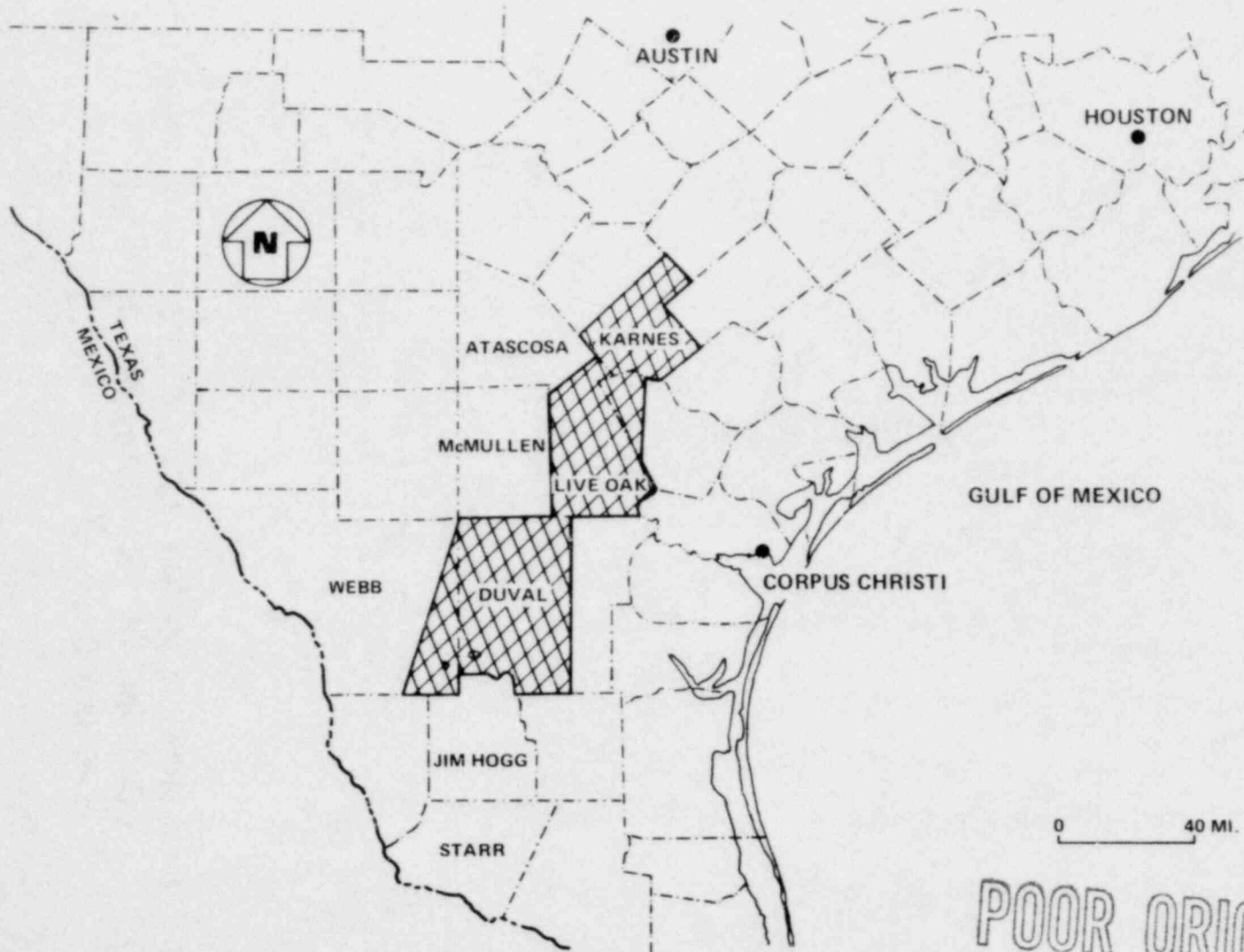
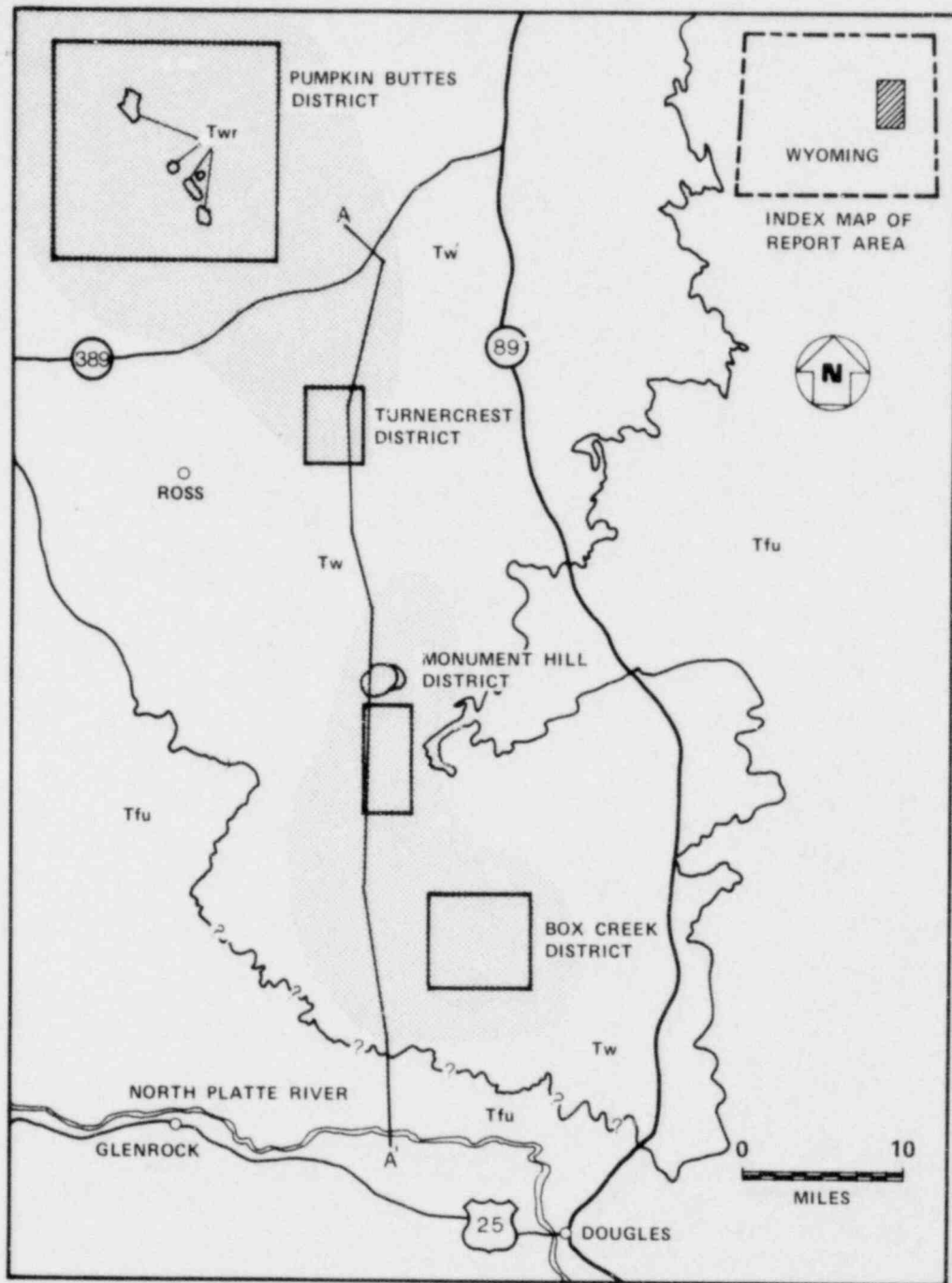


FIGURE 3-5. MAJOR URANIUM MINING DISTRICTS OF TEXAS ⁽³¹⁾



- MINING AREAS/EXPLORATION
- Twr WHITE RIVER (OLIGOCENE)
- Tw WASATCH (EOCENE)
- Tfu FORT UNION (PALEOCENE)

GEOLOGY MODIFIED FROM GEOLOGIC MAP OF WYOMING BY J.D. LOVE AND OTHERS, 1955.

FIGURE 3-6. POWDER RIVER BASIN URANIUM AREAS (2)

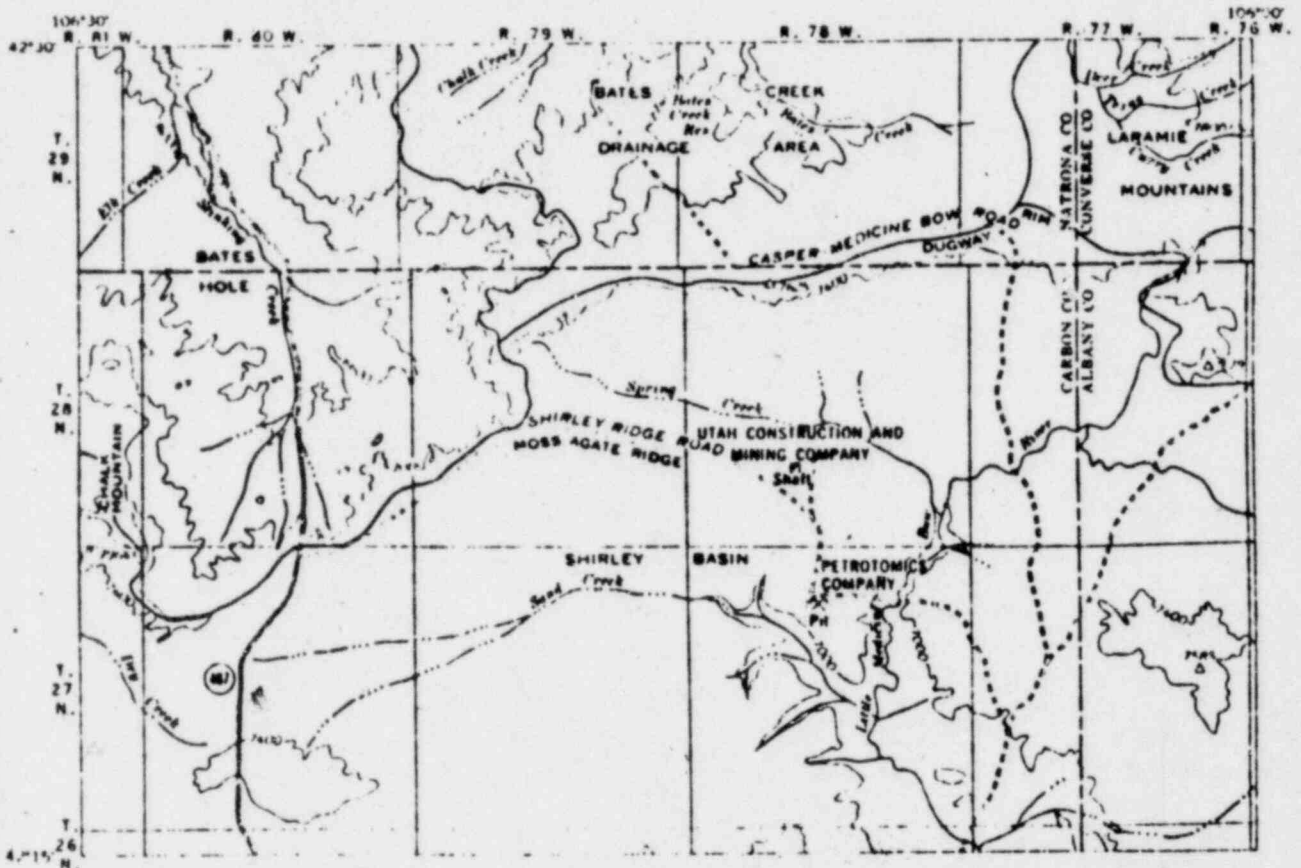


FIGURE 3-7. SHIRLEY BASIN AREA, WYOMING^⑦

POOR ORIGINAL

ERA	SYSTEM	SERIES	FORMATION	THICK- NESS (ft)	DEPTH TO TOP OF FORMATION (ft)	GENERAL PHYSICAL CHARACTER
CENOZOIC	QUATERNARY	PLEISTOCENE AND HOLOCENE	ALLUVIUM	0-30(?)	CROPS OUT	SAND, SILT, AND CLAY. CONTAINS SOME INDIGENOUS PEBBLES, GENERALLY IN LOWER PART.
	TERTIARY	EOCENE	WASATCH FORMATION	100-400	CROPS OUT	COARSE TO FINE-GRAINED SANDSTONE INTERBEDDED WITH SILTSTONE, CARBONACEOUS SHALE, AND COAL BEDS.
		PALEOCENE	FORT UNION FORMATION	2,800	400	FINE-GRAINED TO CONGLOMERATIC SANDSTONE INTERBEDDED WITH SILTSTONE, CARBONACEOUS SHALE, AND COAL BEDS.
MESOZOIC	CRETACEOUS	UPPER	LANCE FORMATION	3,000	3,200	FINE TO MEDIUM-GRAINED SANDSTONE AND INTERBEDDED SHALE AND CLAYSTONE.
			FOX HILLS SANDSTONE	700	6,200	FINE TO MEDIUM-GRAINED SANDSTONE AND INTERBEDDED THIN BEDS OF SANDY SHALE.
			LEWIS SHALE	600	6,900	SHALE AND INTERBEDDED THIN BEDS OF FINE-GRAINED SANDSTONE.
			MESAVERDE FORMATION	900	7,500	THIN-BEDDED TO MASSIVE SANDSTONE AND INTERBEDDED SHALE.
			CODY SHALE	4,000	8,400	SHALE AND FINE-GRAINED SANDSTONE BEDS.
			FRONTIER FORMATION	900	12,400	SANDSTONE AND INTERBEDDED SHALE.
	JURASSIC	LOWER	MOWRY SHALE	200	13,300	SILICEOUS SHALE.
			THERMOPOLIS SHALE	200	13,500	SOFT BLACK SHALE. CONTAINS THIN BEDS OF SANDSTONE AND BENTONITE.
			CLOVERLY FORMATION	150	13,700	MEDIUM TO COARSE-GRAINED SANDSTONE AND INTERBEDDED SILTSTONE.
			MORRISON FORMATION	150	13,850	VARICOLORED CLAYSTONE AND INTERBEDDED FINE-GRAINED SANDSTONE.
	TRIASSIC		SUNDANCE FORMATION	400	14,000	GREENISH GRAY SHALE AND INTERBEDDED GRAY FINE-GRAINED SANDSTONE.
			CHUGWATER FORMATION	700	14,400	DARK RED SILTSTONE, SANDSTONE, AND SHALE.
			PERMIAN	GOOSE EGG FORMATION	350	15,100
PALEOZOIC	PENNSYLVANIAN	TENSLEEP SANDSTONE	500	15,450	FINE TO MEDIUM-GRAINED SANDSTONE.	
		AMSDEN FORMATION	50(?)	15,950	SANDSTONE, SHALE AND THIN-BEDDED LIMESTONE AND DOLOMITE.	
	MISSISSIPPIAN	MADISON FORMATION	300	16,000	MASSIVE TO THIN-BEDDED LIMESTONE AND DOLOMITE.	
	CAMBRIAN	FLATHEAD SANDSTONE	100	16,300	FINE TO COARSE-GRAINED QUARTZITIC SANDSTONE.	
PRECAMBRIAN					16,400	IGNEOUS AND METAMORPHIC ROCKS.

TABLE 3-1. STRATIGRAPHIC SECTION IN THE POWDER RIVER BASIN, WYOMING^③

TABLE 3--2

ESTIMATED PROPERTIES OF SET 2 SOIL SAMPLES⁺

Sample	% Passing 200 Mesh	Estimated Composition	Liquid Limit	Plastic Index	Coarse Material	USCS Class.	AWC*	Shrink/ Swell Potential	CaCO ₃
Powder River Soil #1	90%	80-90% Silt 10-20% Clay	20-25%	5-10%	None	CL-ML	2.1	Low	Absent
Powder River Soil #2	90%	80-90% Silt 10-20% Clay	20-25%	5-10%	Little	CL-ML	2.1	Low	Absent
Shirley Basin Soil #1	30%	25-30% Silt 20-30% Clay 55-60% Silty Clay	25-30%	7-12%	Some	CL	1.9	Low- Moderate	Present
Shirley Basin Soil #2	40%	30-35% Clay 35-40% Silty Clay 25-35% Sandy Clay	35%	13%	Some	CL	1.9	Moderate	Absent
Ambrosia Lake Soil #1	40%	55-65% Silt 20-25% Clay 25-30% Fine Sand	25-30%	7-12%	None	CL	2.1	Low- Moderate	Absent
Ambrosia Lake Soil #2	70%	60-70% Silt 15-20% Clay 5-20% Silty Clay 5% Fine Sand	25%	5%	None	CL-ML	2.1	Low	Present

⁺Visual Classifications using (a) Unified Soil Classification System Chart
and (b) U.S. Department of Agriculture, Soil Conservation Service Soil
Identification Property Charts.

A reverse order sequence was used in conjunction with the charts.

*Average available water holding capacity (in./ft).

CENOZOIC

MESOZOIC

PALEOZOIC

GEOLOGIC TIME UNIT		ROCK UNIT	APPROXIMATE THICKNESS (ft)	DESCRIPTION	
QUATERNARY	HOLOCENE	STREAM ALLUVIUM AND TERRACE GRAVEL	0-50	SURFICIAL DEPOSITS OF SILT, SAND, AND GRAVEL. IN SOME AREAS INCLUDES TERRACE GRAVEL.	
	PLEISTOCENE				
TERTIARY	MIOCENE	ARIKAREE FORMATION	180	TUFFACEOUS SILTSTONE, SANDSTONE, CONGLOMERATE, AND FRESH WATER LIMESTONE OF FLUVIAL AND LACUSTRINE ORIGIN.	
	OLIGOCENE	WHITE RIVER FORMATION	750	UPPER MEMBER - TUFFACEOUS SILTSTONE AND CONGLOMERATE, FLUVIAL AND LACUSTRINE. LOWER MEMBER - TUFFACEOUS SILTSTONE AND CLAYSTONE, PREDOMINANTLY FLUVIAL AND LACUSTRINE.	
	EOCENE	LATE AND MIDDLE	WAGON BED FORMATION	150	TUFFACEOUS SILTSTONE, SANDSTONE, CONGLOMERATE, AND LIMESTONE, FLUVIAL AND LACUSTRINE.
		EARLY	WIND RIVER FORMATION	500	SILTY CLAYSTONE, SILTSTONE, ARKOSIC SANDSTONE, AND CONGLOMERATE, FLUVIAL.
CRETACEOUS		STEELE SHALE	2,000	THIN-BEDDED CARBONACEOUS SHALE, LENTICULAR SANDSTONES NEAR TOP.	
		NIOBRARA FORMATION	900	THIN-BEDDED CARBONACEOUS SHALE, IN PART CALCAREOUS.	
		FRONTIER FORMATION	860	THIN-BEDDED CARBONACEOUS SHALE AND SANDSTONE, WALL CREEK SANDSTONE MEMBER AT TOP.	
		MOWRY SHALE	110	THIN-BEDDED SILICEOUS SHALE, CONTAINS FISH SCALES.	
		THERMOPOLIS SHALE	185	THIN-BEDDED CARBONACEOUS SHALE, MUDDY SANDSTONE MEMBER NEAR BASE.	
		CLOVERLY FORMATION	200	SANDSTONE, MODERATELY CEMENTED, EVEN-BEDDED TO CROSS-BEDDED, CARBONACEOUS SHALE IN MIDDLE.	
	JURASSIC		MORRISON FORMATION	200	VARIEGATED WAXY MUDSTONE AND SILTSTONE, SANDSTONE NEAR BASE, LIMESTONE CONCRETIONS.
			SUNDANCE FORMATION	240	THIN-BEDDED AND FISSILE SHALE, SANDSTONE, AND SANDY LIMESTONE.
	TRIASSIC		JELM FORMATION	125	SHALE AND LEDGE FORMING SANDSTONE, RED TO BUFF.
			ALCOVA LIMESTONE	20	CRINKLY LIMESTONE AND LIMY SANDSTONE.
			RED PEAK FORMATION	580	SILTSTONE AND SHALE, RED, SPARSE SANDSTONE.
	PERMIAN		GOOSE EGG FORMATION	400	SILTSTONE AND SANDSTONE, RED, INTERBEDDED LIMESTONE.
	PENNSYLVANIAN		CASPER FORMATION	660	DOLOMITIC LIMESTONE AND SANDSTONE, OVERLAIN BY CROSS-BEDDED SANDSTONE AND QUARTZITE.
MISSISSIPPIAN		MADISON LIMESTONE	150	DOLOMITIC LIMESTONE, CHERTY NEAR TOP, CONGLOMERATE AND SANDSTONE AT BASE.	
PRECAMBRIAN	GRANITIC AND METAMORPHIC ROCKS AND MAFIC DIKES.				

TABLE 3-3. STRATIGRAPHIC SECTIONS IN THE SHIRLEY BASIN AREA, WYOMING ⁽⁷⁾

NORTH WALL

TOP OF EXPOSURE.

WIND RIVER FORMATION:

1. CLAYEY SILTSTONE, BUFF TO YELLOW, LIGHT-BROWN, OLIVE-GREEN	12.0
2. CLAYEY SILTSTONE, DARK-BROWN, YELLOW, LIGNITIC, GYPSIFEROUS; A FEW THIN SANDY GRAY INTERBEDS....	4.9
3. SANDSTONE, FINE- TO MEDIUM-GRAINED, POORLY CEMENTED, BUFF; A FEW THIN LIGNITIC CLAY INTERBEDS.....	5.5
4. CLAYEY SILTSTONE, YELLOWISH-GREEN TO BLUISH-GRAY; A FEW THIN GYPSIFEROUS BEDS AND LIGNITIC BEDS.....	13.8
5. CLAYEY SILTSTONE, GREENISH- AND BLUISH-GRAY.....	10.7
6. SANDSTONE, MEDIUM-GRAINED, POORLY CEMENTED, YELLOW; TRACE OF CARBON.....	5.5
7. CLAYEY SILTSTONE, GRAY-GREEN; TRACE OF CARBON.....	19.9
8. SILTSTONE, YELLOWISH-GREEN.....	5.6
9. SILTY CLAYSTONE AND SILTSTONE, GRAY AND DARK-GREEN	13.0
10. CLAYSTONE, RED, BLOCKY.....	1.3
11. SILTY CLAYSTONE, GRAY-GREEN.....	2.4
12. SILTY CLAYSTONE, REDDISH-PURPLE TO YELLOWISH-GREEN, BLOCKY.....	6.9
13. SILTSTONE AND SILTY CLAYSTONE, GREENISH-GRAY.....	25.4
14. SILTY CLAYSTONE, RED, ORANGE.....	2.7
15. SANDY SILTSTONE, GRAY, PYRITIC; SLIGHT CaCO ₃ CEMENT.....	3.2
16. SANDSTONE, UNALTERED, GRAY, PYRITIC, MEDIUM- TO VERY COARSE-GRAINED; IN PART CROSSBEDDED; COMPACTED BUT UNCEMENTED. CARBONACEOUS MATERIAL CHIEFLY ON CROSS BEDS. THIS IS THE UPPER ORE-BEARING SANDSTONE.....	30.0
TOTAL MEASURED WIND RIVER FORMATION.....	162.8

WEST WALL

TOP OF EXPOSURE.

WIND RIVER FORMATION:

1. TOPSOIL, BROWN, SANDY.....	3.0
2. GRAVEL, PINK; 1½-IN. MAXIMUM DIAMETER.....	.5
3. SANDSTONE, VERY COARSE GRAINED, POORLY CEMENTED, GREENISH-YELLOW.....	6.0
4. CLAYSTONE, SILTY, YELLOWISH-GREEN; CONTAINS LENSES OF POORLY CEMENTED VERY COARSE GRAINED SANDSTONE.....	15.0
5. SANDSTONE, SILICEOUS, POORLY CEMENTED, YELLOW; GRAVEL AS MUCH AS 3 IN. IN DIAMETER.....	4.0
6. SILTY CLAYSTONE, GREEN; INTERBEDDED WITH BROWN LENTICULAR LIGNITE BEDS.....	4.0
7. SANDSTONE, VERY COARSE GRAINED, CROSSBEDDED, YELLOW TO BUFF; SOME GRAVEL AS MUCH AS 1 IN. IN DIAMETER; CHANNELS-CUT IN UPPER PART.....	22.5
8. CLAYEY SILTSTONE, DENSE, BLOCKY, GRAY-GREEN.....	15.0
9. LIGNITE, SILTY, DARK-GRAY.....	6.5
10. CLAYSTONE, SILTY, BLOCKY, GREEN; SANDY IN LOWER THIRD.....	17.5
11. SANDSTONE, MEDIUM- TO VERY COARSE-GRAINED, SILTY, CROSSBEDDED, GRAY; CALCITE CEMENT IN TOP BEDS.....	10.5
12. LIGNITE, SILTY, DARK-GRAY.....	1.5
13. CLAYSTONE, SILTY, BLOCKY, GREEN; SANDY IN SOME BEDS.....	21.0
14. SANDSTONE, VERY COARSE GRAINED, POORLY CEMENTED, CROSSBEDDED, GRAY.....	10.5
15. LIGNITE, SILTY, DARK-GRAY.....	1.0
16. SILTSTONE, CLAYEY, GREENISH-GRAY; INTERBEDDED IN LOWER HALF WITH FINE-GRAINED GRAY SANDSTONE.....	14.0
17. SANDSTONE, VERY COARSE GRAINED, CROSSBEDDED, PYRITIC, CARBONACEOUS, UNCEMENTED, GRAY. THIS IS THE LOWER ORE-BEARING SANDSTONE.....	33.5
TOTAL MEASURED WIND RIVER FORMATION.....	186.0

TABLE 3-4. SOIL/BEDROCK SECTIONS IN THE SHIRLEY BASIN, WYOMING. ⁷

ERAS	AGE	UNIT	THICKNESS (FT)	DOMINANT LITHOLOGY			
CENOZOIC	TERTIARY	QUATERNARY	SURFICIAL DEPOSITS	0-10+	UNCONSOLIDATED SAND AND GRAVEL DEPOSITS IN TERRACES, PEDIMENTS, GLACIAL MORAINES, AND VALLEY ALLUVIUM		
		PLIOCENE	MOONSTONE FORMATION	0-1,350	CLAYSTONE, SHALE, AND TUFFACEOUS SANDSTONE. SOME CONGLOMERATE AND LIMESTONE		
		MIOCENE	ARIKAREE FORMATION	0-3,000	TUFFACEOUS SANDSTONE AND CONGLOMERATE		
		OLIGOCENE	WHITE RIVER FORMATION	0-1,500	WIDESPREAD CONGLOMERATE AT BASE OVERLAIN BY TUFFACEOUS SILTSTONE, CLAYSTONE, AND SANDSTONE		
		EOCENE	MIDDLE AND LATE	WAGON BED FORMATION	0-1,000	ARKOSIC SANDSTONE AND CONGLOMERATE, TUFFACEOUS SILTSTONE, CLAYSTONE, AND SANDSTONE	
			EARLY	WIND RIVER FORMATION	0-9,000	SANDSTONE, CONGLOMERATE, SILTSTONE, AND CLAYSTONE	
		INDIAN MEADOWS FORMATION		CONGLOMERATE, SANDSTONE, AND SILTSTONE			
		PALEOCENE	FORT UNION FORMATION	0-8,000	SANDSTONE, SILTSTONE, AND SHALE		
		MESOZOIC	CRETACEOUS	LATE	LANCE FORMATION	0-6,000	SANDSTONE, SHALE, AND CLAYSTONE
					MEETEETSE FORMATION	200-1,335	SANDSTONE, SILTSTONE, CARBONACEOUS SHALE, AND COAL
MESAVERDE FORMATION	700-2,000				SANDSTONE, SILTSTONE, CARBONACEOUS SHALE, AND COAL		
CODY SHALE	3,600-5,000				SHALE IN LOWER HALF; SHALY SANDSTONE AND SHALE IN UPPER HALF		
FRONTIER FORMATION	600-1,000				SANDSTONE AND SHALE		
EARLY	MOWRY SHALE			250-700	SHALE AND BENTONITE		
	THEMOPOLIS SHALE		125-250	SHALE, MUDDY SANDSTONE MEMBER AT TOP CONTAINS SANDSTONE AND MINOR AMOUNT OF SHALE			
	CLOVERLY AND MORRISON FORMATIONS		200-700	SANDSTONE, CLAYSTONE, AND LENTICULAR CONGLOMERATE			
JURASSIC	SUNDANCE FORMATION		200-550	SANDSTONE, LIMESTONE, AND SHALE			
	GYPSUM SPRING FORMATION		0-250	LIMESTONE, SHALE, CLAYSTONE, AND GYPSUM			
JURASSIC(?) AND TRIASSIC(?)	NUGGET SANDSTONE		0-500	SANDSTONE, SOME SHALE IN LOWER PART			
TRIASSIC	CHUGWATER GROUP		1,000-1,300	SILTSTONE, SHALE, AND SANDSTONE, ALCOVA LIMESTONE IS A THIN (MAX 15FT) PERSISTENT UNIT ABOVE BASE			
	DINWOODY FORMATION		50-70	SILTSTONE, SHALE, AND SANDSTONE			
PALEOZOIC	PERMIAN		PHOSPHORIA FORMATION	350-480	SHALE AND GYPSUM, SOME THIN BEDS OF LIMESTONE		
		TENSLEEP SANDSTONE	200-400	LIMESTONE, CHERT, SANDSTONE, AND SILTSTONE			
	PENNSYLVANIAN	TENSLEEP SANDSTONE	200-600	SANDSTONE			
		AMSDEN FORMATION	0-400	SANDSTONE AT BASE, OVERLAIN BY LIMESTONE, DOLOMITE, AND SHALE			
	MISSISSIPPIAN	MADISON LIMESTONE	300-700	LIMESTONE			
	DEVONIAN	DERBY FORMATION	0-300	DOLOMITE, LIMESTONE, SHALE, AND SILTSTONE			
	ORDOVICIAN	BIGHORN DOLOMITE	0-300	DOLOMITE			
		GALLATIN LIMESTONE	0-365	LIMESTONE			
	CAMBRIAN	CROS VENTRE FORMATION	0-700	SHALE, LIMESTONE, AND SHALY SANDSTONE			
		FLATHEAD SANDSTONE	50-500	SANDSTONE AND QUARTZITE			
PRECAMBRIAN	IGNEOUS AND META MORPHIC ROCKS		GRANITE, GRANITE GNEISS, SCHIST, AND METASEDIMENTARY ROCKS				

TABLE 3-5. STRATIGRAPHIC UNITS WIND RIVER BASIN AND GAS HILLS MINING DISTRICT ⑨

POOR ORIGINAL

SOIL SERIES NAME	PARENT MATERIAL	PROFILE CHARACTERISTICS OF TYPICAL PEDON	DEPTH OF SOIL, INCHES (cm)	TOPOGRAPHY AND SLOPE	EROSION HAZARD ^b	PERMEABILITY ^c	VEGETATION
HAVRE	ALLUVIUM	STRONGLY CALCAREOUS. Ap: 0-8", CLAY LOAM, pH 7.8 C: 6-60", CLAY LOAM, pH 8.4	60 (152)	NEARLY LEVEL TO GENTLY SLOPING SLOPE 0-3%	LOW TO MODERATE ^d	MODERATE ^d	SAGEBRUSH ^d
SINKSON	RED SILTSTONE	CALCAREOUS. A1: 0-3", LOAM, pH 8.2 C: 3-60", LOAM, pH 8.3	60 (152)	NEARLY LEVEL TO STEEP SLOPE 10-30%	MODERATE TO SEVERE ^d	MODERATE ^d	WESTERN WHEATGRASS, SANDBERG BLUEGRASS, NEEDLE AND THREAD, SAGEBRUSH
THERMO-POLIS	RED SILTSTONE	CALCAREOUS A1: 0-4", LOAM, pH 8.2 C: 4-15", LOAM, pH 8.4 Cr: 15-25", SILTSTONE	10-20 (25-51)	MODERATE TO STEEP SLOPE 10-30%	SEVERE	MODERATE	SANDBERG BLUEGRASS, WESTERN WHEATGRASS, SAGEBRUSH, SCATTERED JUNIPER
BLAZON	SOFT SHALE AND SOFT CLAYEY SANDSTONE	STRONGLY CALCAREOUS. A1: 0-12", CLAY LOAM, pH 8.4 C: 12-20", CALC. SHALE	10-20 (25-51)	SLOPING TO STEEP SLOPE 6-20%	MODERATE TO SEVERE	MODERATE	BLUEBUNCH WHEATGRASS, INDIAN RICEGRASS, SAGEBRUSH
PATENT	ALLUVIUM, SOFT CLAY SHALES	STRONGLY CALCAREOUS. A1: 0-7", CLAY LOAM, pH 8.2 C: 7-60", CLAY LOAM, pH 8.3	60 (152)	NEARLY LEVEL TO STEEP SLOPE 6-20%	MODERATE TO SEVERE	MODERATE	BLUEBUNCH WHEATGRASS, WESTERN WHEATGRASS, SAGEBRUSH
DIAMOND-VILLE	LIMESTONE, SANDSTONE, SHALE	NONCALCAREOUS SURFACE HORIZONS, A AND B HORIZONS, LOAM TO CLAY LOAM, pH 7.3-7.6. Cca: 12-22", LOAM, pH 8. CALCAREOUS Cr: 22-40", SANDSTONE	20 (51)	GENTLY SLOPING TO MODERATELY STEEP SLOPE 3-10%	MODERATE ^d	MODERATE ^d	WESTERN WHEATGRASS, BLUEBUNCH WHEATGRASS, SAGEBRUSH
FORELLE	ALLUVIUM	A AND B HORIZONS FINE SANDY LOAM TO CLAY LOAM, pH 7.4-7.6. CALCAREOUS B AND C HORIZONS, pH 8.2-8.4	60 (152) OR MORE	UNDULATING TO HILLY SLOPE 3-10%	MODERATE	MODERATE	WESTERN WHEATGRASS, BLUEBUNCH WHEATGRASS, SAGEBRUSH
HIGHPOINT	HARD SHALE	NONCALCAREOUS A1: 0-7", CHANNERY SILTY CLAY LOAM, pH 7.2 Cr: 7-20", BEDROCK WITH SILTY CLAY LOAM, pH 7.2	6-20 (15-51)	STEEP SLOPE 20-50%	MODERATE TO SEVERE	MODERATE	BLUEBUNCH WHEATGRASS, THREAD-LEAF SAGE, SANDBERG BLUEGRASS
CROWNEST	HARD, NON-CALCAREOUS SANDSTONE	(NO IMMEDIATE INFORMATION AVAILABLE)	10-20 (25-51)	UPLANDS	MODERATE TO SEVERE	MODERATE TO RAPID	BLUEBUNCH WHEATGRASS, SANDBERG WHEATGRASS, SAGEBRUSH
COTHA	SANDSTONE	0-3", FINE SANDY LOAM 3-14", SANDY LOAM 14-26", LOAM	20-40 (51-101)	UPLANDS	MODERATE TO SEVERE	MODERATE TO RAPID	BLUEBUNCH WHEATGRASS, NEEDLE THREAD, SAGEBRUSH

^a INFORMATION OBTAINED FROM APPLICANT'S REPORT.

^b THE EROSION HAZARD OF A SOIL IS A JUDGMENT MADE BY THE INDIVIDUAL SOIL SURVEYOR, AND IS BASED ON THE PRINCIPAL CHARACTERISTICS OF THE SOIL AND ITS INFERRED QUALITIES.

^c IN THE ABSENCE OF PRECISE MEASUREMENTS, SOILS CAN BE CLASSIFIED INTO RELATIVE PERMEABILITY CLASSES ON THE BASIS OF THEIR STRUCTURE, TEXTURE, POROSITY, CRACKING, AND OTHER CHARACTERISTICS IN RELATION TO LOCAL USE EXPERIENCE. TENTATIVE SUGGESTED PERMEABILITY RATES (IN INCHES PER HOUR) THROUGH SATURATED, UNDISTURBED CORES UNDER A 1/2-INCH HEAD OF WATER ARE AS FOLLOWS:

VERY SLOW	LESS THAN 0.05	MODERATELY RAPID	2.50 TO 5.00
SLOW	0.05 TO 0.20	RAPID	5.00 TO 10.00
MODERATELY SLOW	0.20 TO 0.80	VERY RAPID	OVER 10.00
MODERATE	0.80 TO 2.50		

^d STAFF'S ESTIMATES HAVE BEEN GIVEN WHERE INFORMATION WAS NOT IMMEDIATELY AVAILABLE.

TABLE 3-6. SOIL CHARACTERISTICS NEAR THE LUCKY Mc MINE AND MILL SITE, GAS HILLS, WYOMING⁽⁸⁾

SYSTEM	ROCK	UNIT		
CRETACEOUS	MESA VERDE GROUP	POINT LOOKOUT FORMATION	HOSTA MEMBER	RED, HEMATITIC, & BGS
			GIBSON MEMBER	BLACK SH
		CREVASSE CAN-YON FORMATION	CALTON MEMBER	SH TO ORANGE F-GR SS
			MULATTO TONGUE	GRAY BLACK SH MANGOS TONGUE
			STRAY	SH F-GR TO M-GR SS
			DILCO COAL MEMBER	
			GALLUP FORMATION	TAN, M-GR, MASSIVE SS
		MANGOS FORMATION		TAN, F-GR TO M-GR SS
				GRAY OR BLACK SH FOSSILIFEROUS, CALCAREOUS
			TRAY HERMOND	TAN, F-GR TO M-GR SS
	TRAY		SH OR TAN, M-GR SS	
	JURASSIC	MORRISON FORMATION	BRUSHY BASIN MEMBER	OR MOST W/INFSD WHITE OR RED SS UNITS
			WESTRATER CANYON MEMBER	F-GR TO C-GR, RED OR WHITE SS W/MDY LENSES
			RECAPTURE MEMBER	RED OR GR SANDY, MDY W/SS LENSES
BLUFF FORMATION			LT RED TO TAN, MASSIVE, F-GR TO M-GR SS	
SAN RAFAEL GROUP		SUMMERVILLE FORMATION	RED SILTY SH	
		ENTRADA FORMATION	RED, M-GR SS	
		MINIATE FORMATION	RED TO TAN, M-GR SS	
		MINIATE FORMATION	RED TO TAN, M-GR SS	
		MINIATE FORMATION	RED TO TAN, M-GR SS	
		MINIATE FORMATION	RED TO TAN, M-GR SS	
TRIASSIC	CHINLE FORMATION		DOMINATELY RED SH W/INTD RED OR MOTTLED SS UNITS	
		COARSED T ¹ MEMBER		
		SHINARUMP MEMBER	RED CONGL SS LS	
	PERMIAN	SAN ANDRES FORMATION	GLICRIETA MEMBER	WHITE TO TAN, F-GR, & BU SS W/SS F&Z
TRADITION				
YESO FORMATION		SAN YEBRO MEMBER	DOMINATELY LT RED TO MAROON OR MOTTLED, F-GR, & BU SS W/BD CLAYST & EVAPORITES NEAR TOP	
		TRANSITION		
		MESITA BLANCO MEMBER	RED TO ORANGE, MASSIVE, F-GR SS	
		ABO FORMATION	DOMINATELY RED SILT & CLAYST W/SS & IS NODULES OR INCL W/BD SS & IS LENSES	
PENN.		UNDIFFERENTIATED	INDD SS, LS, & SH	
PRE-CAMBRIAN			GRANITE GNEISS & SCHIST	

PHILLIPS PETROLEUM COMPANY MEASURED SECTION
SECTION 26, T14N, R10W

PHILLIPS PETROLEUM COMPANY WATER WELL
SECTION 26, T14N, R10W

AMCONDA COMPANY DISPOSAL WELL
SECTION 24, T12N, R11W

TABLE 3-7. STRATIGRAPHIC SECTION, SOUTHEASTERN AMBROSIA LAKE AREA, GRANTS, NEW MEXICO⁽¹⁴⁾

SYSTEM	SERIES	GROUP	FORMATION	MEMBER	THICKNESS (FT)	LITHOLOGY AND WATER BEARING CHARACTERISTICS
QUATERNARY	HOLOCENE		GOLD BASIN FORMATION			EOLIAN AND FLUVIAL SILT AND SAND, ROUNDED TO SUBROUNDED GRAVEL, COBBLES AND BOULDER IN A CLEAN SANDY MATRIX. POORLY SORTED. TERRACE DEPOSITS, ALLUVIAL-TAN DEBRIS, LOCAL DEPOSITS IN THE HIGH PLATEAUS AND MOUNTAIN AREAS. IN SPANISH VALLEY, EOLIAN AND ALLUVIAL DEPOSITS OR FORMATIONS (UNDIFFERENTIATED) COMPOSE THE PRINCIPAL WATER-BEARING MATERIAL AND SOURCE OF GROUND WATER.
			BEAVER BASIN FORMATION		0-300-	
TERTIARY	PLEISTOCENE		PLACER CREEK FORMATION			
			HARPOLT MESA FORMATION			
CRETACEOUS	UPPER CRETACEOUS		MANCOS SHALE	UNNAMED UPPER SHALE MEMBER		IGNEOUS ROCKS, MOSTLY DIORITE, MONZONITE, AND SYENITE PORPHYRY THAT INTRUDE OLDER SEDIMENTARY FORMATIONS AS DIKES, SILLS, STOCKS, AND LACCOLITHS. PRECIPITATION MAY ENTER THESE ROCKS WHERE THEY ARE INTENSELY FRACTURED AND SUBSEQUENTLY RECHARGE ADJACENT PERMEABLE SEDIMENTARY ROCKS.
				FERRON SANDSTONE MEMBER	410-800-	DARK-GRAY AND GRAY-BROWN MARINE SHALE WITH DISCONTINUOUS THIN BEDS OF GRAY SANDSTONE, RELATIVELY IMPERMEABLE. DOES NOT YIELD WATER IN THIS AREA.
CRETACEOUS	LOWER CRETACEOUS		DAKOTA SANDSTONE	UNNAMED LOWER SANDSTONE MEMBER		TAN AND GRAY THIN-BEDDED FINE-GRAINED SANDSTONE AND SANDY SHALE ABOUT 160 FT THICK. PERMEABLE, BUT NOT KNOWN TO YIELD WATER IN THIS AREA.
				UNNAMED SANDSTONE MEMBER	50-120	DARK-GRAY AND GRAY-BROWN MARINE SHALE WITH DISCONTINUOUS THIN BEDS OF GRAY SANDSTONE, RELATIVELY IMPERMEABLE. DOES NOT YIELD WATER IN THIS AREA.
JURASSIC	UPPER JURASSIC	SAN RAFAEL GROUP	SUMMERVILLE FORMATION	SLICK ROCK MEMBER		PURPLE, BROWN AND YELLOWISH-BROWN CARBONACEOUS SANDSTONE WITH INTERBEDS OF DARK-GRAY SILTSTONE AND LENTICULAR TAN CONGLOMERATIC SANDSTONE. PERMEABLE, BUT NOT KNOWN TO YIELD WATER IN THIS AREA.
				DEWEY BRIDGE MEMBER	50-250	LIGHT-GRAY SILTIFIED SANDSTONE, LENTICULAR CONGLOMERATIC BROWNISH-GRAY CROSS-BEDDED SANDSTONE WITH THIN INTERBEDS OF GREEN MUDDSTONE, AND THIN SPARSE BEDS OF GRAY LIMESTONE. HAS A LOW INTRINSIC HYDRAULIC CONDUCTIVITY BUT YIELDS WATER. SPRINGS WHERE THE BEDS ARE INTENSELY FRACTURED.
JURASSIC	LOWER JURASSIC	GLEN CANYON GROUP	ENTRADA SANDSTONE	BEIGHTY BASIN SHALE MEMBER	250-450	VARIGATED RED, GREEN AND PURPLE MUDDSTONE WITH SANDY CLAY AND GREENISH-GRAY BENTONITE WITH INTERBEDS OF CONGLOMERATIC SANDSTONE. HAS A LOW INTRINSIC HYDRAULIC CONDUCTIVITY AND IS NOT KNOWN TO YIELD WATER IN THIS AREA.
				MOAB MEMBER	60-220	TAN TO GRAY MEDIUM-SORTED FLUVIAL CROSS-BEDDED SANDSTONE WITH INTERBEDS OF RED AND GRAY MUDDSTONE. PERMEABLE IN PART, BUT NOT KNOWN TO YIELD WATER IN THIS AREA.
TRIASSIC(?)	UPPER TRIASSIC(?)		KAYENTA FORMATION	SALT WASH SANDSTONE MEMBER		RED THIN-BEDDED SANDSTONE, RED SANDY MUDDSTONE, RED SHALE AND THIN GRAY LIMESTONE LAYERS WITH SOME LARGE GRAY-WHITE TO RED CHERT CONCRETIONS. HAS A LOW INTRINSIC HYDRAULIC CONDUCTIVITY, AND IS NOT KNOWN TO YIELD WATER IN THIS AREA.
				UNNAMED SANDSTONE MEMBER	300-550	PALL-TAN TO GRAYISH-WHITE MASSIVELY CROSS-BEDDED MEDIUM-GRAINED SANDSTONE. PERMEABLE, BUT NOT KNOWN TO YIELD WATER IN THIS AREA.
TRIASSIC(?)	LOWER TRIASSIC(?)		NAVAJO SANDSTONE	SLICK ROCK MEMBER		LIGHT-TAN TO RED EOLIAN SANDSTONE. PERMEABLE, BUT NOT KNOWN TO YIELD WATER IN THIS AREA.
				DEWEY BRIDGE MEMBER	300-400	LIGHT-RED AQUOUS SILTSTONE AND FINE-GRAINED SANDSTONE. CONCRETED BEDS COMMON. PERMEABLE, BUT NOT KNOWN TO YIELD WATER IN THIS AREA.
TRIASSIC(?)	UPPER TRIASSIC(?)		KAYENTA FORMATION	UNNAMED SANDSTONE MEMBER		PALL YELLOWISH-ORANGE TO PALL REDDISH-BROWN FINE TO MEDIUM-GRAINED SANDSTONE. HAS A LOW INTRINSIC HYDRAULIC CONDUCTIVITY, AND IS NOT KNOWN TO YIELD WATER IN THIS AREA.
				UNNAMED SANDSTONE MEMBER	230-270	IRREGULAR BEDS OF RED-TAN GRAY-AND LAVENDER SHALE, SILTSTONE AND SANDSTONE. LOCALLY HAS A DISPERSED, BUT NOT KNOWN TO YIELD WATER IN THIS AREA.

TABLE 3-8. GEOLOGIC SECTION FOR THE SPANISH VALLEY AREA PARADOX BASIN, UTAH/COLORADO

POOR ORIGINAL

SYSTEM	SERIES	GROUP	FORMATION	MEMBER	THICKNESS (FT)	LITHOLOGY AND WATER BEARING CHARACTERISTICS
TRIASSIC	UPPER TRIASSIC	GLEN CANYON GROUP	WINGATE SANDSTONE		275-260	MEDIUM-REDDISH-ORANGE FINE-GRAINED SANDSTONE IN TABULAR STRIPS OF MASSIVE EOLIAN CROSS STRATA. PERMEABILITY NOT GREAT BUT WHERE INTENSELY FRACTURED THIS WATER TO SPRINGS. HAS POTENTIAL FOR MODERATE YIELDS OF WATER TO WELLS.
			CHINLE FORMATION	CHURCH ROCK MEMBER MOSSBACK MEMBER	170-270 30-80	REDDISH-BROWN AND VARIEGATED GRAY-BROWN SILTSTONE. REDDISH-GRAY SANDS* IN GRAY-GREEN CONGLOMERATE SANDSTONE. LENTICULAR CONGLOMERATE SPARS* IN TRANSIT LAMINAE OF GYPSUM. LOW INTRINSIC HYDRAULIC CONDUCTIVITY. NOT KNOWN TO YIELD WATER IN THIS AREA. GRAY TO GREENISH-GRAY THINLY TO THICKLY CROSS-BEDDED FINE-GRAINED SANDSTONE LAYERS OF SILTSTONE, CALCAREOUS SANDSTONE, AND CONGLOMERATE. LIGHTNIC DEBRIS, PYRITE, AND OTHER METALLIC DEPOSITS COMMON. PERMEABLE BUT NOT KNOWN TO YIELD WATER IN THIS AREA.
PERMIAN	MIDDLE AND LOWER TRIASSIC		UNCONFORMITY			
			MOSEKOPF FORMATION		470-530	MOSTLY REDDISH-BROWN LAMINATED TO THIN-BEDDED SILTSTONE AND GRAY FINE-GRAINED SANDSTONE. SPARSE THIN LAYERS OF QUARTZ, GRANULE CONGLOMERATE, CURRENT RHYOLITE MARKS AND CRACKS. INTRASTRA TAL LAMINAE OF GYPSUM AND GYPSUM VEINLETS COMMON. LOW INTRINSIC HYDRAULIC CONDUCTIVITY. NOT KNOWN TO YIELD WATER IN THIS AREA.
			UNCONFORMITY			
			QUELLES FORMATION	UNNAMED ARKOSIC MEMBER	750-700*	RED-BROWN AND DARK-RED FLUVIAL ARKOSIC AND ARKOSIC CONGLOMERATE. RED ARKOSIC SANDSTONE WITH MASSIVE CROSSBEDDING AND TABULAR-BEDDED RED-BROWN SANDSTONE. PERMEABLE BUT NOT KNOWN TO YIELD WATER TO A FEW WELLS FOR DOMESTIC USE IN SPANISH VALLEY. BUT IS NOT AN IMPORTANT ADQUIER IN THIS AREA.
PENNSYLVANIAN	UPPER PENNSYLVANIAN		RICO FORMATION		200-450*	REDDISH-BROWN AND GREENISH-GRAY FINE TO MEDIUM-GRAINED CROSS-BEDDED FLUVIAL SANDSTONE. GRAY THIN TO THICK-BEDDED CHESTNUT MARINE LIMESTONE AND REDDISH-GRAY MICACEOUS SILTSTONE. THE SANDSTONES ARE PERMEABLE BUT THE FORMATION HAS A GENERALLY LOW INTRINSIC HYDRAULIC CONDUCTIVITY AND IS NOT KNOWN TO YIELD WATER IN THIS AREA.
	MIDDLE PENNSYLVANIAN		HEMLOCK FORMATION	UNNAMED UPPER ARKOSIC MEMBER PARADOX MEMBER	800-17 2,000-15	SILTSH-GRAY MARINE LIMESTONE AND DOLOMITE CONTAINING GRAY AND RED CHERT. GRAY FINE-GRAINED SANDSTONE AND SILTSTONE. REDDISH-GRAY SANDY SHALE AND SANDSTONE AND GRAY ARKOSIC CONGLOMERATE. NOT KNOWN TO YIELD WATER IN THIS AREA. LIGHT-COLORED SALT GYPSUM ANHYDRITE AND OTHER EVAPORITES. BLACK SHALE. DARK-GRAY SANDY SHALE. GRAY SANDSTONE AND GRAY DOLOMITIC MARINE LIMESTONE. NOT KNOWN TO YIELD WATER IN THIS AREA.
			UNCONFORMITY			METAMORPHIC COMPLEX OF GNEISS, SCHISTS, AND SIMILAR ROCK TYPES WITH ASSOCIATED INTRUSIVE ROCKS. NOT KNOWN TO YIELD WATER IN THIS AREA.

TABLE 3-8. GEOLOGIC SECTION FOR THE SPANISH VALLEY AREA, PARADOX BASIN, UTAH/COLORADO (CONTINUED)¹⁹

SYSTEM	SERIES	GROUP	STRATIGRAPHIC UNIT	APPROXIMATE THICKNESS (FEET)	CHARACTER OF ROCKS	WATER-BEARING PROPERTIES
QUATERNARY	RECENT AND PLEISTOCENE		ALLUVIUM	0-30	TERRACE DEPOSITS COMPOSED OF CLAY, SILT, SAND, AND GRAVEL	NOT AN AQUIFER IN KARNES COUNTY
			INTERSTREAM SAND AND GRAVEL DEPOSITS	0-30	PREDOMINANTLY GRAVEL AND SAND	DO
TERTIARY	PLIOCENE (?) PLIOCENE MIOCENE (?) MIOCENE MIOCENE (?) OLIGOCENE (?)		UNCONFORMITY	0-100	SAND AND SANDSTONE INTERBEDDED WITH CLAY, GRAVEL, AND CALICHE	DO
			GOLIAD SAND	0-100	SAND AND SANDSTONE INTERBEDDED WITH CLAY, GRAVEL, AND CALICHE	DO
			UNCONFORMITY	0-500	CLAY AND SANDY CLAY AND INTERCALATED BEDS OF SAND AND SANDSTONE	YIELDS SMALL TO MODERATE QUANTITIES OF FRESH TO SLIGHTLY SALINE WATER
			LAGARTO CLAY	0-500	CLAY AND SANDY CLAY AND INTERCALATED BEDS OF SAND AND SANDSTONE	YIELDS MODERATE TO LARGE QUANTITIES OF FRESH TO SLIGHTLY SALINE WATER
			UNCONFORMITY	0-800	MEDIUM TO FINE GRAINED SAND AND SANDSTONE AND SANDY, ASHY, AND BENTONITIC CLAY BEDS	YIELDS SMALL TO MODERATE QUANTITIES OF FRESH TO MODERATELY SALINE WATER
			UNCONFORMITY	0-500	PREDOMINANTLY TUFF, TUFACEOUS CLAY, SANDY CLAY, BENTONITIC CLAY, AND SANDSTONE	YIELDS SMALL QUANTITIES OF SLIGHTLY TO MODERATELY SALINE WATER
			CATAHOULA TUFF	0-500	PREDOMINANTLY TUFF, TUFACEOUS CLAY, SANDY CLAY, BENTONITIC CLAY, AND SANDSTONE	YIELDS SMALL QUANTITIES OF SLIGHTLY TO MODERATELY SALINE WATER
			UNCONFORMITY	0-200	CLAY, SAND, AND SANDY SILT	NOT AN AQUIFER IN KARNES COUNTY
			FRIJO CLAY	0-200	CLAY, SAND, AND SANDY SILT	NOT AN AQUIFER IN KARNES COUNTY
			UNCONFORMITY (?)	0-1,200	CLAY, SILT, TUFACEOUS SAND, AND VOLCANIC ASH	YIELDS SMALL QUANTITIES OF FRESH TO MODERATELY SALINE WATER
TERTIARY	Eocene	JACKSON	YEGUA FORMATION	500-1,000	SAND, SILT, AND CLAY	YIELDS SMALL QUANTITIES OF SLIGHTLY TO MODERATELY SALINE WATER
			UNCONFORMITY	400-171	CLAY AND SHALE CONTAINING SMALL AMOUNTS OF SAND, SILT, LIMESTONE, GLAUCONITE, AND SELENITE	NOT AN AQUIFER IN KARNES COUNTY
		CLAIBORNE	UNCONFORMITY	100-171	MEDIUM TO FINE SAND AND CLAY	DO
			SPARTA SAND	130-171	SHALE AND SAND	DO
		MOUNT SELMAN FORMATION	WECHES GREENSAND MEMBER	800-171	MEDIUM TO FINE SAND, SILT, AND CLAY	DO
			UNCONFORMITY (?) QUEEN CITY SAND MEMBER	200-400	MAINLY MARINE CLAY AND SHALE	DO
		WILCOX	REKLAW MEMBER	800-1,000	MEDIUM TO FINE SAND, SILT, AND CLAY	CAPABLE OF YIELDING MODERATE TO LARGE QUANTITIES OF FRESH TO SLIGHTLY SALINE WATER
			CARRIZO SAND	2,200	SILT, CLAY, FINE TO MEDIUM GRAINED SANDSTONE, SANDY SHALE, AND CLAY AND THIN BEDS OF LIGNITE	NOT AN AQUIFER IN KARNES COUNTY
		MIDWAY	UNCONFORMITY	NOT DETERMINED	UNDIFFERENTIATED SAND AND CLAY	DO
			UNDIFFERENTIATED CLAY, SILT, AND SAND	NOT DETERMINED	MAINLY CLAY AND SILT	DO

TABLE 3-9. STRATIGRAPHIC UNITS AND THEIR WATER-BEARING PROPERTIES, KARNES COUNTY, TEXAS (28)

POOR ORIGINAL

CHAPTER 3 REFERENCES

1. A.K. Lobeck; Geologic Map of the United States; The Geographical Press; 1966.
2. J.F. Davis; Uranium Deposits of the Powder River Basin, Wyoming, Union Pacific Railroad Company, 1970; (Twenty-Second Annual Field Conference-Wyoming Geological Assoc.)
3. Geologic Cross Section A-A', B-3 Area, Rocky Mountain Energy Company Bear Creek Operations; 1977.
4. V. A. Mrak, Consultant; Uranium Deposits in the Tertiary Sediments of the Powder River Basin, Wyoming; Wyoming Geological Association Guide Book; 1958.
5. Soil Survey, Converse and Natrona Counties, Wyoming; National Cooperative Soil Survey; U.S. Soil Conservation Service; 1975.
6. "Final Environmental Impact Statement, Bear Creek Project Rocky Mountain Energy Company, Converse County, Wyoming;" U.S. Nuclear Regulatory Commission; June 1977.
7. E.N. Harshman; Geology, Uranium Deposits of Shirley Basin Area, Wyoming; USGS; 1969.
8. "Final Environmental Statement, Lucky Mc Gas Hills Uranium Mill;" U.S. Nuclear Regulatory Commission; 1977.
9. W.R. Keefer; "Structural Geology of the Wind River Basin;" USGS Paper 495-D; 1970.
10. "Geology and Technology of the Grants Uranium Region, The Society of Economic Geologists;" NMIMT Memoir No. 15; Vincent C. Kelly, General Chairman, Uranium Field Conference, State Bureau of Mines and Mineral Resources; 1963.
11. "Phase II - Title I Engineering Assessment of Inactive Uranium Mill Tailings, Phillips/United Nuclear Site, Ambrosia Lake, New Mexico;" Ford, Bacon & Davis Utah Inc.; Dec 1977.
12. J.D. Purtymun, Caroline L. Wienke, David R. Dreesen; "Geology and Hydrology in the Vicinity of the Inactive Uranium Mill Tailings Pile, Ambrosia Lake, New Mexico;" Los Alamos Scientific Laboratory; June 1977.
13. "Water Quality Impacts of Uranium Mining and Milling Activities in the Grants Mineral Belt, New Mexico;" U.S. Environmental Production Agency, Region VI; Dallas, Texas; Sept 1975.

14. "Hydrology and Geology of Uranium Tailings Site at Ambrosia Lake, New Mexico;" Center for Health and Environmental Studies, Brigham Young University; Nov 1976.
15. Maker et al.; "Soil Associations and Land Classification for Irrigation, McKinley County, NM;" Agricultural Experimental Station Resource Progress Report No. 262.
16. "Applicants Environmental Report on the Church Rock, New Mexico Uranium Mill and Mine;" Vol II and Appendices; United Nuclear Corporation, 1975.
17. Geologic Atlas of the Rocky Mountain Region; Rocky Mountain Association of Geologists; Denver, Colorado; 1972.
18. W.L. Stokes, ed; Guidebook to the Geology of Utah, Uranium Deposits and General Geology of Southeastern Utah; Bulletin No. 9; Utah Geological Society; 1954.
19. "Geology and Water Resources of the Spanish Valley Area and San Juan Counties;" Utah Technical Publication No. 32; Department of Natural Resources; 1971.
20. W.L. Stokes; Utah Geological and Mineralogical Survey, Uranium-Vanadium Deposits of the Thompsons Area, Grand County, Utah (with emphasis on the origin of Carnotite ores); Bulletin No. 46; Dec 1952.
21. R.P. Fischer and L.S. Hilbert; "Geology of the Uravan Mineral Belt;" USGS Bulletin 988 - A; 1952.
22. H.S. Johnson Jr. and W. Thordaison; "Uranium Deposits of the Moab, Monticello, White Canyon, and Monument Valley Districts, Utah and Arizona;" USGS Bulletin 1222 - M; 1966.
23. B.B. Hanshaw and G.A. Hill; "Geochemistry and Hydrodynamics of the Paradox Basin Region, Utah, Colorado and New Mexico;" Chemical Geology; 4., p. 263 - 294; 1969.
24. D. Price and T. Arnow; "Summary Appraisals of the Nation's Ground Water Resources - Upper Colorado Region;" USGS Professional Paper 813 - C; 1974.
25. "Draft Environmental Statement Related to Operation of Moab Uranium Mill;" U.S. Nuclear Regulatory Commission; Nov 1977.
26. C.H. Hunt; Physiography of the United States, W.H. Freeman and Co.; 1967.

27. H.D. Eargle, and J.L. Snider; "A Preliminary Report on the Stratigraphy of the Uranium Bearing Rocks of the Karnes County Area, South Central Texas;" Bureau of Economic Geology; University of Texas Report of Investigations No. 30; July 1957.
28. R.B. Anders; "Ground Water Geology of Karnes County, Texas;" USGS Water Supply Paper 1539 - G; 1962.
29. Folk et al.; Field Excursion Central Texas 10th National Clay Conference, Guidebook No. 3; Bureau of Economic Geology; Oct 1961.
30. E. Raisz; "Landforms of the United States;" to accompany Atwood's "Physiographic Provinces of North America;" 1957.
31. W.C. Larson; Uranium In Situ Mining in the United States; Information Circular 8777; Bureau of Mines, U.S. Department of the Interior; 1978.

CHAPTER 4

DIFFUSION THEORY EXPRESSIONS USED TO INTERPRET THE LABORATORY DATA

Previous studies of radon diffusion have not considered sources of radon within the cover material.⁽¹⁻³⁾ The following theoretical development incorporates a source in the cover material and allows the effective diffusion coefficient of the cover material to be different from that of the tailings. This gives unique definition of the sources in the tailings and cover material as well as their diffusion properties.

4.1 RADON SOIL GAS CONCENTRATION USING FINITE SOURCES

As the radon flux approaches background values, sources within the cover material will contribute to the radon flux and limit the lower value of the flux attainable. For this reason, a radon source in the cover material has been incorporated in the diffusion equation to determine the radon soil gas concentration and flux.

4.1.1 General Diffusion Equation

Diffusion theory was used to model the radon concentration and radon exhalation from a test chamber as shown in Figure 4-1. The main limitation of the theory is a result of assuming that the flux is proportional to the concentration gradient as given by Fick's law:

$$J'(x) = -D \frac{dC(x)}{dx} \quad (1)$$

or equivalently

$$J(x) = -D_e \frac{dC(x)}{dx}$$

where

$J'(x)$ = the radon flux in the pore space (pCi/m²s)

$J(x)$ = the radon flux from the cover material (pCi/m²s)

D = the diffusion coefficient of radon in the soil gas
(m²/s)

$dC(x)/dx$ = the radon concentration gradient in the soil gas
(pCi/m⁴)

The diffusion coefficient, D , applies to the migration of radon through the soil gas. It is often expressed as an effective diffusion coefficient, D_e , by correcting for the fraction

(1) See end of chapter for references.

of a unit volume which is void; i.e. $D_e = pD$, where p is the porosity of the material.

The limitation from Fick's Law occurs because the gradient is not continuous across a boundary with a medium which acts as an infinite sink to radon gas. This is the case when radon leaves the soil and mixes in a turbulent manner with the air.

The general diffusion equation is derived from the steady-state equation of continuity where, for a particular infinitesimal volume in the tailings or cover material, the radon source(s) equals the losses due to leakage and decay or

$$\nabla \cdot \vec{J} + p\lambda C = S' \quad (2)$$

where,

$\nabla \cdot \vec{J}$ = the leakage from the infinitesimal volume in the pore space or the divergence of the flux ($\text{pCi}/\text{m}^3\text{s}$)

λ = the decay constant of radon (s^{-1})

C = the radon concentration in the soil gas (pCi/m^3)

S' = the radon source ($\text{pCi}/\text{m}^3\text{s}$)

Using Fick's law and rearranging yields

$$\frac{d^2C}{dx^2} - a^2C + S = 0 \quad (3)$$

where,

$$a^2 = \frac{\lambda p}{D_e}$$

$$S = \frac{S'}{D_e}$$

4.1.2 Boundary Condition

The solution of equation (3) for the concentration has the general form of

$$C_t = Ee^{a_t X} + Fe^{-a_t X} + \frac{S_t}{a_t^2} \quad (4)$$

in the tailings and

$$C_c = Ge^{a_c X} + He^{-a_c X} + \frac{S_c}{a_c^2} \quad (5)$$

in the cover material. The constants E , F , G , and H are determined by the boundary conditions of the system. The above solutions are general in nature and allow the use of different source terms and diffusion coefficients in the tailing and cover as expressed by a_t and a_c .

The boundary conditions (B.C.) applicable to the experiments performed for this study are:

1. $J_t(0) = 0$ the flux is zero at the bottom of the test chamber,
2. $C_t(a) = C_c(a)$ the concentration is continuous across the interface of the tailings and cover material,
3. $J_t(a) = J_c(a)$ the flux is continuous across the interface,
4. $C_c(b) = C_0$ the concentration must equal the experimentally determined concentration at some position in the test chamber.

The coordinate system used for these equations is shown in Figure 4-1.

Using equation (4) and B.C. (1)

$$J_t(0) = 0 = Ea_t - Fa_t$$

or $E = F$

The concentration in the tailings can then be written as

$$C_t = 2E \cosh(a_t x) + Q_t \tag{6}$$

where

$$Q_t = S_t/a_t^2$$

Using equation (5) and B.C. (4) yields

$$C_c(b) = C_0 = Ge^{a_c b} + He^{-a_c b} + Q_c$$

where

$$Q_c = S_c/a_c^2$$

Solving for H and substituting, C_c can be written as

$$C_c = 2Ge^{a_c b} \sinh[a_c(x - b)] + (C_0 - Q_c)e^{-a_c(x - b)} + Q_c \tag{7}$$

Boundary conditions (2) and (3) can be used to solve for E and G in equations (6) and (7) respectively, yielding the following:

$$E = \frac{Z[1 + Z \coth(a_t a)] (C_o - Q_c) e^{-a_c(a-b)} + Z(Q_c - Q_t)}{2 \sinh(a_t a) [Z \coth(a_t a) - \tanh[a_c(a-b)]]} + \frac{Z(C_o - Q_c) e^{-a_c(a-b)}}{2 \sinh(a_t a)}$$

$$G = \frac{[1 + Z \coth(a_t a)] (C_o - Q_c) e^{-a_c a} + (Q_c - Q_t) e^{-a_c b}}{2 \cosh[a_c(a-b)] [Z \coth(a_t a) - \tanh[a_c(a-b)]]} \quad (8)$$

where

$$Z = \frac{D_c a_c}{D_t a_t}$$

The radon concentration in the tailings and cover material can then be written as

$$C_t = \left[\frac{Z[1 + Z \coth(a_t a)] (C_o - Q_c) e^{-a_c(a-b)} + Z(Q_c - Q_t)}{[Z \coth(a_t a) - \tanh[a_c(a-b)]]} \right] \frac{\cosh(a_t x)}{\sinh(a_t a)} \\ + Z(C_o - Q_c) e^{-a_c(a-b)} \frac{\cosh(a_t x)}{\sinh(a_t a)} + Q_t$$

and

$$C_c = \left[\frac{[1 + Z \coth(a_t a)] (C_o - Q_c) e^{-a_c(a-b)} + (Q_c - Q_t)}{[Z \coth(a_t a) - \tanh[a_c(a-b)]]} \right] \frac{\sinh[a_c(x-b)]}{\cosh[a_c(a-b)]} \quad (9)$$

$$+ (C_o - Q_c) e^{-a_c(x-b)} + Q_c$$

4.1.3 Source Modeling

The radon source S in either the tailings ($i = 1$) or the cover material ($i = 2$) can be modeled by

$$S_i = \frac{R_i \rho_i \lambda E_i}{D_e^i} \quad (10)$$

where

R_i = ^{226}Ra density in the material (pCi/g)

E_i = the emanating power of the material

D_e^i = effective diffusion coefficient of the material (m^2/s)

ρ_i = the density of the material (g/m^3)

λ = the decay constant of radon (s^{-1})

These parameters were determined experimentally for this study.

4.2 FLUX AS A FUNCTION OF THICKNESS OF BARE TAILINGS

The flux across the surface of bare tailings was modeled previously⁽³⁾ and given by the following equation:

$$J_t(a) = \frac{D_e^t}{a_t} \tanh(a_t a) [S_t - C_0 a_t^2] \quad (11)$$

The maximum flux, given in equation (11), is obtained when a , the tailings thickness, increases to infinity, approximately 15-20 ft.

$$J_t(\infty) = \frac{D_e^t}{a_t} [S_t - C_0 a_t^2]$$

The ratio of the flux from tailings of a finite thickness to the infinite thickness flux is:

$$\frac{J_t(a)}{J_t(\infty)} = \tanh(a_t a) \quad (12)$$

In general, $C_0 a_t^2$ is negligible so that equation (11) can be written as

$$J_t(a) = R_t E_t \rho_t \sqrt{\lambda D_e^t / \rho} \tanh \left(\sqrt{\lambda \rho / D_e^t} a \right) \quad (13)$$

4.3 FLUX AS A FUNCTION OF COVER MATERIAL THICKNESS

Using Fick's law, equation (1), and the radon concentration in the cover material as given by equation (9), the flux from the test chamber is found to be:

$$J_c = -D_e^c a_c \left[\frac{[1 + Z \coth(a_t a)] (C_o - Q_c) e^{-a_c(a-b)} + (Q_c - Q_t)}{[-\tanh[a_c(a-b)] + Z \coth(a_t a)]} \frac{\cosh[a_c(x-b)]}{\cosh[a_c(a-b)]} \right] \quad (14)$$

$$+ D_e^c a_c (C_o - Q_c) e^{-a_c(x-b)}$$

4.4 ALTERNATIVE EXPRESSION FOR THE RADON FLUX AS A FUNCTION OF COVER THICKNESS

Additional insight into the function of the diffusion coefficient may be obtained in the following manner. If the co-ordinate system is redefined as shown in Figure 4-1, then $x = 0$ at the interface of the tailings and the cover. The primed letters will differentiate equations using the new co-ordinate system from those used in the preceding sections of Chapter 4. Equation (5) remains the same; i.e.,

$$C_c = A e^{-a_c x} + B e^{a_c x} + \frac{S_c}{a_c^2} \quad (15)$$

and the flux is expressed as

$$J_c = D_e^c a_c A e^{-a_c x} - D_e^c a_c B e^{a_c x} \quad (16)$$

where A and B are defined by the boundary conditions, which in the new coordinate system (see Figure 4-1) are

1. $J_t(-a') = 0$
2. $C_t(0) = C_c(0)$
3. $J_t(0) = J_c(0)$
4. $C_c(b') = C_o$

In all cases the subscripts t and c refer to the tailings and cover, respectively.

The flux at the surface of the cover material may be expressed by

$$J_c(b') = D_e^c a_c (A - B e^{-2 a_c b'}) e^{-a_c b'} \quad (17)$$

Application of the boundary condition number 4 gives the result, after re-arranging

$$J_c(b') = D_e^c a_c \left[2 A e^{-a_c b'} + \left(\frac{S_c}{a_c} - C_0 \right) \right] \quad (18)$$

If the effects of the radon source in the cover are neglected, then equation (18) becomes, for the radon from tailings that is migrating through the cover,

$$J_c(b') = 2 D_e^c a_c A e^{-a_c b'} \quad (19)$$

Application of the remaining boundary condition yields the following expression for A (neglecting S_c and C_0).

$$A = \frac{D_e^t \frac{S_t}{a_t} \tanh a_t a'}{D_e^t a_t (1 - e^{-2 a_c b'}) \tanh a_t a' + D_e^c a_c (1 + e^{-2 a_c b'})}$$

or, from equation (13)

$$A = \frac{J_0}{D_e^t a_t (1 - e^{-2 a_c b'}) \tanh a_t a' + D_e^c a_c (1 + e^{-2 a_c b'})} \quad (20)$$

where J_0 is the bare tailings flux at $x = 0$.

Substituting equation (20) into equation (19) yields

$$J_c(b') = \left[\frac{2 J_0}{1 + \left(\frac{D_e^t}{D_e^c} \right) \left(\frac{a_t}{a_c} \right) \tanh a_t a' \tanh a_c b'} \right] \frac{e^{-a_c b'}}{(1 + e^{-2 a_c b'})} \quad (21)$$

or,

$$J_c(b') = J_0 f(b') e^{-a_c b'} \quad (22)$$

where

$$f(b') = \frac{2}{\left[1 + \left(\frac{D_e^t}{D_e^c} \right) \left(\frac{a_t}{a_c} \right) \tanh a_t a' \tanh a_c b' \right] (1 + e^{-2a_c b'})} \quad (23)$$

It is noted that at $b' = 0$, $f(0) = 1$, and at $b' = \infty$,

$$f(b') = \frac{2}{1 + \left(\frac{D_e^t}{D_e^c} \right) \left(\frac{a_t}{a_c} \right) \tanh a_t a'}$$

Therefore, $f(b')$ varies between 1 and 2 for $D_e^t \leq D_e^c$.

If a new function, $h(b')$, is defined as follows:

$$h(b') = \left[1 - \frac{\ln f(b')}{a_c b'} \right]^{-2} \quad (24)$$

Then, equation (22) can be written

$$J_c(b') = J_0 \exp \left(-\sqrt{\frac{\lambda p}{D_e^c h(b')}} b' \right) \quad (25)$$

$$= J_0 \exp \left(-\sqrt{\frac{\lambda p}{D_A^c}} b' \right) \quad (26)$$

where

$$D_A^c = D_e^c h(b')$$

Examination of equation (23) shows that the ratio of the diffusion coefficients (D_e^t/D_e^c) also affects the value of $f(b')$ and, hence, $h(b')$.

For large values of b' , equation (24) yields

$$h(b') = 1$$

which means that

$$D_A^C = D_e^C$$

In general, when using equation (26) for describing the attenuation of radon through cover material, D_A should be used; however, D_e^C may be used in equation (26) when b' is large and $h(b')$ approaches unity. It should be noted that as b' increases, $f(b')$ approaches a constant value which is not necessarily unity; hence the approximation of using D_e in equation (26) for large b' may not yield the same flux as the exact expression. It is within a factor of two, however, and is a significantly smaller error than the error arising from the uncertainties in the values of the diffusion coefficients. The data reported in Chapter 5 will give further insight into the physical significance of the equations which have been discussed.

When equation (13) is applied to a thick, bare tailings pile or to an exhaling soil surface, it takes the form:

$$J_t(\infty) = R_t \rho_t E_t \sqrt{\lambda D_e^t / P_t} \quad (27)$$

This is due to the large value of a , the tailings or soil thickness. Equation (27) has been used widely for radon flux calculations and is equivalent to the equation given by Junge⁽⁴⁾ if $d = D_e^t / P_t$ is assumed to apply to the interstitial volume. The omission of porosity from radon diffusion calculations in much of the early literature (before 1964) has led to errors and discrepancies in many published diffusion coefficients. These have been reviewed and discussed by Culot et al.,⁽²⁾ and again by Tanner.⁽⁵⁾ Equation (27) was also appropriately used to estimate the bare tailings flux, J_0 , from "thick" tailings piles in the Generic Environmental Impact Statement (GEIS) on Uranium Milling.⁽⁶⁾

More general equations for radon flux from a bare tailings surface do not require a "thick" tailings source. Equation (13) assumes only that the radon flux into the underlying soil is negligible. This assumption originated in the present "sealed bottom" experiments, and is probably valid for many thin tailings piles which lie on wet sand or clay bases. Haywood et al.⁽⁷⁾ have reported an even more general equation, using the symbols in this report:

$$J_t = \frac{D_e^t a_t^2}{P_t} R_t \rho_t E_t \left[\frac{a_s D_e^s \cosh(a_t X) + a_t D_e^t \sinh(a_t X) - a_s D_e^s}{a_t D_e^t \cosh(a_t X) + a_s D_e^s \sinh(a_t X)} \right] \quad (28)$$

This equation explicitly accounts for radon diffusion into the underlying soil, which has an effective diffusion coefficient of D_e^i and an inverse relaxation length α_s . This equation was also used in comparing radon emissions from uranium mills and other enhanced and natural sources. (8)

Radon flux from a cover material placed over a tailings pile is often expressed as a function of the bare tailings flux, J_0 , as in equation (26). In order to accommodate multiple-layered tailings covers as envisioned in some tailings reclamation proposals, equation (26) also can be expressed as

$$J_c = J_0 e^{-\sum_{i=1}^n \alpha_i a_i} \quad (29)$$

In this equation the various cover materials, i , have a cumulative attenuating effect on the bare tailings flux, J_0 . The use of

$$\alpha_i' = \sqrt{\lambda P_1 / D_A^i}$$

in equation (29) should be noted, since D_A^i differs from D_e^i by the factor $h(b')$. The factor

$$h(b') = D_A^i / D_e^i$$

can be shown to approach unity at very large b' , but has values between 1.2 and 10 for typical cover thicknesses, as will be shown in Chapter 5. The substitution of α_i for α_i' in equation (29) thus would suggest an erroneously high flux attenuation compared with the proper use of α_i' . Equation (29) was used in the GEIS on uranium milling (6) in estimating radon flux from a tailings pile covered by layers of clay, overburden, and topsoil.

Radon flux from homogeneous (nonlayered) tailings covers can be calculated from the general equation (14), or as reported by Macbeth et al., (3) as follows:

$$J_c = D_e^c \left[\frac{S \sinh(a a) - C_0 a^2 \sinh(a b)}{a \cosh(a b)} \right] \quad (3)$$

In this equation, a is assumed to be constant for both the tailings and cover material.

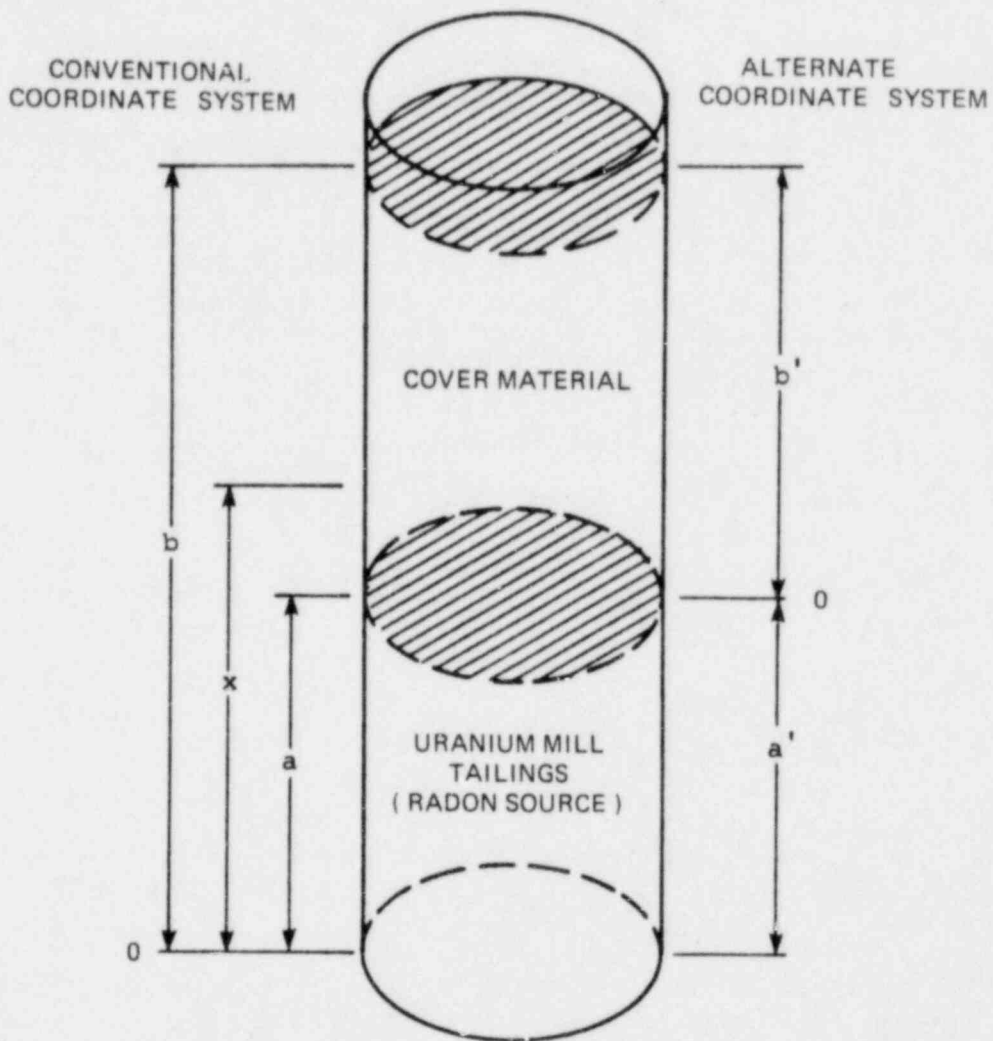


FIGURE 4-1. SCHEMATIC REPRESENTATION OF RADON SOURCE AND COVER MATERIAL

CHAPTER 4 REFERENCES

1. M.V.J. Culot, H.G. Olson, and K.J. Schiager; "Radon Progeny Control in Buildings;" Colorado State University; COO-2273-1 UNCLAS; May 1973.
2. M.V.J. Culot, K.J. Schiager, and H.G. Olson; "Prediction of Increased Gamma Fields After Application of a Radon Barrier on Concrete Surfaces;" Health Physics; 30; pp. 471-478; June 1976.
3. P.J. Macbeth, et al.; "Laboratory Research on Tailings Stabilizations Methods and Their Effectiveness in Radiation Containment;" Department of Energy Report GJT-21; Apr 1978.
4. C.E. Junge; Air Chemistry and Radioactivity; Academic Press; New York; 1963.
5. A.B. Tanner; "Radon Migration in the Ground: A Supplementary Review;" U.S. Geological Survey Open-File Report 78-1050; and Proceedings, Third Int'l. Symposium on the Natural Radiation Environment, Houston, Texas; Apr 1978.
6. U.S. Nuclear Regulatory Commission; "Draft Generic Environmental Impact Statement on Uranium Milling;" NUREG-0511; V2, Appendix P; Apr 1979.
7. F.F. Haywood, W.A. Goldsmith, P.T. Perdue, W.F. Fox and W.H. Shinpaugh; "Assessment of Radiological Impact of the Inactive Uranium-Mill Tailings Pile at Salt Lake City, Utah;" ORNL/TM-5251; Nov 1977.
8. C.C. Travis, A.P. Watson, L.M. McDowell-Boyer, S.J. Cotter, M.L. Randolph, and D.E. Fields; "A Radiological Assessment of Radon-222 Released from Uranium Mills and Other Natural and Technologically Enhanced Sources;" NUREG/CR-0573, ORNL/NUREG-55; Feb 1979.

CHAPTER 5

EXPERIMENTAL RESULTS AND DISCUSSION

5.1 RADON SOURCE PARAMETERS

The determination of any unknown can be made if the number of unknown variables including the unknown of interest is less than or equal to the number of equations which can be generated from the data. If there are fewer unknown variables than equations or data points, the unknown variables are best determined by least-squares-fitting to the available data. Specifically, to determine the diffusion coefficient of a material as accurately as possible, as many unknowns as possible must be eliminated. All unknowns within the equations of concentration and flux given in Chapter 4 can be determined experimentally, leaving only the diffusion coefficient unknown. By the method of least-squares-fitting to the data, the diffusion coefficient can then be determined.

The following sections describe the determination of the diffusion coefficient, the radium content in the source tailings and cover, emanating power, density, and porosity of each.

5.1.1 Radium Content and Emanating Power of the Tailings Source

The tailings radon source as described in Chapter 4 is a function of radium content, emanating power, density, and diffusion coefficient. The tailings used for this study were obtained from the Vitro site in Salt Lake City, Utah; previous data concerning these tailings are available.⁽¹⁾ Some modification of the previous parameters was expected since the tailings were obtained during the winter for the experiments reported in this report and large amounts of moisture were contained within the tailings.

Subsequent measurements of each source determined the moisture content to range from 9 to 27% by weight. The tailings were used as they were obtained. The cold conditions during winter made natural means of drying the tailings impossible, and the high cost of drying the tailings commercially was prohibitive. Tanner indicates that moisture will affect the emanating power as well as the diffusion coefficient and some adjustment must be made to compensate for its effect upon the radon source.⁽²⁾

Each radon source used consisted of 0.61 m of tailings in the bottom of a test chamber 0.61 m in diameter. The flux from the bare tailings is given by the general equation:

(1) See end of chapter for references.

$$J(x) = \frac{D_t S_t \tanh(a_t x)}{a_t} \quad (1)$$

For small values of $a_t x$, the flux is independent of the diffusion coefficient of the tailings and is given by

$$J(x) = R_t \rho_t \lambda E_t x \quad (2)$$

The emanating power determined for dried tailings was found to be $29.8 \pm 1.8\%$ by weight for eight replicate samples. Because satisfactory experimental or theoretical dependence of the emanating power on moisture does not exist, no correction of the emanating power was made.

Large variations in the values of the concentration of the radium in the Vitro tailings have been reported. Listed below are those values of the radium concentration as determined by several sources.

Commercial Laboratory #1	4422 \pm 50	pCi-Ra/g
	3630 \pm 30	pCi-Ra/g
Commercial Laboratory #2	140 \pm 10	pCi-Ra/g
	70 \pm 1	pCi-Ra/g
FB&DU		
(six replicate samples of initial batch of tailings)	1540 \pm 160	pCi-Ra/g
(eight replicate samples, one from each test chamber)	1260 \pm 170	pCi-Ra/g

The radium concentrations measured by FB&DU were obtained by taking a sample of the material and applying the method of Scott and Dodd.⁽³⁾ Values obtained for the radium content and diffusion coefficient of the Vitro tailings which served as the radon source for the cover soil measurements are listed in Table 5-1.

In the subsequent data reduction and analysis that required the parameters associated with the tailings radon source, the actual radium concentration and diffusion coefficient as measured by FB&DU were used. The values given in Table 5-1 were selected for use because they are consistent with average radium concentrations from mill records and with the measured moisture concentrations. The radium concentrations listed in Table 5-1 for set 2 were based on composite analyses, and thus produced an average diffusion coefficient for the entire set when applied to the same measured fluxes used for normalization.

5.1.2 Radium Content and Emanating Power of the Selected Cover Materials

Eight cover materials from three major mining districts and one area removed from any mining activity were selected for this study. The mining regions were the Powder River and Shirley Basins of Wyoming, and the Ambrosia Lake region of New Mexico. The nonmining region selected was Rawlins, Wyoming. Cover material from a non-mining region was selected so that soil with an expected lower ambient concentration of radium might be tested. All major properties of the soils are summarized in Table 5-2.

The radium content of the cover materials selected for this study averaged 3.4 ± 1.9 pCi radium per gram of material. This is higher than the 1 or 2 pCi radium per gram soil expected for naturally occurring background concentrations of radium in soil but is probably typical of overburden taken from a mining area. It was desirable to study covers which would be used to cover actual tailings piles, so the material selected was that suggested by mining personnel in the area. The cover material was obtained during the winter and possibly contained more moisture than normal.

The radium content of the samples from the non-mining region was 1.5 and 2.2 pCi radium per gram soil, which was near expected background values. Of the samples studied, the concentrations in the cover from the Shirley Basin were high and might indicate the ore-bearing material was in closer proximity to the cover than in other regions. It should be noted that the fraction passing through a #200 Tyler sieve is also very large for the Shirley Basin covers. The correlation between percent passing #200 sieve and radium content will be considered in greater detail later.

The emanating power of the selected cover materials ranged from 10 to 75%. Determination of the emanating power for samples with such small concentrations of radium was difficult because of poor counting statistics, although determination of the emanating power in replicate samples showed small variation. The radium concentration in the cover materials has little effect upon the determination of the diffusion coefficient for the cover material because the cover source is small compared to the tailings source.

In addition to the selected cover materials, other materials from the Gas Hills region were analyzed for radium content and emanating power to provide additional data. The diffusion coefficients of these samples were not determined.

5.1.3 Radium Content and Emanating Power of Selected Tailings Samples

In addition to the cover materials selected, tailings

samples were also obtained from each of the four mining regions. Two samples were taken from the Shirley Basin, four from Powder River, four from the Gas Hills and six from the Ambrosia Lake Region. These samples were labeled sandy and slime fractions, depending upon the location from which they were obtained. The sandy fraction was taken from near the discharge point of the mill where the larger and more coarse particles would precipitate. The slime fraction was obtained from a point far from the discharge point where the finer particles had precipitated. There was no attempt to classify the tailings, other than by physical description, in the field.

The radium content of the tailings, as shown in Table 5-2, correlated quite well with particle size. The correlation, shown in Figure 5-1, gives the radium content as a function of particle size. The line is given as an aid to visualize the correlation and no functional fit has been made. The significance of the correlation is that a smaller tailings particle size can be associated with a larger radium content. It should be noted that the same type of correlation was seen in the cover materials (Section 5.1.2) and is consistent with the radium being associated with smaller particles which may be ground from the surface of larger particles.

Figure 5-2, which shows the percent emanating power as a function of percent passing a #200 Tyler sieve, indicates that as the size of the particle increases the emanating power may decrease. There are not enough data points, however, for definitive correlations to be obtained.

5.1.4 Soil Mechanical Properties

Determination of the soil mechanical properties was obtained by Dames & Moore under subcontract to FB&DU. Several of the more important parameters are summarized in Table 5-2 and the complete Dames & Moore report is given in Appendix A. The properties of the set 2 replicate soil samples are summarized in Table 3-2. The soil classification scheme is presented in Figure 5-3. Note that the most sandy classification obtained for the cover materials was SM-SP, indicating that the cover materials were mostly silty-sands or clay material. The maximum dry density reported is the theoretical maximum density obtained by compacting the soil with optimum moisture content and then drying the sample. Moisture aids in compaction; therefore, maximum compaction is obtained when the moisture is closely controlled. Moisture content greater than the optimum moisture degrades the mechanical strength of the soil. At 30% moisture, for example, Powder River clay acts like a highly viscous fluid and is unable to support a shear force.

It is important to understand the difference between porosity and void ratio. Porosity (p) is the ratio of void space to the total volume, whereas the void ratio (v) is the ratio of void space to space occupied by solids. Porosity

may be defined in terms of void ratio in the following manner:

$$P = \frac{v}{1 + v}$$

Typical porosities and void ratios for cohesionless soils are presented in Table 5-3. Cohesionless soils are soils which do not adhere to each other, e.g. sands. "Clay deposits [which are not cohesionless soils] with flocculent structures will have high void ratios, low density, and quite probably high water content." (4) High void ratios give correspondingly high porosities. The most sandy soil obtained for this study was classified as SM or silty sand and is indicated in Table 5-3 as a micaceous sand with silt having porosities in the range of 0.43 to 0.56. All soils for this study had porosities in the range of 0.42 to 0.57 with the exception of the Ambrosia Lake shale at 0.60. Therefore, the porosities obtained in the laboratory are in line with the porosities of typical soils found in nature.

The compaction of soils in the laboratory was performed using tamping tools but no special effort was made to crush the soils into uniform sizes which would compact more easily. Variations in the compaction can be attributed to differences in the sizes of the clay particles and the moisture content of the soils. Compaction in the field would typically approach 90-95% whereas in the laboratory compaction ranged from 65-89%.

5.2 DETERMINATION OF THE EFFECTIVE DIFFUSION COEFFICIENT FOR THE SELECTED COVER MATERIALS

Effective diffusion coefficients were determined two ways for each cover soil tested. First, the diffusion coefficient was determined by least-squares fitting the measured radon flux at 0.31, 0.91, and 1.83 m of cover material for set 1 and 2.74 and 3.66 m for set 2 by varying the diffusion coefficient in the theoretical equations derived for flux in Chapter 4. The second method involved fitting the radon gas profiles in the test chamber with the theoretical equation for the concentration and varying the diffusion coefficient to obtain the best fit. The two values for the diffusion coefficient varied for a common material. The ratio of the diffusion coefficient from flux measurements to the diffusion coefficient of the concentrations measurements ($D_e(\text{flux})/D_e(\text{conc})$) ranged from 0.5 to 1.8; however, the average ratio was 1.3. These values are within those that might be expected when the data are determined from the measurement of two different parameters with uncertainties associated with those parameters. These results lead to confidence in the theoretical models that were used to determine the diffusion coefficients.

5.2.1 Determination of the Effective Diffusion Coefficient Using Radon Flux Profiles

The variability of the radium concentrations in the tailings source makes it difficult to determine the radon source parameters in a consistent manner which would also be applicable to field measurements. Flux measurements are relatively easy to make in the field, so the method of determining the effective radium concentration might be appropriately centered around such measurements. The procedure used to characterize each source is outlined in Section 5.1. Two flux profiles are shown in Figures 5-4 and 5-5. These two figures are representative of the data for each of the cover soils described in Table 5-2. The effects due to different moisture content in sets 1 and 2 also are illustrated. Table 5-4 lists the flux measurements from which the flux diffusion coefficients were determined for each of the soils. The diffusion coefficients corresponding to these data are given in Table 5-5 with the weighted-least-squares value for each cover soil.

Two curves are shown in each of Figures 5-4 and 5-5. The solid line represents the theoretical fit of the exact equation to the data and the dashed line represents the fit of the alternate equation. Both of these curves show a relatively good fit to the flux measurements when the uncertainty of the data is considered. Values of the alternate diffusion coefficient (D_A) calculated from the raw flux data are given in Table 5-6. Table 5-7 shows the diffusion coefficients which result from the exact and the alternate solutions listed in Chapter 4 and the moistures, porosities, and densities associated with each.

The exact diffusion coefficient, D_e , has a range of values from 1.8×10^{-3} to 3.2×10^{-2} cm^2/s . Values of the alternate diffusion coefficient, D_A , vary from 1.6×10^{-3} to 2×10^{-1} cm^2/s . It is to be expected that D_A will be larger than D_e when the conditions which define D_A are considered. The ratios of D_A/D_e calculated for the various soils and from equation (24) are shown in Figure 5-6, and verify the positive bias of D_A . The error in flux which results from using D_e in place of D_A in equation (26) is expressed as $f(b')$ in equation (22). The function $f(b')$, as illustrated in Figure 5-6, increases rapidly from unity in the first meter and approaches a constant (1.5 for the cover materials tested here) at slightly greater cover thicknesses.

5.2.2 Determination of the Effective Diffusion Coefficient Using Radon Concentration Profiles

Figures 5-7 and 5-8 represent the measurements of the radon concentration in the Shirley Basin Soil No. 2 and the Ambrosia Lake Soil No. 1, respectively. The curves shown with the data points are the result of fitting the theory to the actual measurements. Table 5-8 lists the radon concentration values for the cover soils at various distances from the interface of

the tailings and the cover material. Values of the diffusion coefficient that result from the curve fit of the concentration data are shown in Table 5-9. The values of $D_e^{(conc.)}$ vary from $1.4 \times 10^{-3} \text{ cm}^2/\text{s}$ to $1.3 \times 10^{-2} \text{ cm}^2/\text{s}$. As noted previously, these values are generally slightly lower than $D_e^{(flux)}$.

5.3 VARIATION OF THE DIFFUSION COEFFICIENT WITH MOISTURE CONTENT

Moisture can affect the diffusion coefficient of a porous medium in two ways: first, by blocking the pores of the medium and decreasing the porosity; and second, by absorbing radon. The diffusion coefficient measured for various amounts of moisture are then intermediate diffusion coefficients between the system when dry air is the transporting medium in the porous material and the system where water is the transporting medium.

Laboratory measurements of the diffusion coefficient at intermediate moisture contents were performed by adding known amounts of water to the cover material and placing these over the tailings radon source. Moisture probes were used to ascertain the moisture content of the cover material as a function of time. Values measured during this study and others reported by Tanner are given in Table 5-7 and Table 5-10. Plotting on semilogarithmic paper shows the exponential nature of the diffusion coefficient as a function of moisture content in the limited transition region (Figure 5-9).

A least-squares fit to the data yields the curve given in Figure 5-9. The equation describing the fit is

$$\begin{aligned} D_e &= 0.106 p \exp(-0.261 M) \\ &= 0.106 p \exp(-0.261 pm) \end{aligned} \quad (5)$$

where

- p = porosity of dry system
- M = percent moisture of system
- m = fractional moisture saturation of system

The goodness of fit for this relation is 0.95. In fitting the data, the Wyoming No. 2 value was omitted because of the exceeding low moisture, and Ambrosia Lake No. 1 was also omitted. Flux and concentration measurements on the test chamber containing Ambrosia Lake Soil No. 1 were anomalous. The high porosity (0.60) of the shale soil is thought to be the reason for the lack of consistency in the measurements.

It is also noted that D_e can be represented as a function of moisture by the geometric mean for dry tailings and saturated tailings, weighted with respect to the fractional moisture saturation. Mathematically, this is expressed as equation (6) which yields the same line as plotted in Figure 5-9 for the

exponential function of equation (5).

$$D_{e(m)} = D_{e(m=0)}^{(1-m)} D_{e(m=1)}^m \quad (6)$$

5.4 RADON FLUX REDUCTION DUE TO THE BEAR CREEK CONFIGURATION

Alternative 3 of the Bear Creek proposal (6) was modeled in the laboratory using a 0.61-m thickness of Vitro tailings as a radon source. The initial flux from the tailings before covering was 175 pCi/m²s. A 0.30-m thickness of Rocky Mountain Energy (RME) clay containing 30% moisture by weight was added to the column. The moisture content was above the optimum moisture content for maximum compaction but conformed to the alternative specifications. The clay behaved like a viscous fluid and would not support a shear force. Another 1.54 m of RME soil was added above the moist clay and the column allowed to come to equilibrium.

As shown in Figure 5-10, the final flux obtained was 16 pCi/m²s. Figure 5-10 also shows the flux and the moisture content of the clay as a function of time as they approached equilibrium.

Changes in the moisture content of the clay can be attributed to redistribution within the clay due to the nonuniform addition of moisture. Moisture probes were placed in the clay 7.6 cm, 15.2 cm and 22.8 cm from the clay-tailings interface. The lower and center probes indicated increase in moisture content with time while the top probe indicated the clay was drying out. No probes were placed in the tailings to verify fluctuation in the moisture content. The errors in the absolute moisture measurements were generally $\pm 5\%$ moisture.

The alternate formula of Chapter 4 for the flux reduction was used to predict the resultant flux of the Bear Creek configuration and a value of 1.4 pCi/m²s was obtained. The additional flux from the cover material was calculated by considering the cover to be a radon source. Using the properties of the cover material an additional radon flux of 10.9 pCi/m²s was calculated. The sum of the reduced flux from the tailings and the background flux from the cover material is 12.3 pCi/m²s. This value is in good agreement with the experimental determination, which is 16 pCi/m²s.

5.5 SURFACE RADON FLUX AS A FUNCTION OF BARE URANIUM TAILINGS DEPTH

The surface radon flux of Ambrosia Lake tailings #1-1 was studied as a function of its depth. A diffusion coefficient of 8.8×10^{-2} cm²/s was determined by least-squares fittings of the flux profile. Previous measurements of similar Vitro

tailings gave diffusion coefficients in the range of 3.8×10^{-2} to 6.0×10^{-2} cm^2/s . (1)

The test chamber was similar in design to that used by Macbeth et al., and consisted of a cylindrical tube 0.31 m in diameter. It was in three sections, each section being 1.52 m in length. The test was performed by filling the first section with tailings, waiting approximately one week for equilibrium to be established, and then performing several flux measurements. The second section was then added to the first section, filled with tailings and the process repeated. Similar steps were taken for the third section.

A plot of the normalized flux as a function of tailings thickness is given in Figure 5-11. The highest flux, measured for the three sections together, was 115 $\text{pCi}/\text{m}^2\text{s}$. All flux measurements were normalized to this value in Figure 5-11. The shape of the curve showed an exponential approach to the maximum flux value. This result means that the effective upper limit to the obtainable flux for the Ambrosia Lake tailings is 115 $\text{pCi}/\text{m}^2\text{s}$.

5.6 RADON FLUX ALTERATIONS DUE TO VEGETATIVE ROOT PENETRATION

Plants typical of those proposed in Wyoming reclamation plans for mill tailings piles were planted in cover soil over tailings in test columns. During the fore part of this experiment, the test columns containing the plants were under the supervision of Native Plants, Inc., a Salt Lake City nursery. Their final report is reproduced as Appendix B of this document. FB&DU was responsible for making the flux measurements while the plants were in the nursery. These measurements were made using the Lewis flask technique which is described in Section 2.1.4 of this report.

The data collected during the summer months from May through September showed a large variation in flux values. Moisture is known to effect the radon exhalation in a major way. Since FB&DU was not able to control the watering schedule of the nursery, it was determined to move three of the test columns from the nursery to controlled surroundings in an FB&DU laboratory. Two of the test columns were growing wheat grass and one column had the wheat grass removed so as to be used as a control.

Beginning at the latter part of August the test columns were no longer watered and the drying process began. Figure 5-12 shows the flux measurements obtained in column 4, a grass growing column, from May through October. The flux variations discussed above can be observed. As the drying began in the early part of September, a large increase in the measured value of the flux was evident. The other two columns gave results that were similar to those in column 4 except for flux values. Average flux values for the three columns after two months of

drying were:

Column 3 (grass) - 354 ± 37 pCi/m²s
Column 4 (grass) - 228 ± 21 pCi/m²s
Column 5 (bare) - 202 ± 21 pCi/m²s

Both of the columns with plants had higher radon levels associated with them than did the base or control column.

After the three columns reached flux equilibrium an effort was made to determine the qualitative effect of moisture on radon escape from the three columns. Three moisture probes, described in Section 2.3, were inserted in each of the columns to monitor the moisture content 5 in. below the surface of the cover soil, 5 in. above the tailings-clay interface and 1 ft from the bottom of the tailings. The probes indicated that the tailings were very wet; the clay in columns 4 and 5 was damp, while the clay in column 3 was dry; the top cover soil was dry in all three columns.

Water was applied to the test columns twice, with an 8-day interval between the two events. First, 1.15 liters of water (equivalent to 0.5 in. of rainfall) were added to each column. Eight days later, 2.3 liters (equivalent to 1 in. of rainfall) were added to the columns. The effect on the radon flux of adding the water to the columns is shown in Figures 5-13, 5-14, and 5-15. These figures show the flux and the top moisture probe voltage plotted against time. An eye fit curve of the flux data has been added to assist in visualizing the water effect on radon exhalation.

Each of the columns exhibited an immediate decrease in the flux level at each watering. This effect was expected because of the previously observed effect of moisture on radon exhalation. Columns 3 and 4 (the plant columns) recovered in a few hours and appeared to have a flux 25 to 30% above the pretest baseline. The flux in column 5 (the control column) returned to its pretest level in a few hours. The flux in the plant columns also seemed to exhibit a wide variation in value from sample to sample, while the flux in the control column remained relatively constant. The top moisture probe voltage displayed very little variation during the first watering. None of the other probes showed any variation during either watering episode.

The second application of water (equivalent to one inch of rain) produced an immediate decrease in flux with an attendant recovery to the original baseline values of flux in approximately one day. The recovery rate was less rapid and the equilibrium value of the flux was lower than that observed when water was first added to the test columns. The top moisture probe voltages decreased for all of the columns when water was added the second time.

Several conclusions can be deduced from this experiment: A slight increase in radon exhalation seems to be present when root penetration occurs. The variation in value from flux sample to flux sample was much more pronounced in those columns in which vegetation was growing. Increasing moisture at the surface sharply reduces the flux values. Evaporation seems to increase the flux values and produces a pumping effect. The observed effects of moisture are greater than those due to vegetation growing in the test columns. Much more work needs to be done in this area.

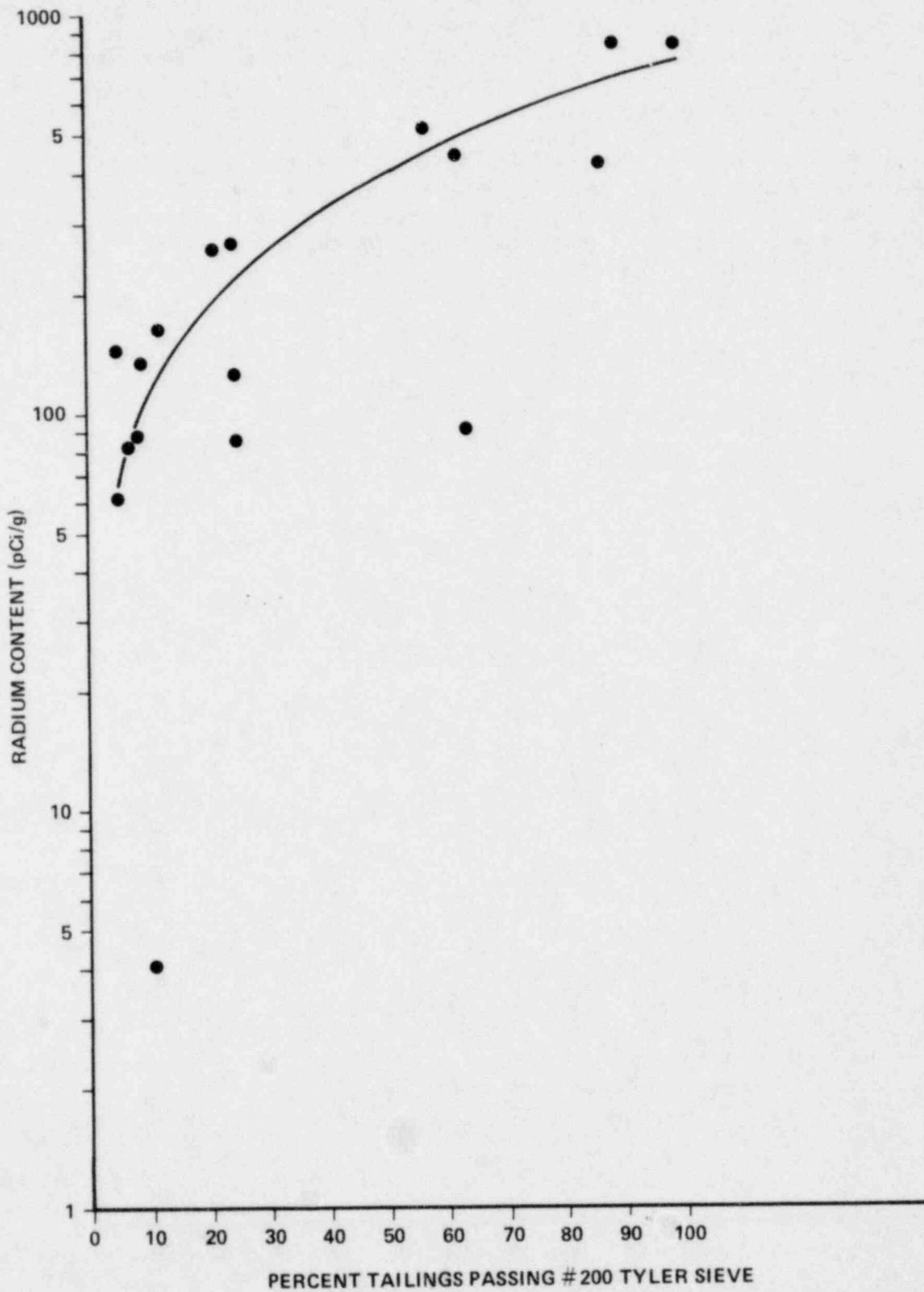


FIGURE 5-1. CORRELATION OF RADIUM CONTENT OF TAILINGS SAMPLES WITH PARTICLE SIZE

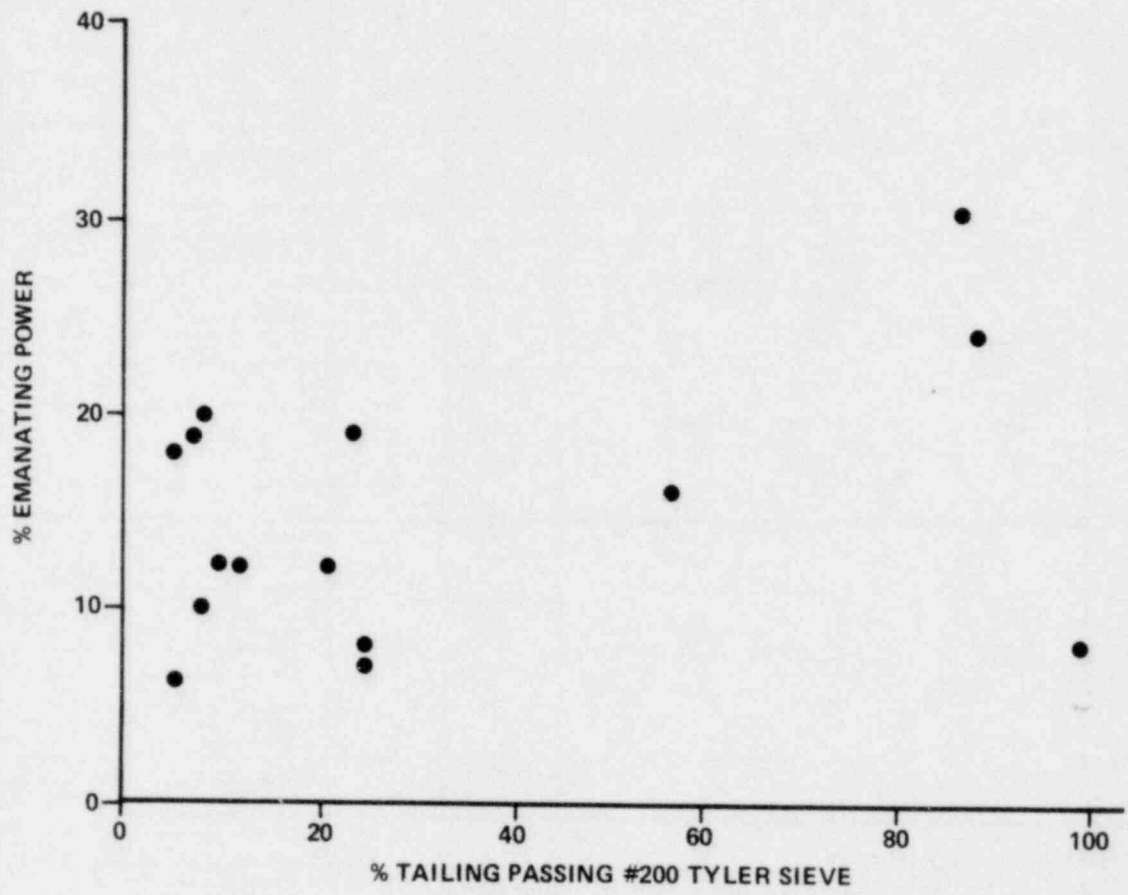


FIGURE 5-2. CORRELATION OF PERCENT EMANATING POWER OF TAILINGS SAMPLES WITH PARTICLE SIZE

MAJOR DIVISIONS			GRAPH SYMBOL	LETTER SYMBOL	TYPICAL DESCRIPTIONS
COARSE GRAINED SOILS	GRAVEL AND GRAVELLY SOILS	CLEAN GRAVELS (LITTLE OR NO FINES)		GW	WELL-GRADED GRAVELS, GRAVEL-SAND MIXTURES, LITTLE OR NO FINES
		GRAVELS WITH FINES (APPRECIABLE AMOUNT OF FINES)		GP	POORLY-GRADED GRAVELS, GRAVEL-SAND MIXTURES, LITTLE OR NO FINES
				GM	SILTY GRAVELS, GRAVEL-SAND-SILT MIXTURES
			GC	CLAYEY GRAVELS, GRAVEL-SAND-CLAY MIXTURES	
	SAND AND SANDY SOILS	CLEAN SAND (LITTLE OR NO FINES)		SW	WELL-GRADED SANDS, GRAVELLY SANDS, LITTLE OR NO FINES
				SP	POORLY-GRADED SANDS, GRAVELLY SANDS, LITTLE OR NO FINES
		SANDS WITH FINES (APPRECIABLE AMOUNT OF FINES)		SM	SILTY SANDS, SAND-SILT MIXTURES
				SC	CLAYEY SANDS, SAND-CLAY MIXTURES
FINE GRAINED SOILS	SILTS AND CLAYS	LIQUID LIMIT LESS THAN 50		ML	INORGANIC SILTS AND VERY FINE SANDS, ROCK FLOUR, SILTY OR CLAYEY FINE SANDS OR CLAYEY SILTS WITH SLIGHT PLASTICITY
				CL	INORGANIC CLAYS OF LOW TO MEDIUM PLASTICITY, GRAVELLY CLAYS, SANDY CLAYS, SILTY CLAYS, LEAN CLAYS
				OL	ORGANIC SILTS AND ORGANIC SILTY CLAYS OF LOW PLASTICITY
	SILTS AND CLAYS	LIQUID LIMIT GREATER THAN 50		MH	INORGANIC SILTS, MICACEOUS OR DIATOMACEOUS FINE SAND OR SILTY SOILS
				CH	INORGANIC CLAYS OF HIGH PLASTICITY, FAT CLAYS
				OH	ORGANIC CLAYS OF MEDIUM TO HIGH PLASTICITY, ORGANIC SILTS
HIGHLY ORGANIC SOILS				PT	PEAT, HUMUS, SWAMP SOILS WITH HIGH ORGANIC CONTENTS

NOTE: DUAL SYMBOLS ARE USED TO INDICATE BORDERLINE SOIL CLASSIFICATIONS.

SOIL CLASSIFICATION CHART

FIGURE 5-3. UNIFIED SOIL CLASSIFICATION SYSTEM

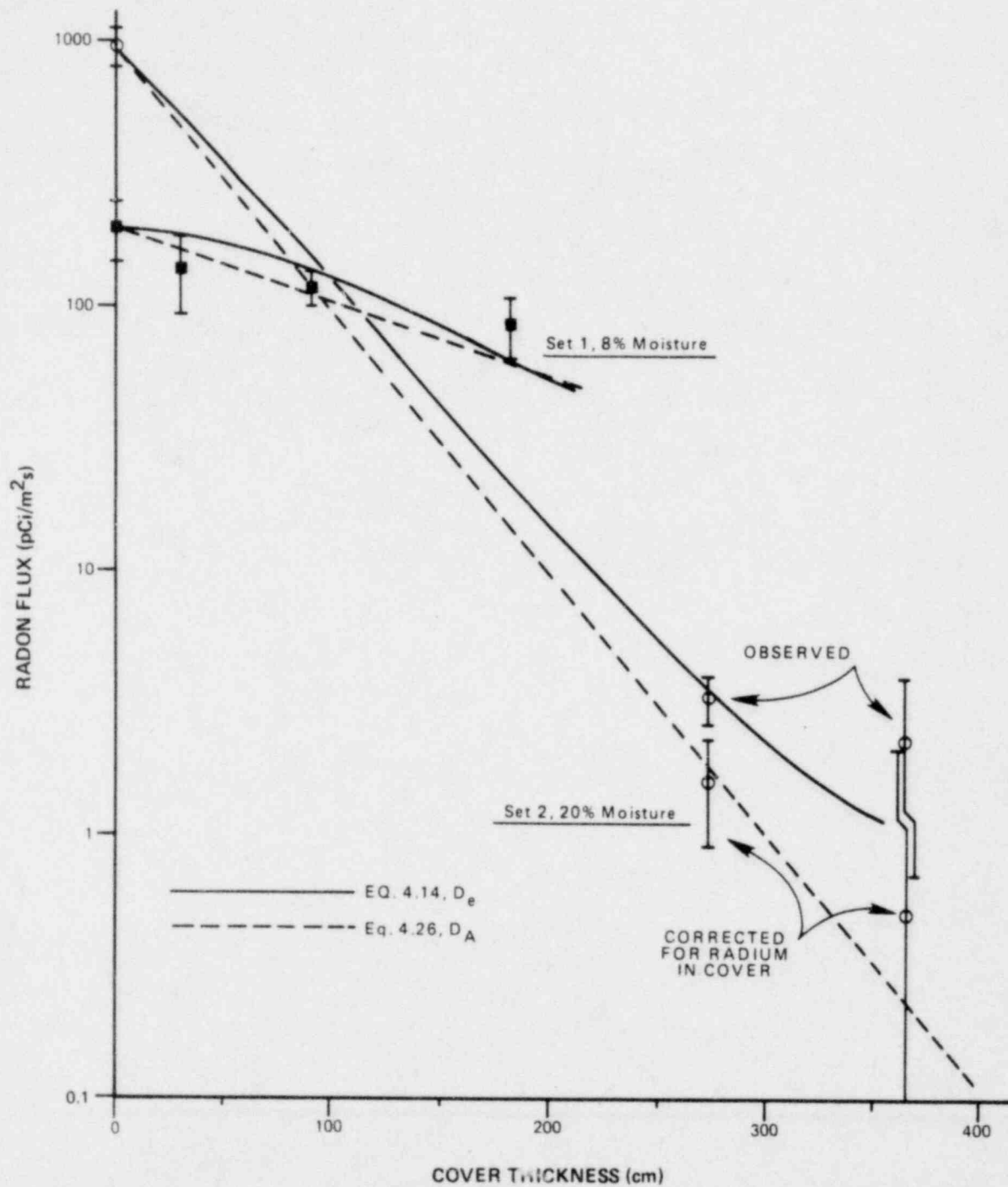


FIGURE 5-4. RADON FLUX PROFILES OF SHIRLEY BASIN SOIL NO. 2

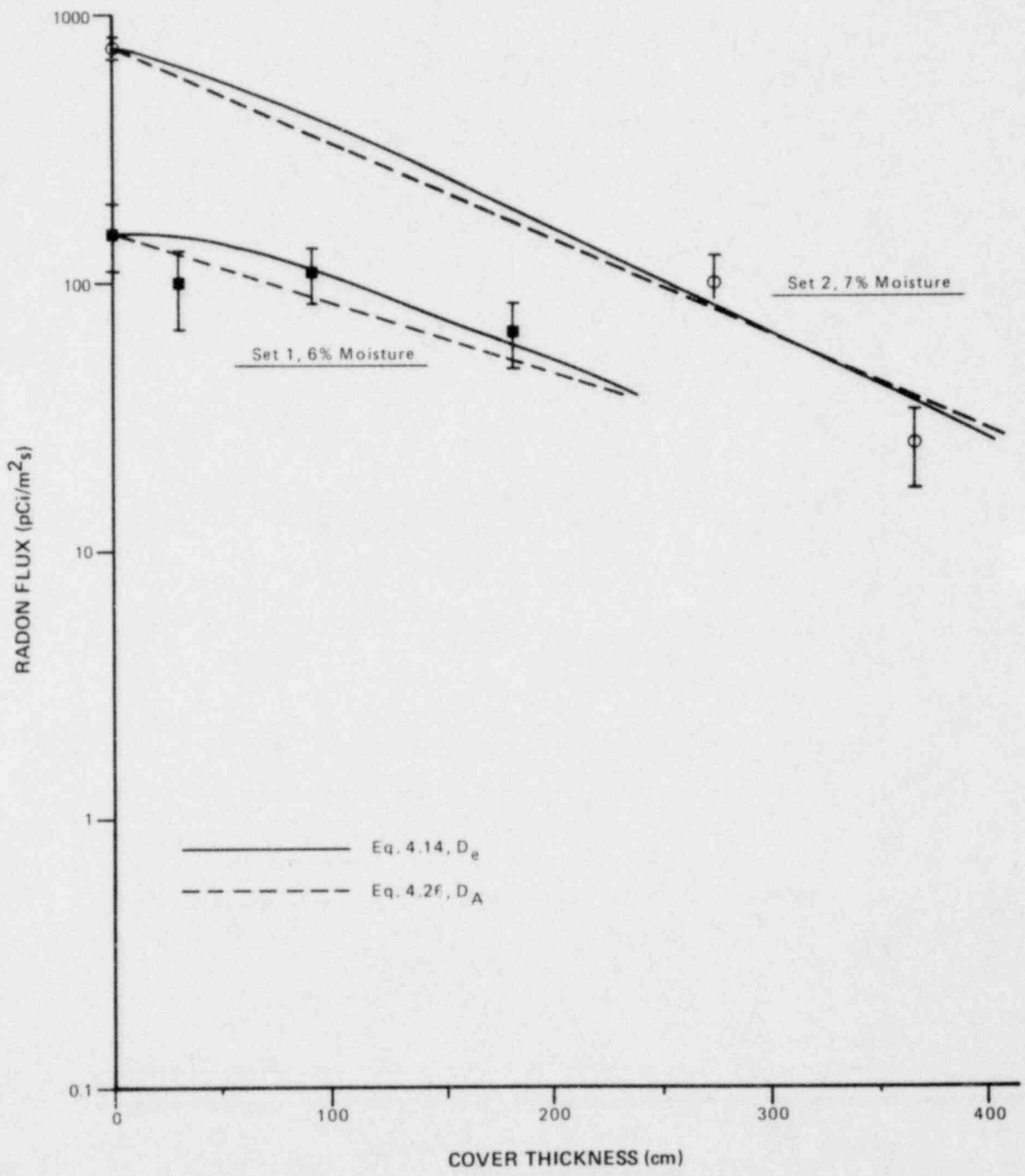


FIGURE 5-5. RADON FLUX PROFILES OF POWDER RIVER SOIL NO. 2

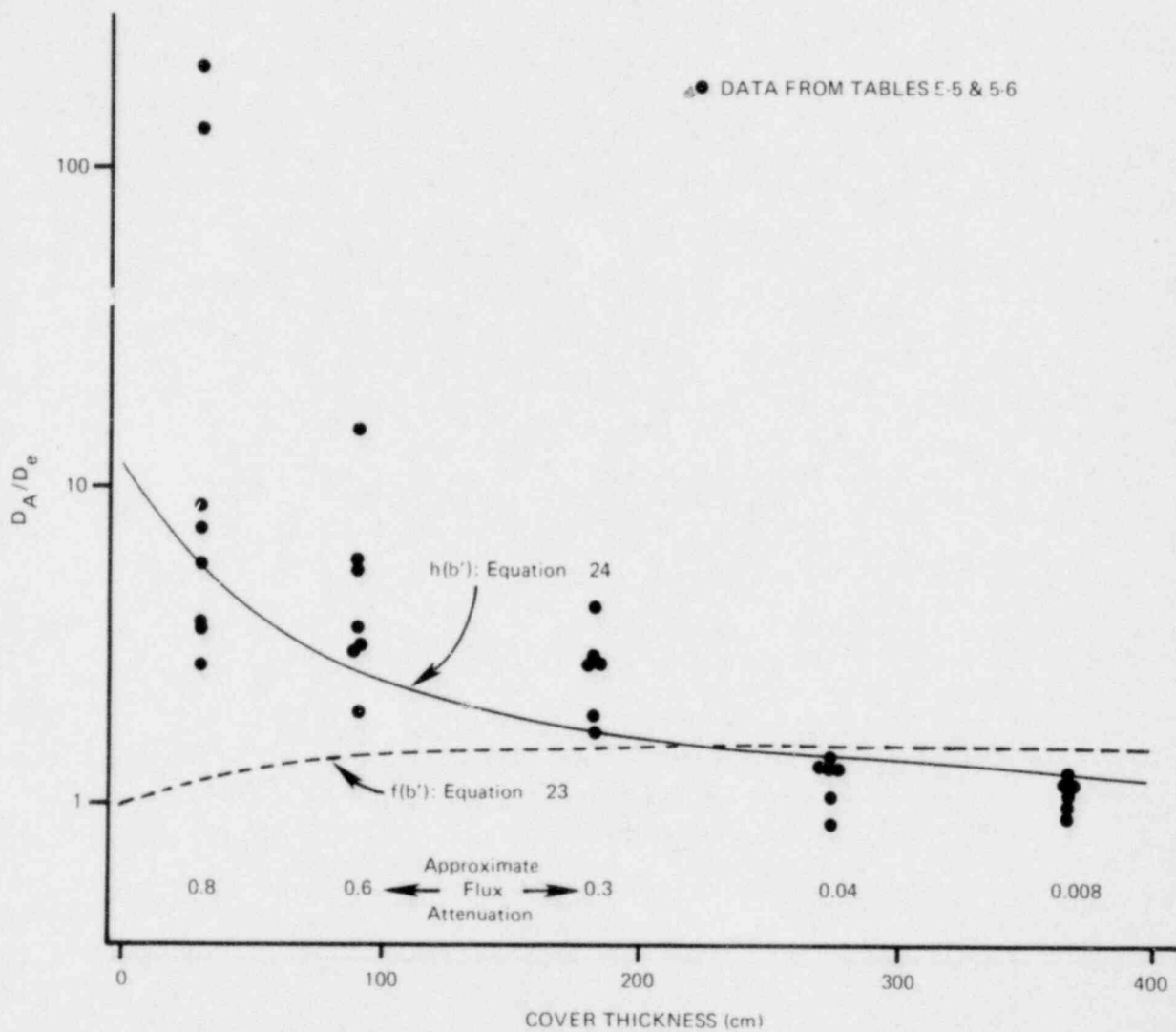


FIGURE 5-6. ILLUSTRATION OF THE COVER THICKNESS DEPENDENCE OF D_A .

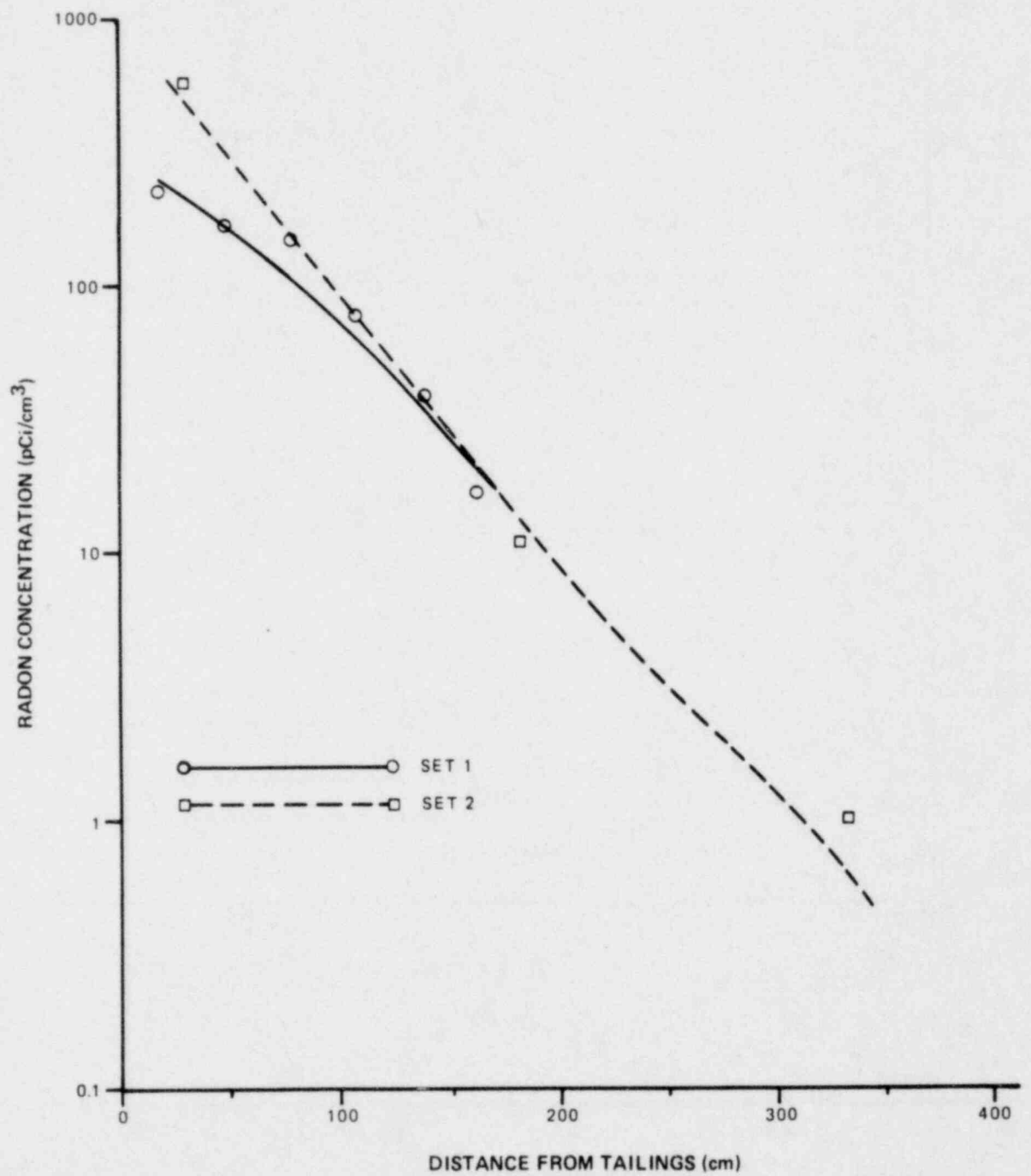


FIGURE 5-7 RADON CONCENTRATION PROFILE OF SHIRLEY BASIN SOIL NO. 2

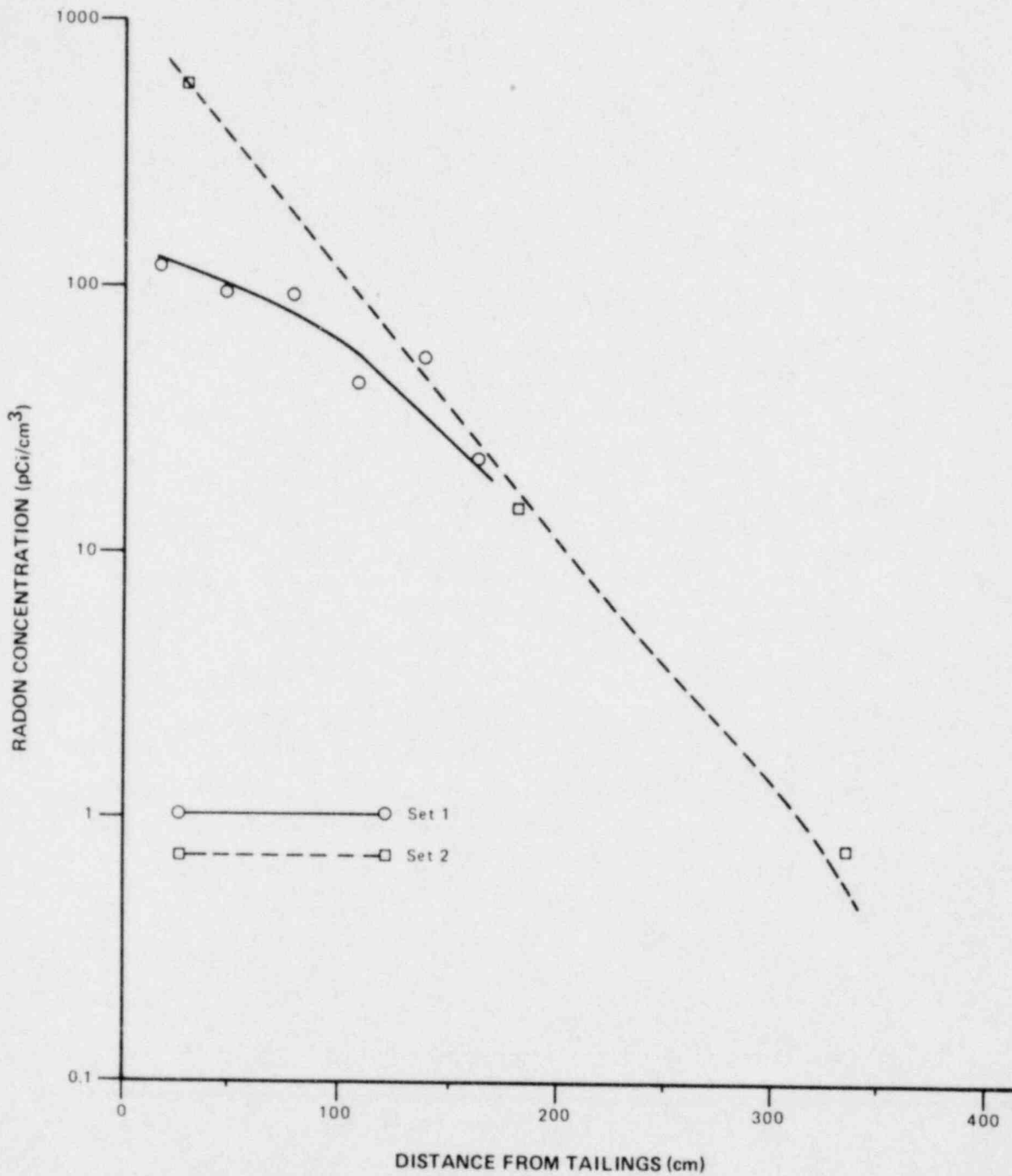


FIGURE 5-8. RADON CONCENTRATION PROFILE OF AMBROSIA LAKE SOIL NO. 1.

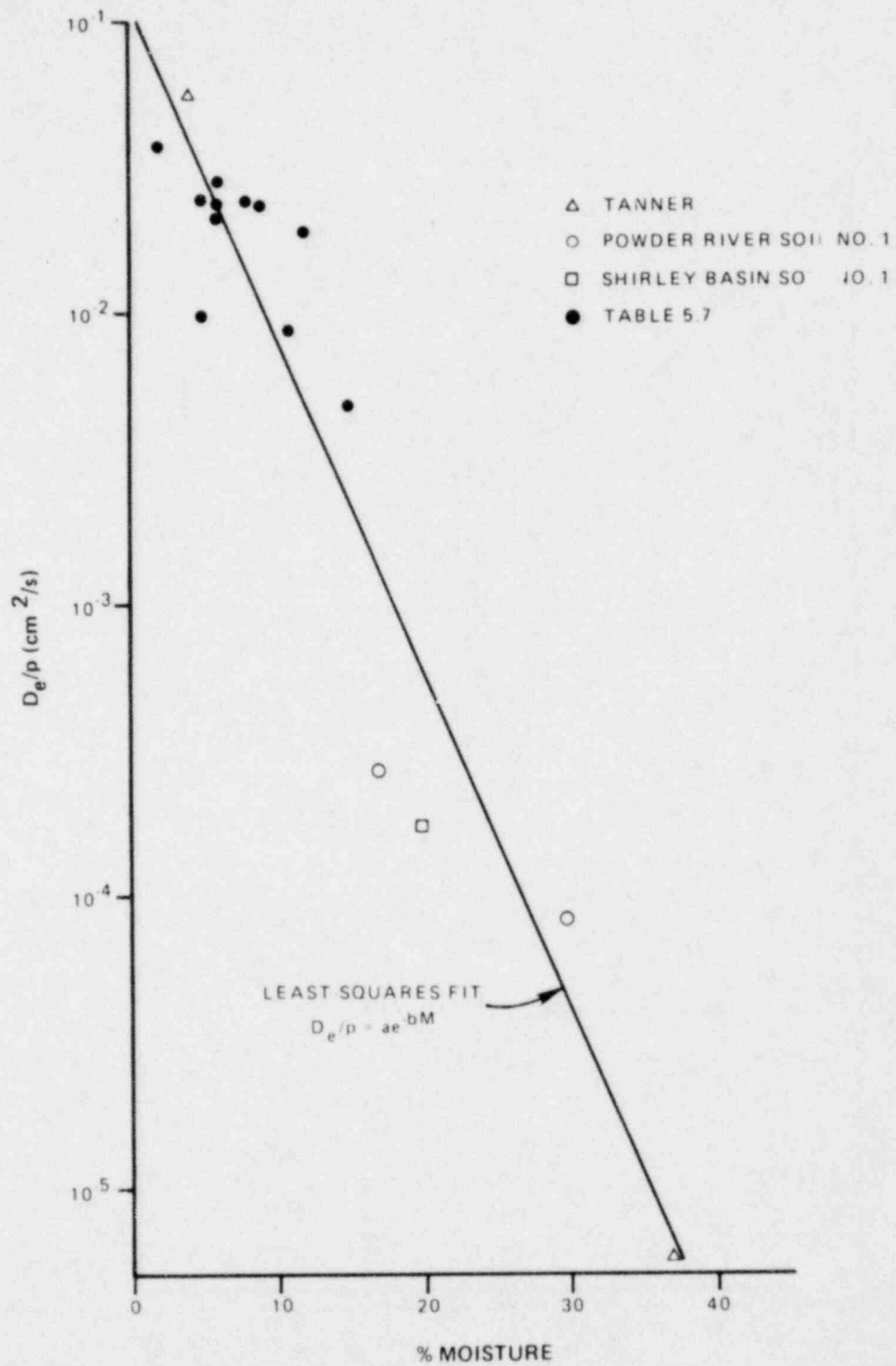


FIGURE 5-9 EXPONENTIAL MOISTURE DEPENDENCE OF THE DIFFUSION COEFFICIENT

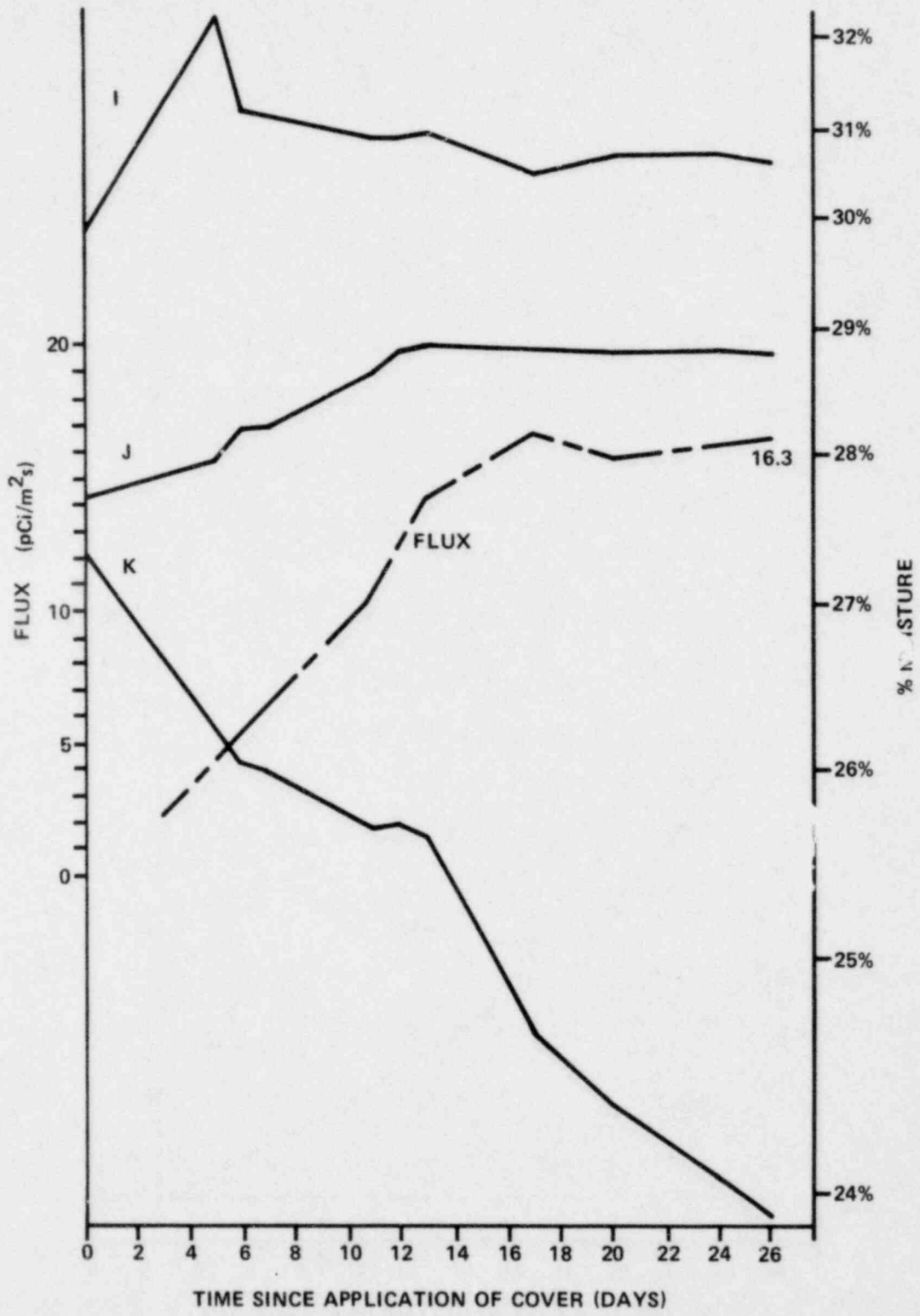


FIGURE 5-10 FLUX AND MOISTURE MEASUREMENTS OF THE RME CONFIGURATION AS A FUNCTION OF TIME

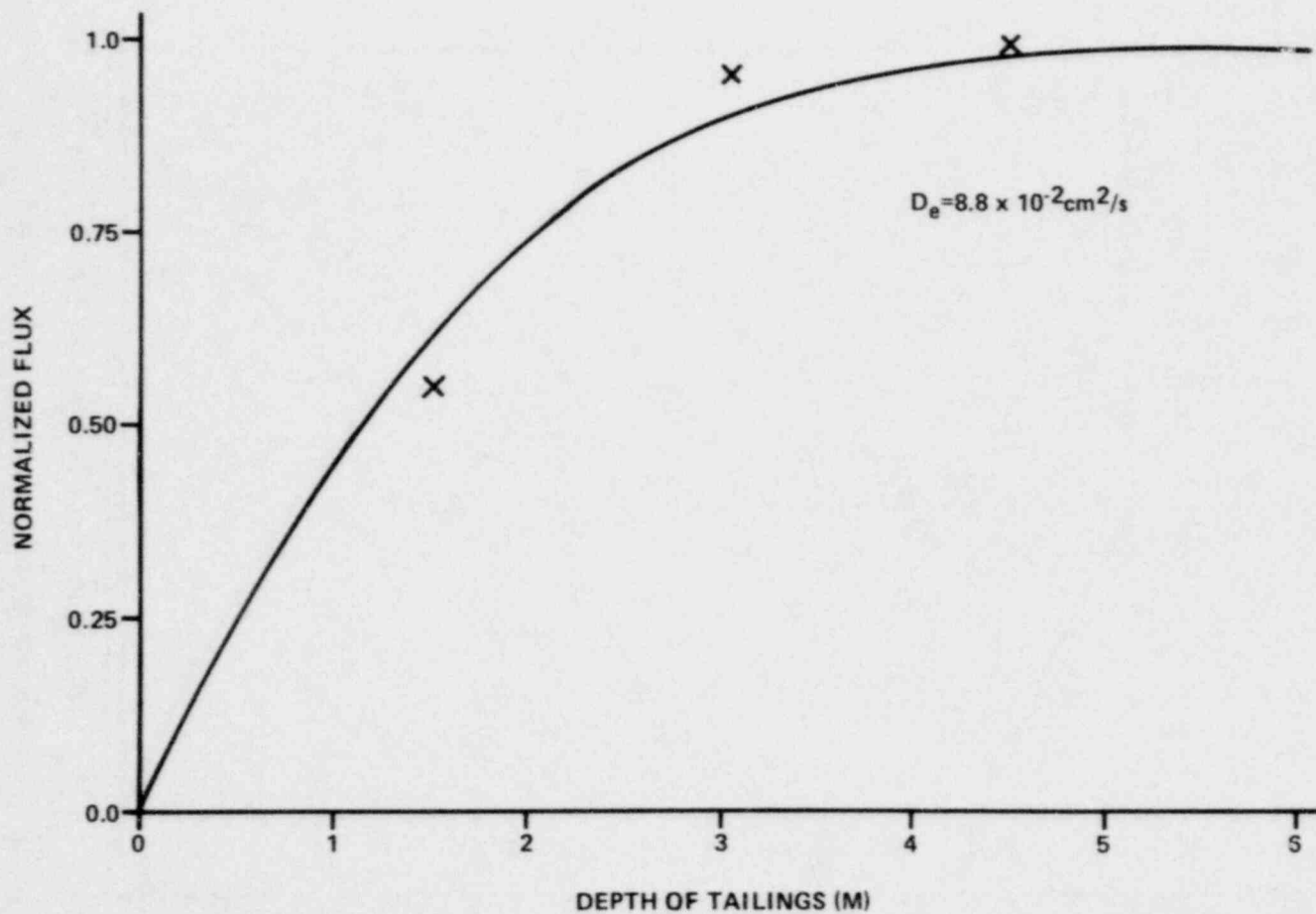


FIGURE 5-11. FLUX AS A FUNCTION OF BARE TAILINGS DEPTH FOR AMBROSIA LAKE TAILINGS #1-1

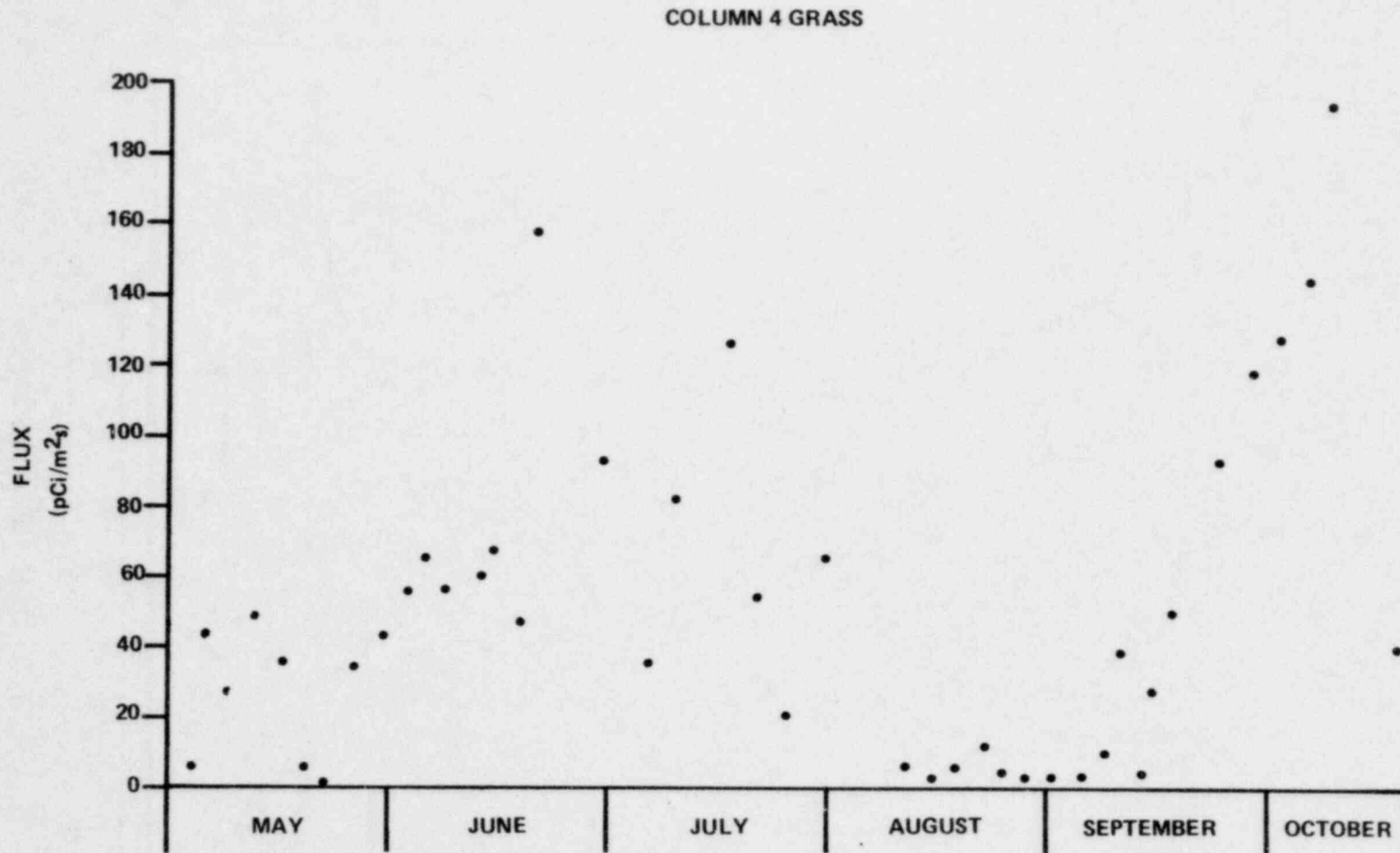


FIGURE 5-12. VARIATION OF RADON FLUX WITH TIME FOR A TYPICAL TEST COLUMN WITH NATIVE GRASS GROWTH (COLUMN #4)

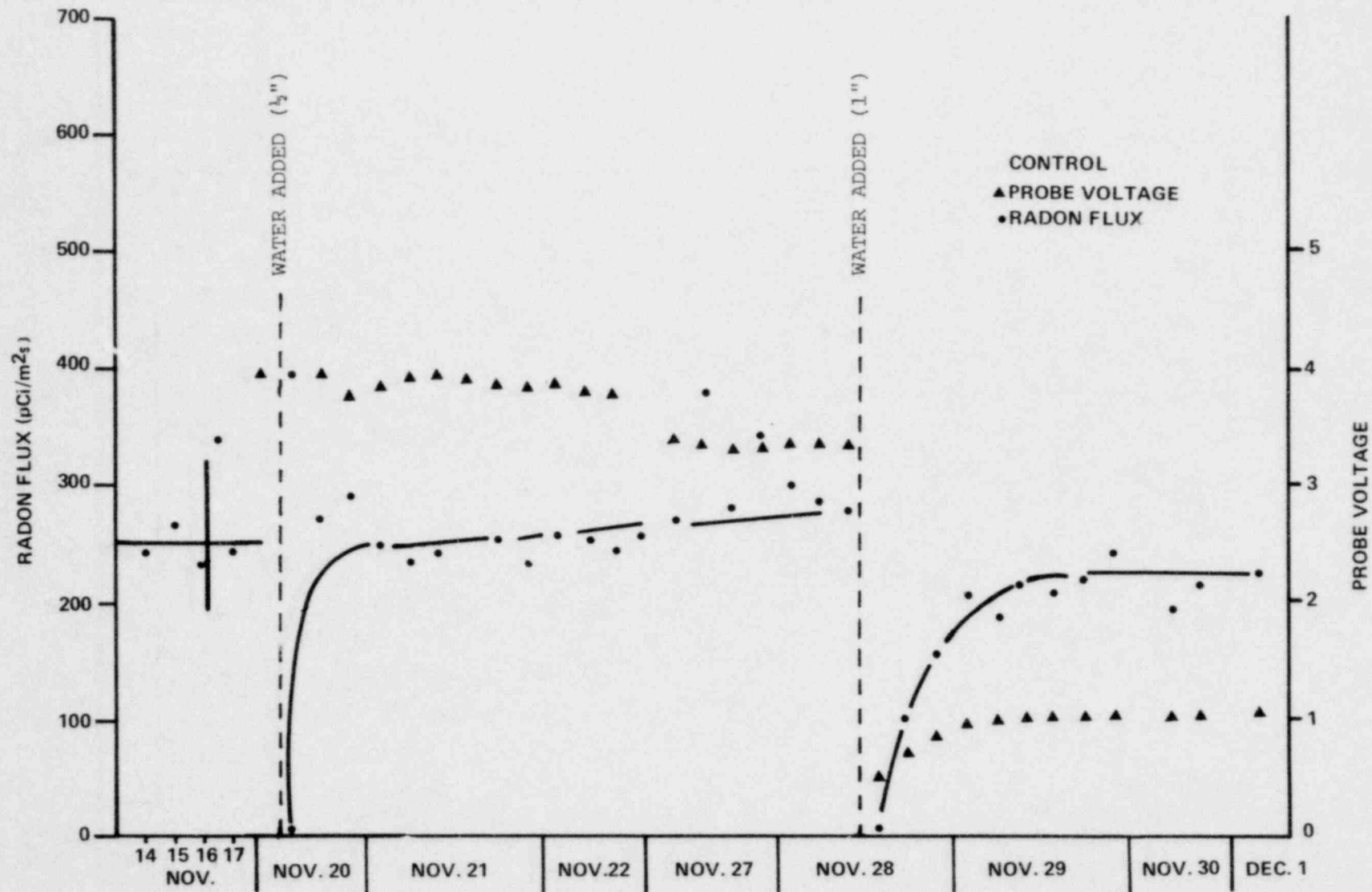


FIGURE 5-13. EFFECT OF MOISTURE ON THE RADON FLUX AND MOISTURE PROBE VOLTAGE AS A FUNCTION OF TIME FOR BARE COVER (COLUMN #5)

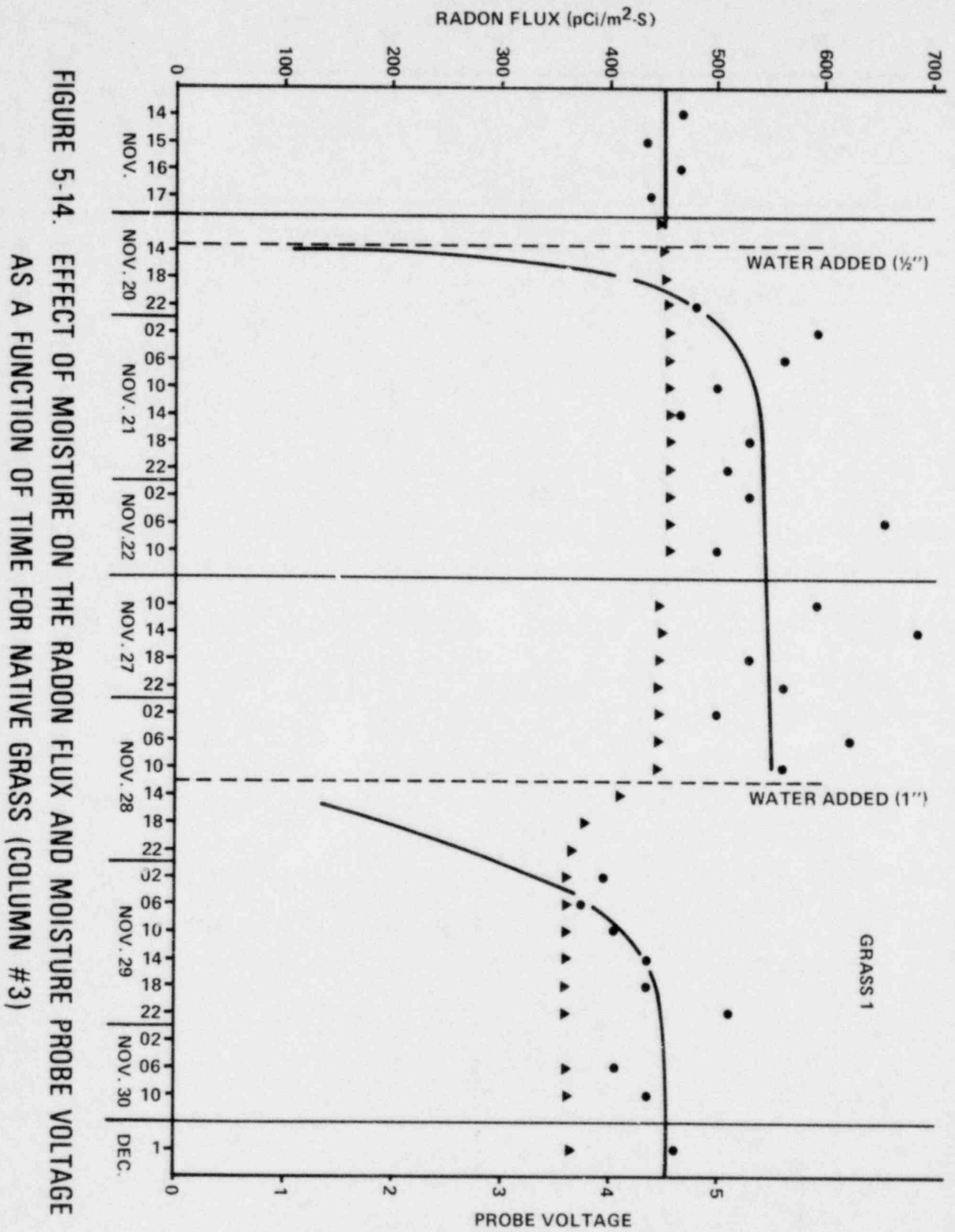


FIGURE 5-14. EFFECT OF MOISTURE ON THE RADON FLUX AND MOISTURE PROBE VOLTAGE AS A FUNCTION OF TIME FOR NATIVE GRASS (COLUMN #3)

GRASS 1

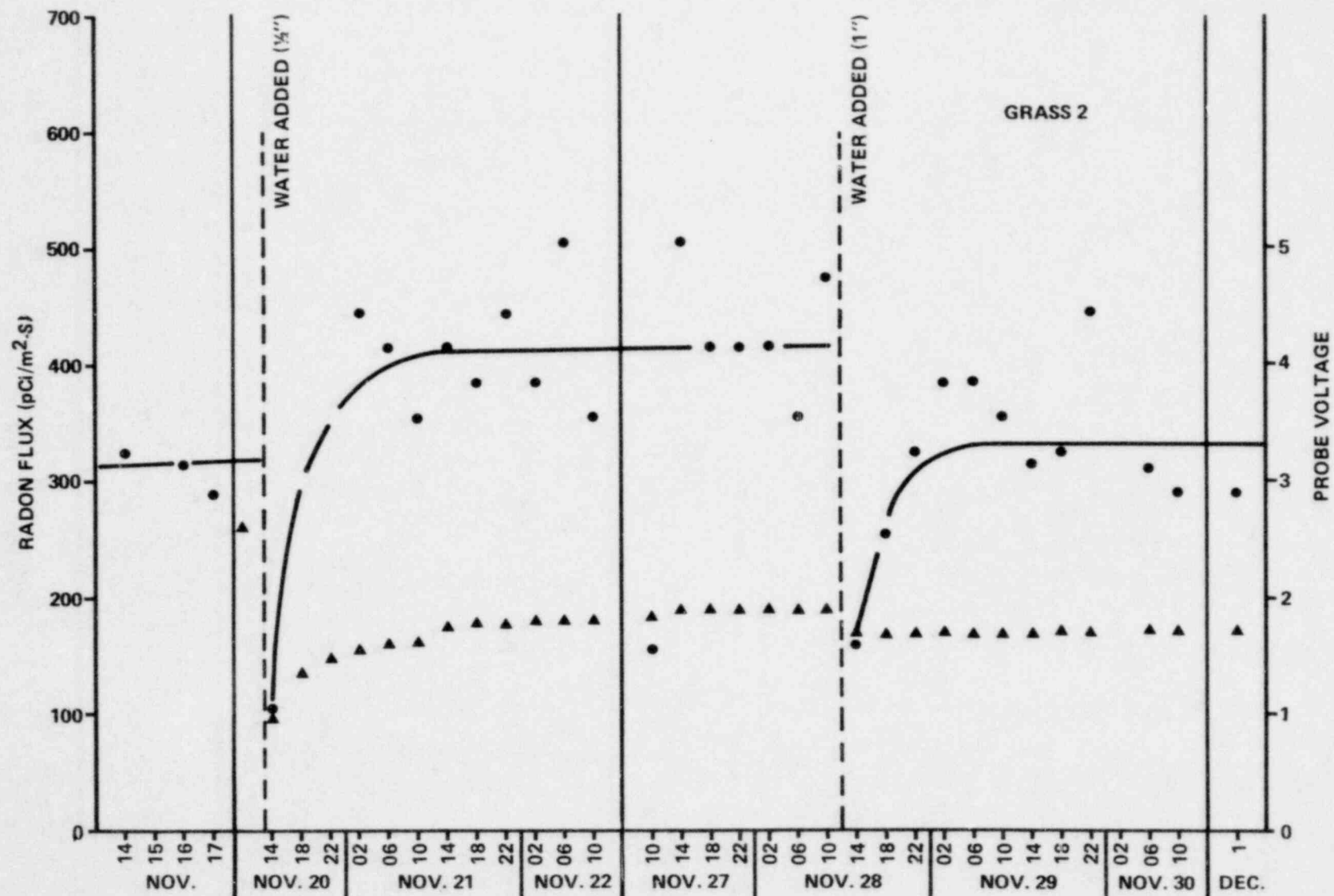


FIGURE 5-15. EFFECT OF MOISTURE ON THE RADON FLUX AND MOISTURE PROBE VOLTAGE AS A FUNCTION OF TIME FOR NATIVE GRASS (COLUMN #4)

TABLE 5-1

RADIUM CONCENTRATIONS AND DIFFUSION COEFFICIENTS*
FOR THE TAILINGS SOURCES USED WITH EACH COVER MATERIAL

	Set 1		Set 2	
	Radium Concentration (pCi Ra/g)	Diffusion Coefficient (cm ² /s)	Radium Concentration [†] (pCi Ra/g)	Diffusion Coefficient (cm ² /s)
Powder River Soil No. 1	1620	8.1x10 ⁻⁵	1130	4.5x10 ⁻³
Powder River Soil No. 2	1190	1.2x10 ⁻⁴	1450	4.5x10 ⁻³
Shirley Basin Soil No. 1	1310	1.7x10 ⁻⁴	1650	4.5x10 ⁻³
Shirley Basin Soil No. 2	1080	2.3x10 ⁻⁴	1860	4.5x10 ⁻³
Ambrosia Lake Soil No. 1	1310	6.8x10 ⁻⁵	1690	4.5x10 ⁻³
Ambrosia Lake Soil No. 2	1190	1.7x10 ⁻⁴	1510	4.5x10 ⁻³
Wyoming Soil No. 1	1300	1.4x10 ⁻⁴	----	----
Wyoming Soil No. 2	1100	1.9x10 ⁻⁴	----	----

*Diffusion Coefficients calculated from Eq. (13), Ch. 4

†Based on a composite Ra analysis, normalized to individual bare tailings flux measurements

TABLE 5 - 2

SUMMARY OF RADON SOURCE PARAMETERS
AND SOIL MECHANICAL PROPERTIES

D&M ID	Sample Identification	pCi Ra/g Tailings (Dry)		Emanating Power %	Soil Classification	% Passing #200 Tyler Sieve	Maximum Dry Density (g/cm ³)	Moisture Content At Maximum Compaction
		Set 1	Set 2					
C1	Shirley Basin Soil #1	5.8 ± .2	7.0 ± .5	16 ± 2	CL-CH	98	1.63	21.3
S1	Shirley Basin Soil #2	6.0 ± .3	4.3 ± .5	10 ± 5	CH	90	1.51	26.0
C2	Powder River Soil #1	2.7 ± .2	2.7 ± .4	25 ± 6	CL	79	1.71	18.0
S2	Powder River Soil #2	1.2 ± .1	2.4 ± .2	40 ± 15	SM	20	1.79	15.0
WC	Wyoming Soil #1	1.5 ± .3	—	72	SM	25	1.88	13.5
W5	Wyoming Soil #2	2.2 ± .3	—	75	SM-SP	7	2.02	8.7
C5	Ambrosia Lake Soil #1	1.2 ± .1	2.4 ± .1	14 ± 3	CH	92	1.51	28.5
S5	Ambrosia Lake Soil #2	4.9 ± .8	2.7 ± .4	26	SM	18	1.81	12.0
C3	Gas Hills Soil #1-1	5.9 ± .9	—	71	CL-SC	62	1.70	18.5
S3	Gas Hills Soil #1-2	12.0 ± .9	—	46	SC-CL	50	1.79	15.3
C4	Gas Hills Soil #2-1	3.1 ± .4	—	26	CL	80	1.86	28.5
S4	Gas Hills Soil #2-2	1.8 ± .3	—	48	SP-SM	10	1.73	6.0
T15	Shirley Basin Tailings #1-1	261.0 ± 8.0	—	12 ± 4	SM	21	—	—
T14	Shirley Basin Tailings #1-2	875.0 ± 15.0	—	8 ± 3	CL	99	—	—
T4	Powder River Tailings #1-1	82.2 ± 4.6	—	19 ± 12	SM-SP	7	—	—
T5	Powder River Tailings #1-2	129.0 ± 6.0	—	7 ± 1	SM	25	—	—
T6	Powder River Tailings #2-1	145.0 ± 6.0	—	6	SM-SP	5	—	—
T7	Powder River Tailings #2-2	163.0 ± 4.0	—	12 ± 4	SP-SM	12	—	—
T8	Gas Hills Tailings #1-1	63.2 ± 2.3	—	18 ± 1	SP	5	—	—
T9	Gas Hills Tailings #1-2	87.0 ± 4.4	—	8 ± 3	SM	25	—	—
T10	Gas Hills Tailings #2-1	4.1 ± .7	—	11 ± 9	SP-SM	10	—	—
T11	Gas Hills Tailings #2-2	411.0 ± 12.0	—	31 ± 4	ML	87	—	—
T1	Ambrosia Lake Tailings #1-1	269.0 ± 7.0	—	19	SM	24	—	—
T2	Ambrosia Lake Tailings #1-2	850.0 ± 18.0	—	24 ± 10	CL	89	—	—
T12	Ambrosia Lake Tailings #2-1	88.1 ± 3.5	—	10 ± 4	SM-SP	8	—	—
T3	Ambrosia Lake Tailings #2-2	449.0 ± 10.0	—	—	SC	62	—	—
T16	Ambrosia Lake Tailings #3-1	138.0 ± 4.0	—	20 ± 1	SP-SM	9	—	—
T13	Ambrosia Lake Tailings #3-2	535.0 ± 2.0	—	18	ML-SM	57	—	—

TABLE 5-3

TYPICAL VOID RATIOS AND POROSITIES
FOR COHESIONLESS SOILS(2)

<u>Soil Description</u>	<u>v_{max}^*</u>	<u>v_{min}^*</u>	<u>P_{max}^*</u>	<u>P_{min}^*</u>
Well graded fine to coarse sand	0.70	0.35	0.41	0.26
Uniform fine to medium sand	0.85	0.50	0.46	0.33
Silty sand and gravel	0.80	0.25	0.44	0.20
Micaceous sand with silt	1.25	0.75	0.56	0.43

* v_{max} = maximum void ratio, v_{min} = minimum void ratio,
 P_{max} = maximum porosity, P_{min} = minimum porosity.

TABLE 5-4

MEASURED RADON FLUX (pCi/m² s) AS A FUNCTION
OF COVER THICKNESS

	Set 1				Set 2		
	Bare Tailings Flux	1-Foot Cover	3-Foot Cover	6-Foot Cover	Bare Tailings Flux	9-Foot Cover	12-Foot Cover
Powder River Soil No. 1	175+47	172+27	123+22	*	585+68	69+21	23+8
Powder River Soil No. 2	154+41	99+32	110+26	66+18	753+67	99+25	25+8
Shirley Basin Soil No. 1	203+46	155+24	100+22	*	855+88	90+51	15+16
Shirley Basin Soil No. 2	199+51	139+45	118+18	86+22	962+160	3.3+0.7	2.3+1.6
Ambrosia Lake Soil No. 1	130+29	106+46	113+22	76+20	876+132	7.5+2.7	3.7+3.3
Ambrosia Lake Soil No. 2	185+48	183+23	196+47	84+11	782+74	73+14	17+17
Wyoming Soil No. 1	186+38	105+16	97+31	33+7	*	*	*
Wyoming Soil No. 2	182+32	154+27	59+25	48+21	*	*	*

*Not determined

TABLE 5-5

EFFECTIVE DIFFUSION COEFFICIENT D_e (cm^2/s)
 DETERMINED FOR EACH COVER MATERIAL AT THE
 SPECIFIED DEPTH

	Set 1				Set 2			
	1-Ft Cover	3-Ft Cover	6-Ft Cover	Wt Least Sq Fit	9-Ft Cover	12-Ft Cover	Wt Least Sq Fit	
Powder River Soil # 1	0.014	0.010	----	0.010	0.011	0.0094	0.010	
Powder River Soil # 2	0.0012	0.011	0.014	0.012	0.010	0.0073	0.0089	
Shirley Basin Soil # 1	0.0026	0.0062	----	0.0053	0.012	0.0077	0.0098	
Shirley Basin Soil # 2	0.0021	0.0088	0.018	0.012	0.0017	0.0025	0.0018	
Ambrosia Lake Soil # 1	0.0032	0.034	0.033	0.032	0.0029	0.0038	0.0030	
Ambrosia Lake Soil # 2	0.017	----	0.017	0.017	0.0090	0.0068	0.0086	
Wyoming Soil # 1	0.0012	0.0069	0.0070	0.0047	----	----	----	
Wyoming Soil # 2	0.0035	0.0027	0.0073	0.0037	----	----	----	

TABLE 5-6

ALTERNATE DIFFUSION COEFFICIENT D_A (cm^2/s)
 DETERMINED FOR EACH COVER MATERIAL AT THE SPECIFIED DEPTH

	Set 1				Set 2		
	1-Ft Cover	3-Ft Cover	6-Ft Cover	Wt Geom Mean [†]	9-Ft Cover	12-Ft Cover	Wt Geom Mean
Powder River Soil # 1	1.9	0.056	----	0.056	0.015	0.011	0.013
Powder River Soil # 2	0.0043	0.065	0.041	0.049	0.014	0.0086	0.012
Shirley Basin Soil # 1	0.015	0.019	----	0.019	0.016	0.0084	0.013
Shirley Basin Soil # 2	0.0078	0.032	0.050	0.047	0.0015	0.0019	0.0016
Ambrosia Lake Soil # 1	0.028	0.52	0.14	0.20	0.0031	0.0038	0.0033
Ambrosia Lake Soil # 2	3.6	----	0.048	0.048	0.012	0.0075	0.011
Wyoming Soil # 1	0.0033	0.022	0.012	0.019	----	----	----
Wyoming Soil # 2	0.026	0.0053	0.014	0.010	----	----	----

[†]Excluding 1 ft. Covers

TABLE 5-7

DIFFUSION COEFFICIENTS FOR EACH
COVER MATERIAL

Set 1	% Moisture	P Porosity	Density (g/cm ³)	% Compaction	D _e (cm ² /s)	D _a (cm ² /s)
Powder River Soil # 1	5	0.43	1.52	89	0.010	0.056
Powder River Soil # 2	6	0.44	1.49	83	0.012	0.049
Shirley Basin Soil # 1	5	0.57	1.12	69	0.0053	0.019
Shirely Basin Soil # 2	8	0.52	1.27	84	0.012	0.047
Ambrosia Lake Soil # 1	10	0.60	1.09	72	0.032	0.20
Ambrosia Lake Soil # 2	2	0.49	1.34	74	0.017	0.048
Wyoming Soil # 1	11	0.57	1.22	65	0.0047	0.019
Wyoming Soil # 2	1	0.42	1.56	77	0.0037	0.010
Set 2						
Powder River Soil # 1	9	0.46	1.45	89	0.010	0.013
Powder River Soil # 2	6	0.39	1.62	85	0.0089	0.012
Shirley Basin Soil # 1	12	0.54	1.22	83	0.0098	0.013
Shirley Basin Soil # 2	15	0.39	1.61	94	0.0018	0.0016
Ambrosia Lake Soil # 1	20	0.47	1.43	86	0.0030	0.0033
Ambrosia Lake Soil # 2	6	0.44	1.44	77	0.0086	0.011

TABLE 5-8

MEASURED RADON CONCENTRATIONS (pCi/cm³) AT SPECIFIED
DISTANCES ABOVE THE TAILINGS-COVER INTERFACE

	Set 1						Set 2		
	18cm	48cm	79cm	109cm	140cm	155cm	30cm	183cm	335cm
Powder River Soil #1	220	170	61	--	--	--	250	47	4.9
Powder River Soil #2	38	220	250	44	42	7.9	340	60	5.6
Shirley Basin Soil #1	220	150	54	--	--	--	380	89	5.5
Shirley Basin Soil #2	230	170	150	79	39	17	580	11	1.0
Ambrosia Lake Soil #1	120	97	94	44	55	23	590	15	0.79
Ambrosia Lake Soil #2	290	230	170	91	60	31	470	58	--
Wyoming Soil #1	260	160	160	76	15	1.6	--	--	--
Wyoming Soil #2	230	180	130	80	39	12	--	--	--

TABLE 5-9

EFFECTIVE DIFFUSION COEFFICIENTS D_e (cm^2/s)
 DETERMINED FROM RADON CONCENTRATION PROFILES

	Set 1	Set 2
	<u>Least Square Fit</u>	<u>Least Square Fit</u>
Powder River Soil # 1	0.0080	0.0086
Powder River Soil # 2	0.0079	0.0063
Shirley Basin Soil # 1	0.0093	0.0082
Shirley Basin Soil # 2	0.0090	0.0014
Ambrosia Lake Soil # 1	----	0.0018
Ambrosia Lake Soil # 2	0.013	0.0048
Wyoming Soil # 1	0.011	----
Wyoming Soil # 2	0.0072	----

TABLE 5-10

DIFFUSION COEFFICIENT DETERMINED FOR VARIOUS
COVER MATERIALS AS A FUNCTION OF MOISTURE ADDED

	<u>% Moisture</u>	<u>Density ρ (g/cm³)</u>	<u>Porosity P</u>	<u>De/p (cm²/s)</u>	<u>De/p (b)</u>
Powder River Soil #1	5.	1.53	0.43	2.3×10^{-2}	1.5×10^{-1}
	17.	1.53	0.43	2.6×10^{-4}	2.7×10^{-2}
	30.	1.53	0.43	8.2×10^{-5}	9.5×10^{-2}
Shirley Basin Soil #1	5.	1.12	0.57	9.1×10^{-3}	4.9×10^{-2}
	20.	1.12	0.57	1.7×10^{-4}	3.6×10^{-1}
Mud (a)	37.2	1.57	?	5.7×10^{-6}	6.8×10^{-2}
Mud (a)	85.5	1.02	?	2.2×10^{-6}	
Sand (a)	4.	1.4	0.39	5.4×10^{-2}	1.5×10^{-1}

(a) Tanner, Allan B. "Radon Migration in the Ground: A Review", The Natural Radiation Environment 1964.

(b) Corrected for moisture

CHAPTER 5 REFERENCES

1. P.J. Macbeth, et al.; "Laboratory Research on Tailings Stabilization Methods and Their Effectiveness in Radiation Containment;" U.S. Department of Energy Report GJT-21; Apr 1978.
2. A.B. Tanner; "Radon Migration in the Ground: A Review;" The Natural Radiation Environment; J.A.S. Adams and W.M. Lowder, eds.; University of Chicago Press; 1964.
3. J.H. Scott and P.H. Dodd; "Gamma-Only Assaying for Disequilibrium Corrections;" RME-135; Geology and Mineralogy; Apr 1960.
4. D.F. McCarthy; "Essentials of Soil Mechanics and Foundations;" Reston Publishing Company, Inc., 1977.
5. H.W. Kraner, L. Schroeder and R.D. Evans; "Measurements of the Effects of Atmospheric Variables on Radon-222 Flux and Soil-Gas Concentrations;" The Natural Radiation Environment; J.A.S. Adams and W.M. Lowder, eds; University of Chicago Press; 1964.
6. "Environmental Statement Related to the Operation of the Bear Creek Project;" Rocky Mountain Energy Company; NUREG-0129; Jan 1977.

CHAPTER 6

CONCLUSIONS

The conclusions determined for this study will be summarized and presented according to task.

6.1 TASK 1

Task 1 dealt primarily with the determination of diffusion coefficients for eight clays and soils from several mining regions. Characterization of the radon source was necessarily a part of this task. The results of this task were as follows:

1. Diffusion coefficients were determined for eight soils. An exact and an alternate solution of the diffusion equation were employed to give D_e and D_A . D_e and D_A were found to be interchangeable at large cover thicknesses. Values of the diffusion coefficient were found to range from approximately 2×10^{-3} to 3×10^{-2} cm^2/s . $D_e(\text{flux})$ was found to differ slightly from $D_e(\text{conc})$, but the variation was within the limits to be expected from using different parameters to determine the values.
2. Diffusion theory leads to a model of radon exhalation which corresponds to measured values.
3. Radon gas flux attenuation may be predicted if the cover soil and the tailings can be characterized as to moisture content, porosity, density, radium content, emanating power and diffusion coefficient.

6.2 TASK 2

This task dealt with the effect of moisture on the diffusion coefficient. Moisture was found to have a profound effect on the exhalation of radon gas. Qualitative and quantitative effects were found and are listed below.

1. When moisture is added to either the tailings or the cover material, an effective attenuating effect is noted.
2. As the cover material dries, there is an increase of radon flux that seems to be due to a pumping effect. It is postulated that the effect is connected with evaporation.
3. A functional relationship was determined relating the moisture to the diffusion coefficient. This relationship is given in Section 5.3.

6.3 TASK 3

Task 3 was concerned with determining the emanating power of ten mill tailings samples. The results are:

1. The emanating power varies from 6 to 31% for the tailings that were tested. There is a rough correlation between soil type and emanating power, but the correspondence is not marked.
2. There is probably a large moisture dependence, but no effort was made to relate emanating power and moisture.
3. No correlation was found between particle size and emanating power.

6.4 TASK 4

Root penetration effects on radon gas exhalation was the major emphasis of Task 4. FB&DU found the following effects:

1. There seemed to be an increase in flux when the plant roots penetrated through the cover to the tailings. A minimum of 13% increase in flux was noted for plant-covered test columns when compared with base cover.
2. Moisture had a much larger effect on the radon exhalation than any other observed phenomena.
3. There seemed to be a more pronounced pumping effect as drying occurred in the test columns in which plants were growing than in those which had no vegetation.

6.5 GENERAL CONCLUSIONS

Modeling of the diffusion of radon gas through tailings and cover was accomplished. Measurements of radon flux and concentration were used to determine diffusion coefficients. The values of the coefficients generally correspond to those found by other investigators. A simple exponential relation may be used with thick cover to predict the flux at the surface of the cover material. Moisture has a large effect on the radon exhalation. More data are necessary in order to define the relationship between radon flux and moisture. Plant growth seems to have an effect on radon gas escape, but this effect appears to be smaller than that due to moisture.

The overall benefit of this study was to increase the understanding of both specific and general movement of radon gas in soil.

APPENDIX A

SOIL MECHANICAL PROPERTIES OF THE SELECTED COVER
AND TAILINGS MATERIAL

BY

DAMES & MOORE

Key to Dames & Moore Sample Identification is given in Table 5.1.

Dames & Moore
250 East Broadway
Suite 200
Salt Lake City, Utah 84111

March 6, 1978

Ford, Bacon & Davis Utah, Inc.
P.O. Box 8009
Salt Lake City, Utah 84108

Attention: Mr. Greg Jensen

Gentlemen:

Results of Laboratory Testing and
Permeability
Data Discussions
Samples Designated C, S and T
For Ford, Bacon & Davis Utah, Inc.

INTRODUCTION

This report summarizes laboratory tests performed on samples provided by Ford, Bacon & Davis Utah, Inc., and delivered to the Dames & Moore laboratory in Salt Lake City, and presents discussions pertaining to the permeability characteristics of the samples tested. All results are labeled with the same sample designation as received. The laboratory test data sheets are maintained in our files. Copies can be forwarded if requested.

PURPOSE AND SCOPE

The purpose and scope of this program were developed in discussions between Messrs. Duane Whiting and Greg Jensen of

Ford, Bacon & Davis Utah, Inc.
February 6, 1978
Page -2-

Ford, Bacon & Davis Utah, Inc., and representatives of Dames & Moore. Test specifications and the contract agreement are contained in Ford, Bacon & Davis Contract Number 218-005, dated December 14, 1977.

The tests performed include the following:

1. Atterberg limits test.
2. Gradation analyses, No. 4 to No. 200 sieve.
3. Compaction tests.
4. Permeability tests.

TEST PROCEDURES AND RESULTS

GENERAL

Soil classifications have been made in accordance with the method described on Plate 1, Unified Soil Classification System.

ATTERBERG LIMITS TEST

Atterberg limits were determined according to ASTM* D-423 (liquid limit) and ASTM D-424 (plastic limit and plasticity index). The results of the tests performed are tabulated on the following page.

*American Society for Testing and Materials

<u>Sample</u>	<u>Liquid Limit</u>	<u>Plastic Limit</u>	<u>Plasticity Index</u>	<u>Soil* Type</u>
S-1	64.2	27.5	36.7	CH
S-2		----- Non Plastic -----		
S-3	39.2	19.1	20.1	CL
S-4		----- Non Plastic -----		
S-5		----- Non Plastic -----		
C-1	50.7	25.4	25.3	CL/CH
C-2	33.8	19.2	14.6	CL
C-3	37.2	20.3	16.9	CL
C-4	28.7	15.2	13.5	CL
C-5	70.5	29.5	41.0	CH

*Based solely on the results of the Atterberg limits test.

GRADATION ANALYSES

Gradation analyses were performed according to ASTM D-422. Wet sieving methods were used. The results of the gradation analyses are presented on Plates 2A through 2D, Gradation Curves.

COMPACTION TESTS

Compaction tests were performed according to the ASTM D-698 method criteria. The results of the compaction tests are presented on Plates 3A and 3B, Compaction Test Data.

PERMEABILITY TESTS

Both constant and falling head permeability tests were performed in conjunction with this testing program. Constant

head tests were performed upon the more permeable samples in accordance with the ASTM D-2434 criteria. Falling head tests which were performed upon the more impermeable samples were performed in accordance with the method described in "Engineering Properties of Soils and Their Measurements," by Joseph E. Bowles, 1970.

All tests were performed upon recompacted samples. Recom-paction of the test samples was performed by compacting soil within cylindrical brass rings. The soil was added in layers of uniform thickness, with each layer receiving approximately the same compactive effort. The surface of each layer was scarified prior to adding the successive layer. The results of these tests are tabulated below.

Sample	Soil Type	Percent* Compaction	Surcharge Pressure lbs/sq ft	Test** Type	Percent Swell or Collapse During Test	Permeability*** Kx10 ⁻⁶ cm/sec
C-1	CL/CH	76.3	1,000	FH	10.9 collapse	8.14
C-1		85.4	1,000	FH	1.4 collapse	104
C-1		90.8	1,000	FH	0.1 collapse	0.965
C-2	CL	75.0	1,000	FH	12.8 collapse	26.0
C-2		85.3	1,000	FH	4.6 collapse	83.0
C-2		90.6	1,000	FH	0.0 collapse	23.0

Ford, Bacon & Davis Utah, Inc.
 February 6, 1978
 Page -5-

Sample	Soil Type	Percent* Compaction	Surcharge Pressure lbs/sq ft	Test** Type	Percent Swell or Collapse During Test	Permeability*** Kx10 ⁻⁶ cm/sec
C-3	CL/SC	74.9	1,000	CH	12.0 collapse	21.9
C-3		84.8	1,000	CH	2.5 collapse	55.3
C-3		90.0	1,000	CH	0.0 collapse	2.4
C-4	CL	75.3	1,000	FH	12.1 collapse	0.240
C-4		85.0	1,000	FH	5.0 collapse	0.230
C-4		90.0	1,000	FH	0.0 collapse	0.128
C-5	CH	74.7	1,000	FH	16.7 collapse	0.320
C-5		84.6	1,000	FH	2.3 collapse	0.250
C-5		90.0	1,000	FH	0.3 collapse	0.217
S-1	CH	74.5	500	CH	3.2 collapse	635
S-1		85.3	500	FH	2.5 swell	0.650
S-1		90.9	500	FH	4.0 swell	0.130
S-2	SM	75.1	500	CH	13.5 collapse	358
S-2		84.8	500	CH	8.5 collapse	90.1
S-2		90.0	500	CH	2.0 collapse	31.5

Sample	Soil Type	Percent* Compaction	Surcharge Pressure lbs/sq ft	Test** Type	Percent Swell or Collapse During Test	Permeability*** Kx10 ⁻⁶ cm/sec
S-3	SC/CL	74.4	500	CH	7.6 collapse	75.7
S-3		84.4	500	CH	0.9 collapse	64.7
S-3		89.4	500	CH	0.0 collapse	4.70
S-4	SP/SM	75.7	500	CH	8.8 collapse	6,640
S-4		85.5	500	CH	2.8 collapse	8,390
S-4		90.4	500	CH	10.0 collapse	2,190
S-5	SM	76.0	500	CH	10.1 collapse	225
S-5		84.9	500	CH	2.5 collapse	1,910
S-5		90.6	500	CH	1.5 collapse	346

*ASTM D-698, Method C
 **FH - Falling Head
 CH - Constant Head
 ***This is the average of a number of permeability readings recorded following stabilization of the permeability rate.

NATURAL CLAY SOILS

The clay samples tested range from sandy clays (SC) to highly plastic clays (CH). As would be expected, the more highly plastic clays exhibit lower permeability rates than do the sandy clays and silty clays. Excluding what obviously appears to be some bad test data, the measured permeability rates for the clays

compacted to 85 to 90 percent of ASTM D-698, Method C range from 1.28×10^{-7} cm/sec to 8.3×10^{-5} cm/sec. At higher compaction percentages, lower permeability rates would be anticipated. However, our experience indicates that it will be difficult to achieve rates of less than 1×10^{-7} cm/sec in the laboratory. In the field, rates this low would be nearly impossible to obtain with the soils tested.

It should be noted that although the CH clays exhibit somewhat lower permeability rates, they are also much more susceptible to shrinkage cracking, if allowed to dry.

NATURAL SAND SOILS

The test results, as would be expected, show that the permeability rates are affected by the degree of compaction and especially by the amount of "fines" within the sample. This can best be seen by reviewing the permeability rates for samples S-2 and S-4. Both are fine to medium sands. However, sample S-2 contains 20.5 percent "fines" and sample S-4 contains 8.5 percent "fines". The measured permeability rate for the S-4 samples are approximately two magnitudes greater than for the S-2 samples.

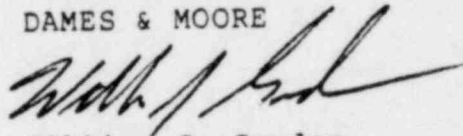
oOo

Ford, Bacon & Davis Utah, Inc.
February 6, 1978
Page -8-

We appreciate the opportunity of performing this service for you. If you have any questions regarding this report or require additional information, please contact us.

Yours very truly,

DAMES & MOORE



William J. Gordon
Associate
Professional Engineer No. 3457
State of Utah

WJG/ph

Attachments: Plate 1 - Unified Soil Classification System
Plates 2A through 2D - Gradation Curves
Plates 3A and 3B - Compaction Test Data

July 14, 1978

Ford, Bacon & Davis Utah Inc.
375 Chipeta Way
Salt Lake City, Utah 84108

Attention: Mr. Greg Jensen

Gentlemen:

Results of Laboratory Testing
Samples WC and WS
For Ford, Bacon & Davis Utah Inc.

INTRODUCTION

This report summarizes laboratory tests performed on samples provided by Ford, Bacon & Davis Utah Inc., which were delivered to the Dames & Moore laboratory in Salt Lake City, and presents discussions pertaining to the permeability characteristics of the samples tested. All results are labeled with the same sample designation as received. The laboratory test data sheets are maintained in our files. Copies can be forwarded, if requested.

PURPOSE AND SCOPE

The purpose and scope of this program were developed in discussions between Mr. Greg Jensen of Ford, Bacon & Davis Utah Inc., and representatives of Dames & Moore. Test specifications and the contract agreement are contained in Ford, Bacon & Davis' Contract Number UC-218-005 Supplement No. C, dated May 25, 1978.

The scope of the testing on the samples received includes the following:

1. Atterberg limits,
2. Gradation Tests, 3" to .175 mm,
3. Compaction Tests,
4. Permeability Tests.

TEST PROCEDURES AND RESULTS

GENERAL

Soil classifications have been made in accordance with the system described on Plate 1, Unified Soil Classification System.

ATTERBERG LIMITS TESTS

Atterberg limits were determined according to ASTM* D-423 (liquid limit) and ASTM D-424 (plastic limit and plasticity index). The results of the tests show that both Sample WS and Sample WC are non-plastic.

GRADATION TESTS

Gradation analyses were performed according to the ASTM D-422 Wet Sieving Method. The results of the gradation tests are presented on Plates 2A and 2B, Gradation Curves.

COMPACTION TESTS

Compaction tests were performed according to the ASTM D-1557-C method criteria. The results of the compaction tests are presented on Plates 3A and 3B, Compaction Test Data.

* American Society for Testing and Materials.

PERMEABILITY TESTS

Both constant and falling head permeability tests were performed in conjunction with this testing program. Constant head tests were performed upon the more permeable WS samples in accordance with the ASTM D-2434 criteria. Falling head tests were performed upon the more impermeable WC samples in accordance with the method described in "Engineering Properties of Soils and Their Measurements," by Joseph E. Bowles, 1970.

All tests were performed upon recompacted samples. Recom-paction of the test samples was performed by compacting soil within cylindrical brass rings. The soil was added in layers of uniform thickness, with each layer receiving approximately the same compactive effort. The surface of each layer was scarified prior to adding the successive layer. The results of these tests are tabulated below.

Sample	Soil Type	Percent* Compaction	Surcharge Pressure In Pounds Per Square Foot	Test** Type	Percent Swell or Collapse During Test	Permeability*** kx10 ⁻⁶ cm/sec
WC	SM	73.9	500	FH	2.4 Collapse	32.1
WC	SM	83.6	500	FH	0.2 Swell	12.9
WC	SM	89.1	500	FH	0.0	0.5
WS	SM-SP	75.5	500	CH	5.4 Collapse	4,380
WS	SM-SP	85.8	500	CH	0.3 Collapse	7,520
WS	SM-SP	9.0	500	CH	0.0	2,730

* ASTM D-1557-C

** FH - Falling Head, CH - Constant Head

*** This is the average of a number of permeability readings recorded following stabilization of the permeability rate.

Ford, Bacon & Davis Utah Inc.
July 14, 1978
Page -4-

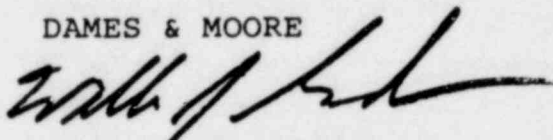
The test results, as would be expected, show that the permeability rates are affected by the degree of compaction and especially by the amount of "fines" within the samples.

oOo

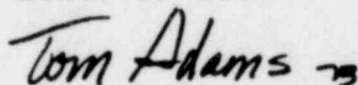
We appreciate the opportunity of performing this service for you. If you have any questions regarding this report or require additional information, please contact us.

Yours very truly,

DAMES & MOORE



William J. Gordon
Associate
Professional Engineer No. 3457
State of Utah

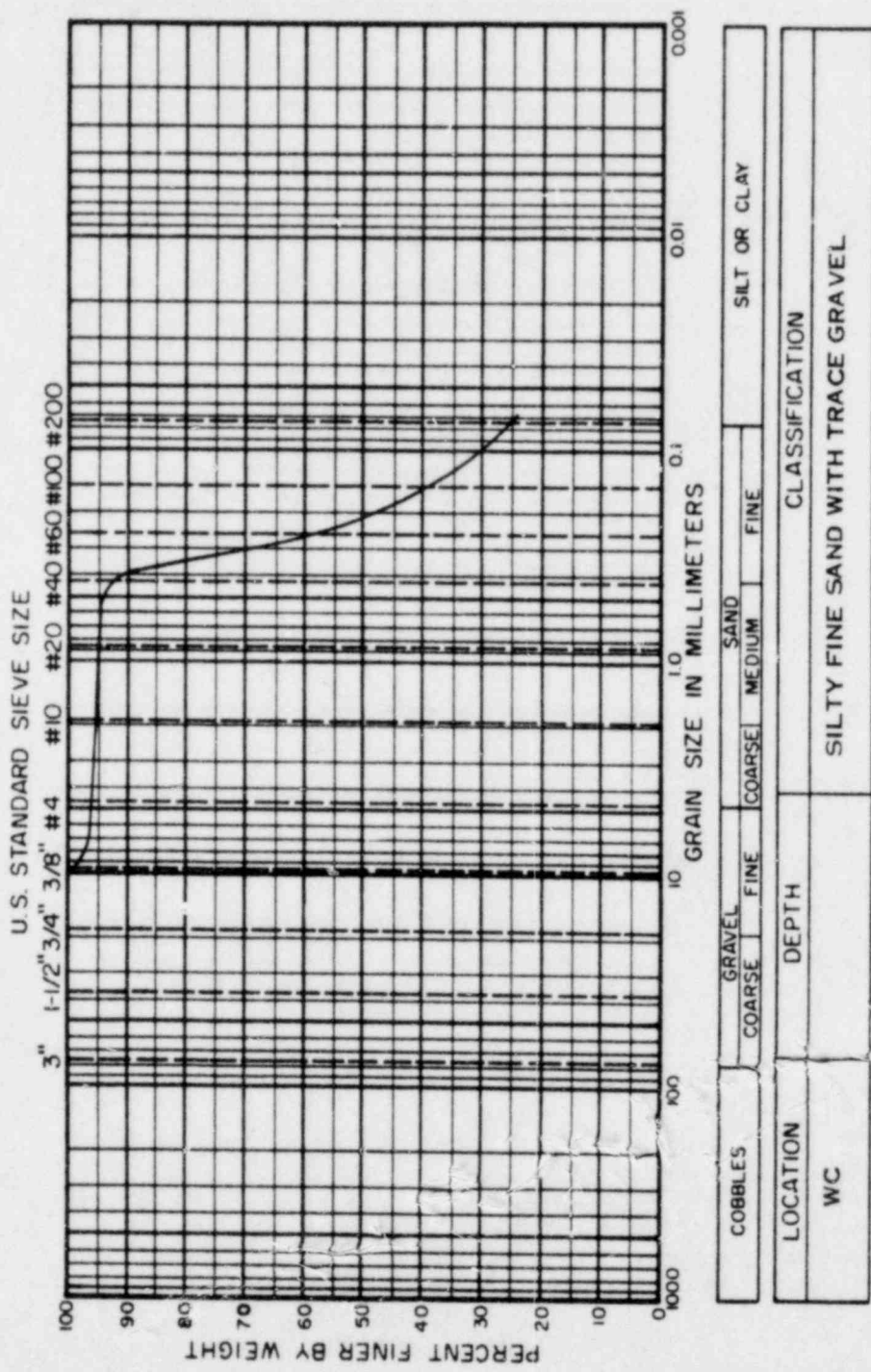


Tom Adams
Laboratory Technician

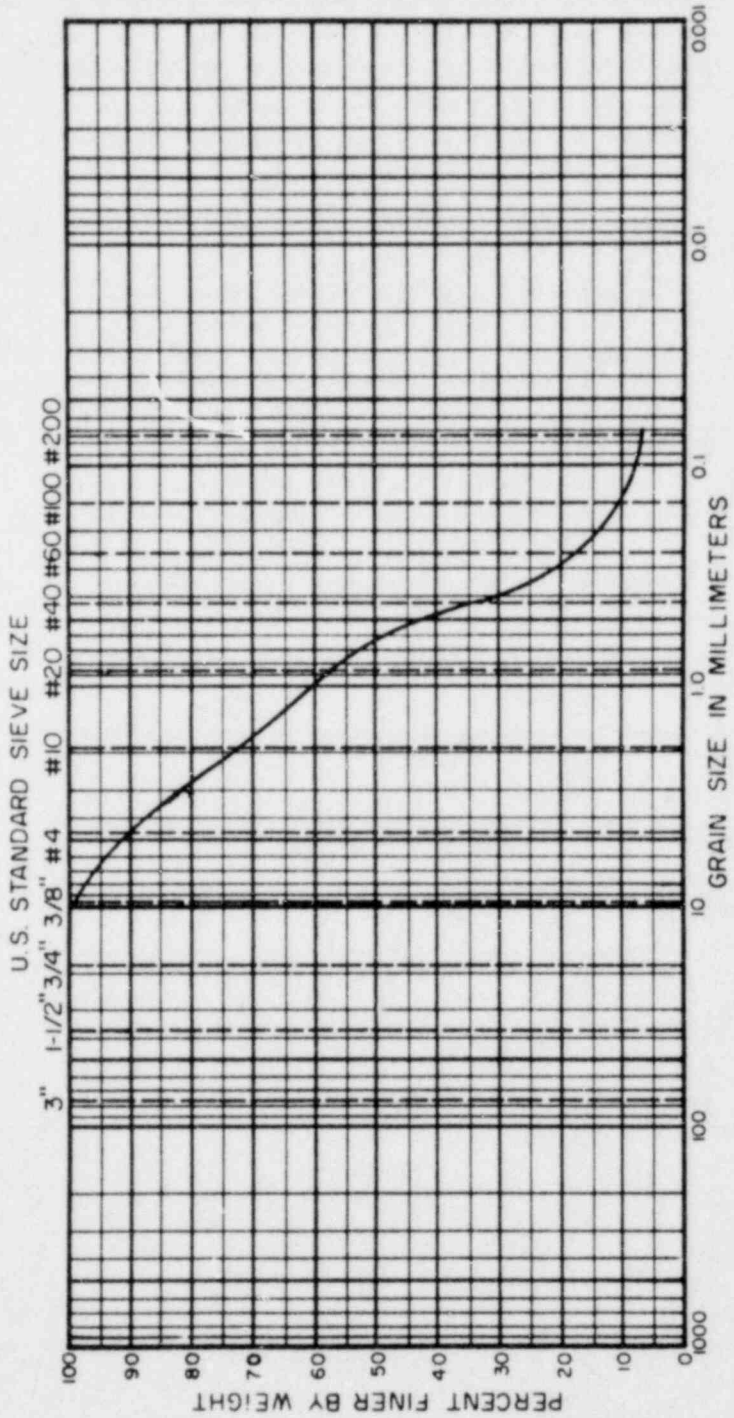
WJG/TA/nb

Attachments:

Plate 1 - Unified Soil Classification System
Plates 2A and 2B - Gradation Curves
Plates 3A and 3B - Compaction Test Data



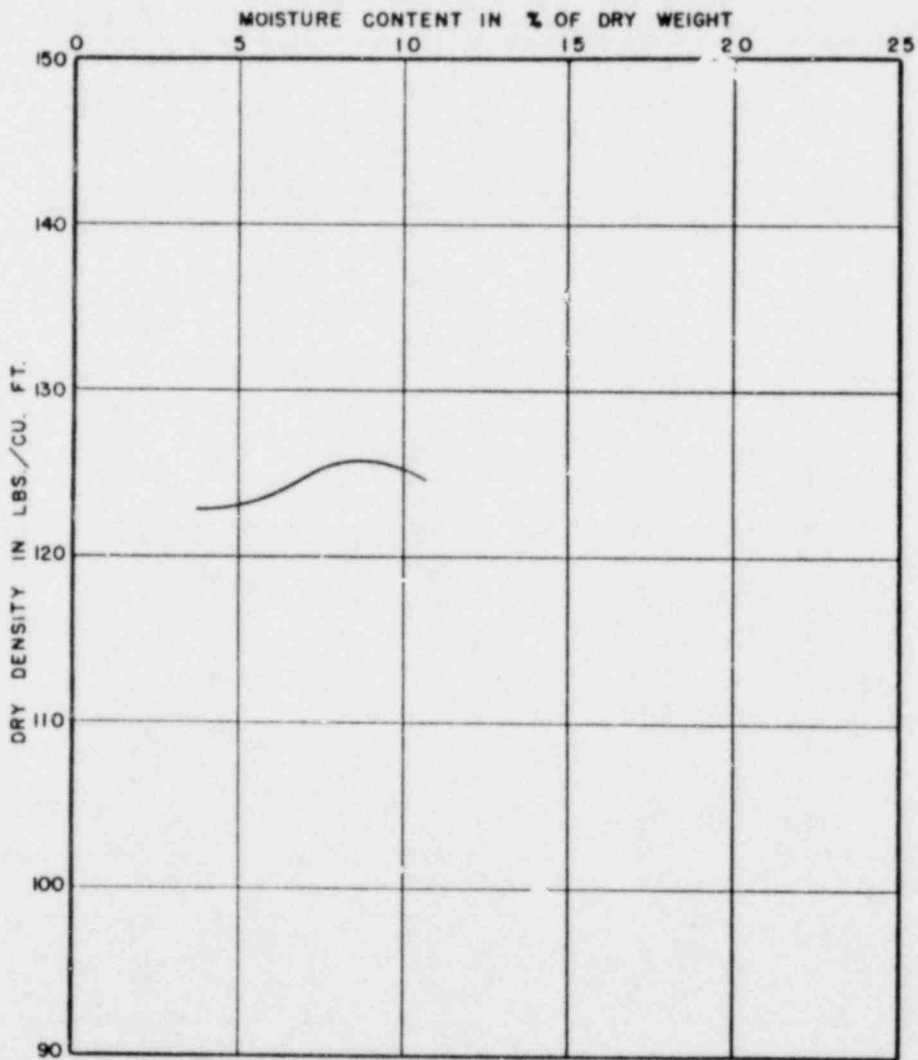
GRADATION CURVE



COBBLES	GRAVEL	SAND	SILT OR CLAY
	COARSE	FINE	
	COARSE	MEDIUM	FINE
LOCATION	CLASSIFICATION		
WS	DEPTH	FINE TO COARSE SAND WITH SOME FINE GRAVEL AND SILT (SP-SM)	

COMPACTION TEST DATA

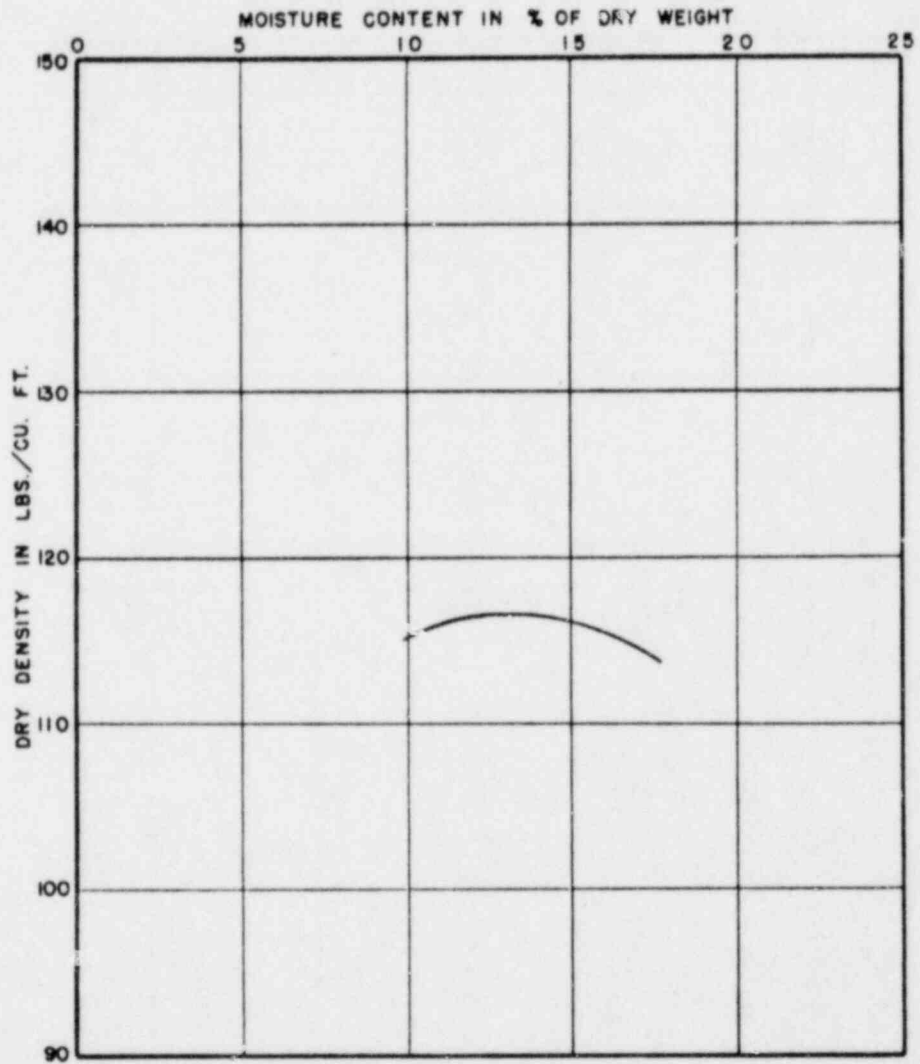
SAMPLE NO. WS _____ DEPTH _____ ELEVATION _____
SOIL FINE TO COARSE SAND WITH SOME FINE GRAVEL
AND SILT (SP-SM)
OPTIMUM MOISTURE CONTENT 8.7 PERCENT
MAXIMUM DRY DENSITY 126 LBS. PER CUBIC FOOT
METHOD OF COMPACTION A.S.T.M. D-1557-C



GRADATION CURVE

SAMPLE NO. WC DEPTH _____ ELEVATION _____
SOIL SILTY FINE SAND WITH TRACE GRAVEL

OPTIMUM MOISTURE CONTENT 13.5 PERCENT
MAXIMUM DRY DENSITY 117 LBS. PER CUBIC FOOT
METHOD OF COMPACTION A. S. T. M. D-1557-C



COMPACTION TEST DATA

APPENDIX B

CHARACTERISTICS OF PLANT SPECIES SELECTED

BY

NATIVE PLANTS, INC.

PLANT GROWTH AS A FACTOR IN
RADON GAS LEAKAGE FROM
URANIUM MILL TAILINGS

FINAL REPORT

Submitted To:

Ford, Bacon, and Davis
375 Chipeta Way
University Research Park
Salt Lake City, Utah 84108

Attention: Mr. Brad Sermon
Mr. Craig Jensen

Submitted By:

Native Plants, Inc.
400 Wakara Way
University Research Park
Salt Lake City, Utah 84108

TABLE OF CONTENTS

<u>Title</u>	<u>Page</u>
Abstract	1
Plant Materials, Species Screening and Selection	2
Experimental Design	4
Conclusions and Recommendations	12

ABSTRACT

In January of 1978, meetings were held between Ford, Bacon, and Davis, and Native Plants, Inc., to design experiments that would help determine whether or not soil covered uranium tailings would leak radon gas via root channels of deep rooted plants. The concern with radon gas leakage as a potentially dangerous health hazard prompted this investigation.

Native Plants, Inc., screened and evaluated plants that had been approved for the client's future reclamation of a tailings pond near Casper, Wyoming. After selection of deep rooted species, methods of growing these plants on simulated soil conditions over spoils were devised and constructed. Seeds and/or growing plants of the subject species were obtained and grown into standardized sizes. Plants were then moved into larger containers that simulated actual soil covered tailings. These larger containers were placed in one of Native Plants' controlled greenhouse facilities for the duration of the experiment. Environmental controls, watering, pest and disease control were monitored on a daily basis by greenhouse technicians. Root penetration by at least one of the grasses and by all shrub plants was noted during the course of the experiment. Ford, Bacon, and Davis personnel designed equipment for monitoring radon gas leakage from the plants. Additional results were sought at the end of the specified growing period by extending the experiment and drought stressing the plants while continuing the gas monitoring.

PLANT MATERIALS, SPECIES SCREENING AND SELECTION

The plant materials parameters of this study included:

1. The natural vegetation of the site where the subject uranium tailings are to be deposited near Casper, Wyoming. The area is dominated by native grasses with shrubs in drainage ways and localized areas.
2. The approved revegetation species which included a number of new or introduced species to the area in addition to native species.

Generally, the shrub species that are native to this region are quite aggressive and deep rooted. Sagebrush (Artemisia spp.) commonly found near the site, is a very deep rooted plant with a strong central tap root and an extensive surface root system as well. This plant would have been selected for testing but the specified capping soils were described as heavy clays. Sage is only found naturally on deep, loose, well-drained soils.

Fourwing saltbrush (Atriplex canescens) is not a common native plant in the area but due to its ability to adapt to a broad range of soil types, disturbances, and climatic conditions, it was the only shrub mentioned in the revegetation plan. Since it does have an aggressive root system and will adapt to clay soils if not kept too wet, fourwing saltbrush was one of the species selected for testing.

The grass species screened included three introduced wheatgrasses and two native wheatgrasses (Agropyron spp.):

- * *Agropyron riparium* Streambank wheatgrass
- * *A. smithii* Western wheatgrass
- A. cristatum* Crested wheatgrass
- Fairway crested wheatgrass
- Intermediate crested wheatgrass

*native species

It was determined that the native wheatgrasses would be the best species for natural deep root penetration. However, to test that hypothesis, Native Plants acquired seed of all of the grass species mentioned and sowed them in January 1978 in 8" and 12" deep containers. The containers used were compartmentalized tubeshaped plastic containers with side grooves that guide roots straightdown. This is Native Plants own patented Tubepak growing system.

The soil used in the Tubepaks was a 3:1:1 mixture of peat: vermiculite: perlite with Osmocote fertilizer added. The exact formulation was 12 ft.³ peat, 4 ft.³ of vermiculite, 4 ft.³ perlite, and 12 oz. Osmocote (14-14-14). CO₂ generation, night lighting, watering, fertilizing and other greenhouse procedures were carried out to optimize growth.

At the end of a three-month growing period, all of the grasses had filled the 8" deep containers but only the two native species, western wheatgrass and streambank wheatgrass, had adequately filled the 12" deep Tubepaks to allow for transplant. Therefore, the selection of these two grasses for the remainder of the experiment was made.

EXPERIMENTAL DESIGN

Containers

To adequately control variables, container size, depth, and makeup were considered critical. Numerous alternatives were reviewed with the following criteria being considered:

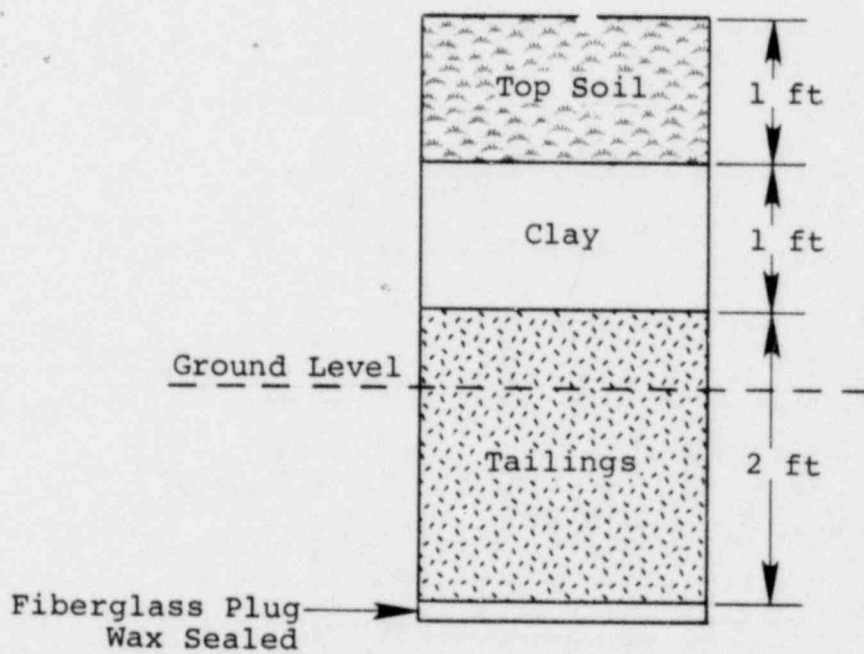
- ability to follow root development
- adequate depth for simulation of actual field conditions
- physical rigidity and ability to withstand growing period constraints
- mobility
- inert reaction with soils and tailings
- permeability of gases and liquids

The container selected was a 13" diameter flexible polyvinyl chloride semi-transparent plastic tube with 1/2" thick sidewalls. 65" sections of this tubing were cut and one end sealed with a custom made fiberglass plug. To ensure a water-tight seal, wax was poured around inside edges of the plug and a metal strapping clamp was tightened in place around the outside of the base.

Container Placement

The cylinders with sealed end down were placed vertically near the back shutter vents in Native Plants' greenhouse number two. The bottom of the containers were buried approximately two feet underground for stabilization and shielding. Alignment and spacing of

Figure 1. Diagrammatic Representation of PVA Container and Layering Profile



All of the plants were planted by hand using a small shovel. One Tubepak plug was centered in the middle of each of the PVC cylinders and care was taken not to disturb soils placement. All plants were watered in after planting.

Table I. Number of Containers in Study

<u>Species</u>	<u>Number of Containers</u>
<u>Atriplex canescens</u>	4
<u>Agropyron smithii</u>	3
<u>Agropyron riparium</u>	3

Growing Conditions

Throughout the growth regime in the greenhouse, the following environmental conditions were recorded:

1. Temperature range 58 - 64⁰ F. (night)
 68 - 84⁰ F. (day)
2. Relative Humidity 30 - 55%
3. Light Intensity Daylight
 20 second 50 ft./c light breaks every
 10 minutes during night period.

There was a single nicotine fumigation applied on August 1, 1978 for pest control. No pest or disease problems were observed.

containers is shown in Figure 2. Essentially, a spacing which would allow for ease of monitoring and 360° observation of root development was selected.

Soil Selection and Placement

Though soil selection and placement were carried out by Ford, Bacon, and Davis, personnel, a brief description is included here for continuity. Soils consisted of the following:

Tailings - supplied by client

Clay capping soil - sterile, light colored, blacky (source, Salt Lake City, west bench)

Topsoil - dark, clay-loam (source, Salt Lake City, orchard)

Two feet of tailings extending 6 to 10 inches above ground level were added. This was covered with one foot of clay and topped with 1 foot of clay loam topsoil (Figure 1 and 2).

Planting Procedures

Selected species had been previously grown to fill the 12-inch Tubepak container with roots as has already been discussed. The fourwing saltbrush were grown as single plants and were approximately 1 1/2 years old and came from a Nevada seed source. Both grasses were grown from multiple seedlings. The western wheatgrass seed came from South Dakota. The stream-bank wheatgrass seed source was Kansas.

A bi-weekly application of 20-20-20, NPK fertilizer with trace elements was used to grow seedlings prior to planting in large containers. Fertilizer was applied aqueously. No further fertilizer was used.

Three times per week, greenhouse technicians checked the condition of all of the plants. Watering was done as soil and plant conditions indicated was necessary. Since these were closed containers, watering was a critical factor -- overwatering would have been lethal to these species.

Greenhouse environmental systems are automatically controlled and the variation shown is within the parameters selected by Native Plants' greenhouse manager. CO₂ generation was automatically set during non-ventilating hours. Measurements of levels of CO₂ were not made but the range sought for was 800 - 1200 ppm.

Observations

Root penetration of the tailings by all of the Atriplex plants was observed. Root penetration of tailings was observed in at least one container of Agropyron. Due to the delicate root structure of grasses, root advance was more difficult to follow. During the growing period, the client took all radon gas readings.

The grasses were clipped once during the growing period and as of October 10, had grown to a height of six inches. The Atriplex which were all about 12 - 18" in height at the start of the treatments, had grown to 24" and had developed extensive branching.

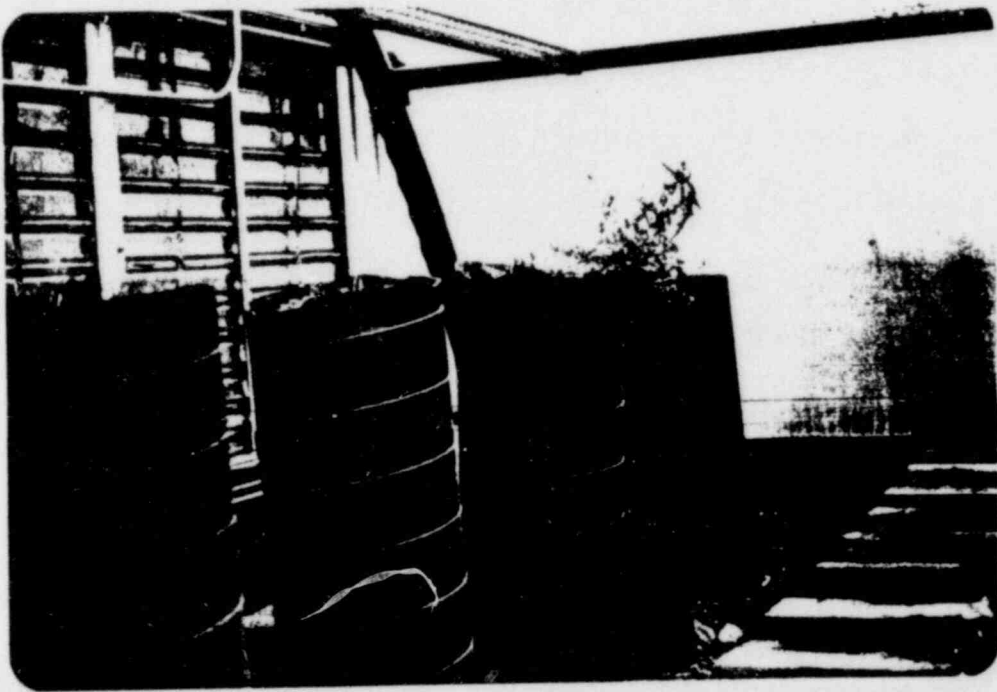
Photographs of the plants taken at the end of the study are shown in Figure 3.

At the beginning of September, 1978, watering of the test plants was terminated at the request of the client. The purpose for this was to stress the plants, the premise being that such stress would either cause accelerated root growth with deeper penetration of the tailings, or it would cause desiccation of the plants with root shrinkage. Either effect might result in increased radon leakage. The results of the readings are in possession of the client.

Regarding overall plant performance, all test plants appeared to grow vigorously up to cessation of watering. Top growth was very good as was observable root growth. Following the stressing treatment, the Atriplex plants continued to exhibit good top growth, but all of the grasses exhibited wilting and obvious shoot stress symptoms. The effect on root growth was not determined.

FIGURE 2

PVC Containers Used in Radon
Gas Leakage Study



POOR ORIGINAL

FIGURE 3. An Atriplex Plant Grown in Uranium Tailings at End of Treatment

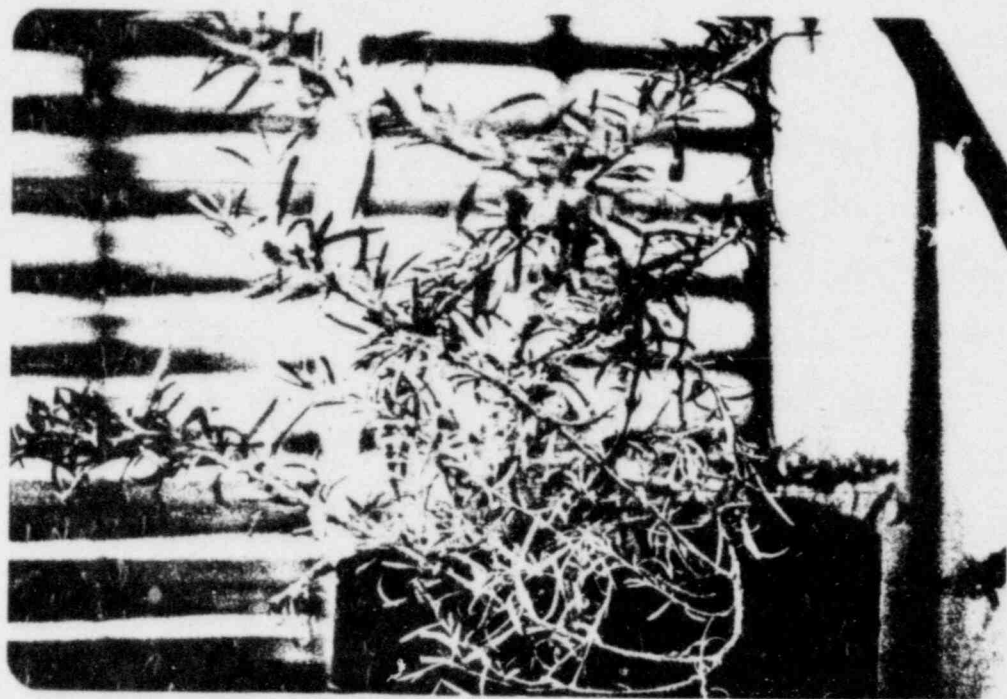
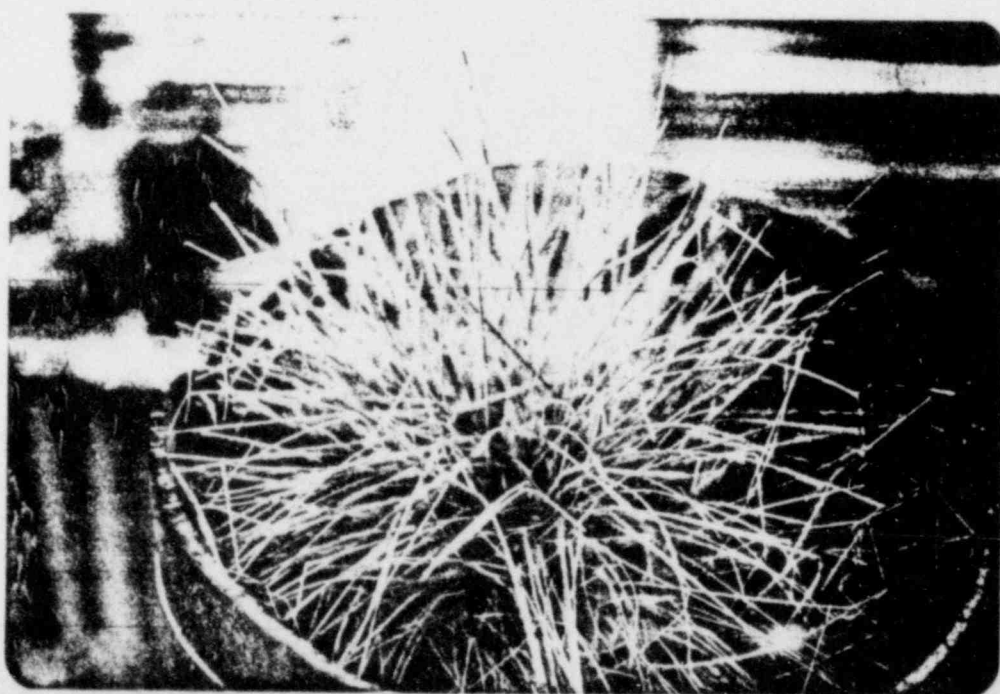


FIGURE 4. A Group of Agropyron Plants Showing Regrowth in Uranium Tailings After Being Clipped to 6 Inches Height



CONCLUSIONS AND RECOMMENDATIONS

The general results of this study indicates no adverse effects on test plants grown in a specialized container with approximately 35% tailings per total volume. Physiological stress was noted in Agropyron plants purposely not watered for six weeks.

It is recommended that to further test the hypothesis plants be allows to grow to a larger size for one year and then be allowed to die. Monitoring should be carried out through the second year after death. Caution on moving containers should be exercised due to damage of delicate root channels.

Field verification of these data should be undertaken if economically feasible. Field conditions are dramatically different than greenhouse conditions though data may remain the same.

Additional greenhouse studies indicated include:

- variations in capping soil depths
- variations in volume of tailings and capping soils
- additional species that might invade reclaimed areas that could be more deeply rooted than those previously tested.
- fertilized vs. non-fertilized replications to test rate of growth vs. gas leakage.

NRC FORM 335 (7-77)		U.S. NUCLEAR REGULATORY COMMISSION BIBLIOGRAPHIC DATA SHEET		1. REPORT NUMBER (Assigned by DDC) NUREG/CR-1081	
4. TITLE AND SUBTITLE (Add Volume No., if appropriate) Characterization of Uranium Tailings Cover Materials for Radon Flux Reduction				2. (Leave blank)	
7. AUTHOR(S) Vern C. Rogers and others				3. RECIPIENT'S ACCESSION NO.	
9. PERFORMING ORGANIZATION NAME AND MAILING ADDRESS (Include Zip Code) Ford, Bacon & Davis Utah, Inc. 375 Chipeta Way Salt Lake City, Utah 84108				5. DATE REPORT COMPLETED MONTH January YEAR 80	
12. SPONSORING ORGANIZATION NAME AND MAILING ADDRESS (Include Zip Code) Waste Management Research Branch Division of Safeguards, Fuel Cycle & Environmental Res. Office of Nuclear Regulatory Research Washington, D. C. 20555				DATE REPORT ISSUED MONTH March YEAR 1980	
13. TYPE OF REPORT Technical/Formal				PERIOD COVERED (Inclusive dates)	
5. SUPPLEMENTARY NOTES				6. (Leave blank)	
14. (Leave blank)				8. (Leave blank)	
16. ABSTRACT (200 words or less) <p>The attenuation of radon through uranium tailings cover material is usually described with diffusion theory expressions. One of the main parameters characterizing the diffusion is the diffusion coefficient. Measured values of the diffusion coefficient for several Wyoming and New Mexico soils are presented. An interpretation of various approximations to the diffusion equation is also given. Finally, the diffusion coefficient dependence on moisture is presented and the data are represented by a simple correlation.</p>				10. PROJECT/TASK/WORK UNIT NO.	
17. KEY WORDS AND DOCUMENT ANALYSIS uranium mill tailing radon attenuation cover materials diffusion coefficient				11. CONTRACT NO. A-2046	
17b. IDENTIFIERS/OPEN-ENDED TERMS				19. SECURITY CLASS (This report) Unrestricted	
18. AVAILABILITY STATEMENT Unlimited				21. NO. OF PAGES	
19. SECURITY CLASS (This page) Unrestricted				22. PRICE \$	

UNITED STATES
NUCLEAR REGULATORY COMMISSION
WASHINGTON, D. C. 20555

OFFICIAL BUSINESS
PENALTY FOR PRIVATE USE, \$300

POSTAGE AND FEES PAID
U.S. NUCLEAR REGULATORY
COMMISSION



POOR ORIGINAL